UNIVERSITÀ DEGLI STUDI DI MILANO

Dottorato in Scienze Farmacologiche Sperimentali e Cliniche

Dipartimento di Scienze Farmacologiche e Biomolecolari

XXXI ciclo

The long pentraxin 3 plays a key role in the immunomodulation of diet-induced obesity

Bio/14

Studente:

Annalisa Moregola

R11331

Supervisore:

Chiarissimo Prof. Giuseppe D. Norata

Coordinatore del Dottorato:

Chiarissimo Prof. Alberico L. Catapano

Anno Accademico

2017/2018

The long pentraxin 3 plays a key role in the immunomodulation of diet-induced obesity

AIM: Obesity is characterized by a state of chronic low-grade inflammation. PTX3 is the prototype of long pentraxins, it is an essential component of the humoral arm of innate immunity and is involved in many inflammatory processes. There are several conflicting data about the role of PTX3 in obesity. Aim of this project was to clarify whether PTX3 behaves as a bystander or actively participates to obesity-related inflammation.

METHODS: PTX3 KO and WT littermates were fed a high fat diet (HFD; 45% Kcal from fat) or a standard fata diet (SFD;10% Kcal from fat) for 20 weeks. Body weight was measured weekly; fat distribution (magnetic resonance for imaging, MRI) and glycemia (glucose-GTT and insulin-ITT tolerance tests) was checked at 10 and 20 weeks. Immunophenotyping and gene expression, in particular of the adipose tissue, was performed at 20 weeks. Ectopic fat deposition in h1/h1 and h2/h2 individuals was determined by DEXA.

RESULTS: PTX3 KO mice on HFD exhibit a decreased weight gain compared to WT (AUC weight gain WT=190.8±17.45, KO=134.8±10.09), coupled to a decreased accumulation of visceral (VAT) and subcutaneous (SCAT) fat both at 10 ($p<0.05$) and 20 weeks ($p<0.01$) of diet measured by MRI and confirmed weighing the tissues after the sacrifice (VAT% WT=7.609±0.6776, KO=4.390±0.8235; SCAT% WT=5.953±0.9682, KO=3.144±0.6129, $p<0.05$). Basal glycemia and the results of the glucose and insulin tolerance test were superimposable. PTX3 deficiency results in the reduction of monocytes markers and pro-inflammatory cytokines gene expression in VAT (MCP-1, IL-6, $p<0.05$) which is associated to a reduced infiltration of monocytes and macrophages in the tissue as assessed by cell sorting. Of note vascularization was enhanced (increased gene expression of *Cd31* and *Vegfa* in VAT, $p<0.05$) in VAT from PTX3 KO mice. Sorted VAT macrophages showed enhanced expression of

molecules associated with M2-polarization (*Arg1*, *Ym-1*, $p<0.01$). In humans, carriers of the h2/h2 haplotype for PTX3, characterized by lower PTX3 plasma levels compared to h1/h1 carriers, presented with lower BMI and lower abdominal obesity compare to h1/h1 carriers (android fat% h2/h2=45.34±10.32, h1/h1=47.17±9.23, $p<0.05$).

CONCLUSIONS: Our results demonstrate that PTX3 might contribute to the development of obesity by limiting adipose tissue vascularization and promoting macrophage infiltration.

La lunga pentraxina 3 gioca un ruolo chiave nella modulazione della risposta immuno-infiammatoria associata all'obesità

SCOPO: L'obesità è caratterizzata da uno stato di infiammazione cronica. PTX3, il prototipo delle pentraxine lunghe, è una componente essenziale del braccio umorale dell'immunità innata ed è coinvolta in diversi processi infiammatori. Il ruolo di PTX3 nell'obesità è dibattuto. Scopo di questo progetto è stato quello di chiarire quale sia il ruolo di PTX3 nell'obesità e se contribuisce allo sviluppo della patologia.

METODI: Topi PTX3 KO e WT sono stati messi a dieta ad alto contenuto di grassi (High Fat Diet – HFD, 45% delle Kcal derivante dai grassi), o dieta standard (Standard Fat Diet-SFD, 10% delle Kcal derivante dai grassi) come dieta controllo, per 20 settimane. Il peso degli animali è stato registrato settimanalmente. A 10 e 20 settimane di dieta sono stati valutati la distribuzione di grasso corporeo (risonanza magnetica), e la risposta glicemica (Test di Tolleranza al Glucosio – GTT, Test di Tolleranza all'Insulina – ITT). Al termine delle 20 settimane è stata fatta un'analisi immunofenotipica delle cellule immunitarie circolanti e tissutali tramite citofluorimetria e una valutazione dell'espressione genica nel tessuto adiposo. Il grasso ectopico nei soggetti h1/h1 e h2/h2 è stato valutato tramite DEXA.

RISULTATI: I PTX3 KO dopo 20 settimane di dieta HFD hanno guadagnato significativamente meno peso rispetto ai topi WT (area sotto la curva del guadagno di peso: WT=190.8±17.45, KO=134.8±10.09), ed hanno accumulato meno tessuto adiposo a livello viscerale (VAT) e sottocutaneo (SCAT) misurato tramite MRI sia a 10 ($p<0.05$) che a 20 ($p<0.01$) settimane dall'inizio della dieta e confermato al momento del sacrificio (VAT% WT=7.609±0.6776, KO=4.390±0.8235; SCAT% WT=5.953±0.9682, KO=3.144±0.6129, $p<0.05$). Non abbiamo riscontrato differenze tra animali PTX3 KO e WT nelle risposte ai test di tolleranza al glucosio e all'insulina. La mancanza di PTX3 si è rivelata essere

associata a ridotta espressione genica di citochine pro-infiammatorie (MCP-1, IL-6, $p<0.05$) e infiltrazione di monociti e macrofagi nel VAT valutato tramite cell sorter, mentre la vascolarizzazione del tessuto è risultata essere maggiore rispetto ai WT (aumentata espressione di *Cd31* e *Vegfa*, $p<0.05$ e $p<0.01$). I macrofagi isolati dal VAT dei topi PTX3 KO hanno mostrato un'aumentata espressione di marker tipici dei macrofagi M2, più pro-risolutivi (*Arg1*, *Ym-1*, $p<0.01$) rispetto a quelli degli animali WT. Studi nell'uomo hanno mostrato come individui portatori dell'aplotipo h2/h2 per PTX3, caratterizzati da livelli più bassi di PTX3 rispetto ai soggetti dell'aplotipo h1/h1, mostrano un ridotto BMI e una ridotta obesità addominale rispetto ai soggetti h1/h1 (% grasso androide h2/h2=45.34±10.32, h1/h1=47.17±9.23, $p<0.05$).

CONCLUSIONI: I nostri risultati mostrano che PTX3 potrebbe contribuire allo sviluppo di obesità limitando la vascolarizzazione del tessuto adiposo e promuovendo l'infiltrazione di macrofagi.

Index

Introduction 8

1. OBESITY 9

1.1 OBESITY COMORBIDITIES and METABOLIC SYNDROME 10

1.2 ADIPOSE TISSUE 12

1.2.1 Adipose tissue inflammation 14

1.2.2 Role of macrophages in adipose tissue immune-inflammatory response 15

1.2.3 Importance of adipose tissue vascularization 18

1.3 ANIMAL MODELS OF OBESITY 20

1.3.1 Genetically obese mouse models 20

1.3.2 Diet-induced obesity model 22

2. IMMUNITY 23

2.1 INNATE IMMUNITY 23

2.2 PENTRAXIN 3 25

2.2.1 PTX3 gene and protein structure 25

2.2.2 PTX3 production 26

2.2.3 PTX3 ligands 27

2.2.4 Relevance in humans: PTX3 and genetic variants 29

2.3 OTHER PENTRAXINS 30

2.3.1 Long Pentraxins 30

2.3.2 Short Pentraxins 31

3. ROLE OF PTX3 IN PATHOLOGIES 32

3.1 PTX3 AND INFECTIONS 32

3.2 PTX3 IN CARDIOVASCULAR DISEASES 33

3.3 PTX3 DURING OBESITY 34

3.4 PTX3 IN TUMORS 36

Aim of the project 38

Materials and Methods 40

1. Animal models 41

2. Genotyping 41

3. Diet-induced obesity model 42

4. Magnetic resonance for imaging (MRI) 42

5. Glucose and Insulin tolerance test 43
6. Samples preparation for immunophenotyping by flow cytometry 43
7. Blood biochemistry measurements 44
8. Histology 45
9. Real time PCR 45
10. Immunoblotting 46
11. Human study – the PLIC cohort 47
12. Human study – Anthropometric measurements 48
13. Statistical analysis 49
Results 50
1. Diet-induced obesity model 51
2. Effect of diet-induce obesity in PTX3 KO mice 51
3. Glucose and lipid homeostasis evaluation 52
4. Circulating and bone marrow immune cell profiling 53
5. PTX3 deficiency promotes pro-resolution macrophage skewing 54
6. Enhanced vascularization limits visceral adipocytes hypertrophy in PTX3 KO mice 55
7. Genetic determined lower PTX3 levels in humans relates with a reduced visceral adipose tissue accumulation 56
Discussion 57
Figures and Tables 62
References 95

Introduction

1. OBESITY

Obesity is one of the most prevalent and common disease worldwide and it is become a major concern for public health because of the related comorbidities such as diabetes, hypertension, atherosclerosis and some type of cancer. Obesity is considered the result of disequilibrium between energy intake and expenditure. Different determinants contribute to the onset of obesity: behavioural, environmental and genetic factors (***Figure 1***). Behavioural factors comprehend increased calorie intake, physical inactivity and sedentary lifestyle, insufficient sleep and smoking cessation. In a study evaluating the impact of sleep on the physiopathology of obesity, researchers show that sleep deprivation associate with a decrease in leptin levels, with a consequent decrease sense of satiety, leading in turn to excessive food intake [1]. Environmental factors inducing obesity can be the change of the value that is now given to food, is no more something needed for survival, but eating is become a pleasure and an entertainment. Furthermore, there is an inverse correlation between obesity and socioeconomic status [2]. People with limited economic power usually choose junk compared to healthy food. Furthermore every culture has their values that influence health behaviour [3]. Biological factors are numerous [4]. First, obesity may be caused leading to monogenic, polygenic or syndromic (chromosomal abnormalities, e.g. Prader-Willis syndrome). Among described mutations are listed those encoding for leptin and melanocortin 4 gene. More than 300 genes associated to obesity have been identified using genome wide association technics.

A person is considered obese when its BMI (Body Mass Index), corresponding to a person's weight in kilograms divided by the square of height in meters, is higher than 30, with class 1 obesity between 30 and 35, class 2 obesity between 35 and 40, and class 3 obesity or severe obesity for a BMI over 40.

Obesity is characterized by the accumulation of fat that can occur at the visceral level, in particular in the abdomen, or subcutaneously. Abdominal obesity is identified when waist circumference is > 102 cm in men and > 88 cm in women according to the criteria provided by the ATP (Adult Treatment Panel). Abdominal obesity is the one driving the progression of multiple cardiometabolic risk, as type 2 diabetes, and it can correlate to those risks independently from body mass index. Accumulation of fat in the visceral area is usually associated with hypertrophy and hyperplasia if adipocytes, alterations of the supportive extracellular matrix, infiltration of immune cells, in particular monocytes and macrophages, that promote an inflammatory milieu. Indeed, obesity is not only defined as an excess or abnormal fat accumulation, but also as a disease characterized by chronic low-grade inflammation and by positive association with inflammatory circulating markers as CRP [5, 6], IL6 [7] and TNFa [8]. Indeed, cytokines are produced by hypertrophic adipocytes and contribute to the maintenance of the chronic inflammatory circuit that characterizes obesity. Obesity has been related to immune dysfunction after the observation of higher rates of infections and impaired would healing in obese subjects [9].

1.1 OBESITY COMORBIDITIES and METABOLIC SYNDROME

Obesity is associated with a persistent state of chronic low-grade inflammation that seems to play a pivotal role in the onset of obesity-related pathologies as dyslipidemia, hypertension, insulin-resistance, diabetes, cardiovascular diseases and chronic stress [10].

Dyslipidemia is characterized by high levels of triglycerides, high levels of LDL small and dense particles and low levels of HDL cholesterol [11]. This condition is known as the “atherogenic lipoprotein phenotype” [12]. This phenotype is

associated with higher risk of coronary diseases, as angina pectoris, unstable angina and myocardial infarction.

Insulin-resistance is the condition where response to insulin is dampened in insulin-sensitive tissues, such as liver, fat and skeletal muscles, thus causing hyperglycaemia. Insulin role is to lower glucose blood levels binding its receptor on responsive tissues after a meal. During obesity inflammation contributes to insulin-resistance in different ways. TNFα, hypoxia and free fatty acids produced during obesity, activates intracellular signalling pathways involving IKKβ and JNK1, two serine kinases. The activation of these enzymes by TNFα leads to the inhibition of IRS-1 (Insulin Receptor Substrate 1), inducing insulin-resistance in adipocytes and hepatocytes [13, 14]. In addition, TNFα promotes insulin-resistance through the inhibition of PPARγ [15], a transcription factor involved in lipids synthesis and fat storage in adipocytes. Insulin-resistance is directly correlated to type 2 diabetes. During insulin-resistance, pancreatic β cells produce higher amount of insulin in order to counteract peripheral insulin intolerance, however, after years, this is not sufficient to maintain glucose homeostasis and glucose levels remain high in the blood. More than 125 ml/dL at fasting are usually considered markers of type 2 diabetes and leads to long-term complications such as diabetic retinopathy, stroke and heart disease. The compensatory hyperinsulinemia can cause hypertension as in some circumstances insulin leads to an enhanced sodium tubular reabsorption, thus resulting in elevated blood pressure [16]. Another mechanism by which obesity can determines hypertension is through the sympathetic activation by leptin, a hormone produced by the adipocytes. Leptin induces the sense of satiety and thermogenesis activating the sympathetic nervous system while its inhibition limits hypertension.

Obesity is the principal risk factor for the development of metabolic syndrome. Metabolic syndrome (MetS) is a complex and multifactorial pathology

characterized by an interconnection of physiologic, biochemical and metabolic factors. In accordance with the National Educational Program's Adult Treatment Panel III report (NCEPT-ATP III) the diagnosis of Mets is attributed when three of these criteria occur: abdominal obesity (waist circumference > 102 cm in men and > 88 cm in women); triglycerides >150 mg/dL; fasting blood glucose > 110 mg/dL; HDL cholesterol < 40 mg/dL for men and < 50 mg/dL for women; blood pressure > 130/80 mmHg [11]. However, fat accumulation in adipose tissue is considered the trigger of an inflammatory response that exacerbate the MetS.

1.2 ADIPOSE TISSUE

In mammals there are two principal types of adipose tissue: the white adipose tissue (WAT) and the brown adipose tissue (BAT). BAT and WAT are characterized by different structures, functions, and regulations. In humans, WAT is found in the body in intra-abdominal depots around the omentum, intestine, and perirenal area, as well as in subcutaneous depots in the buttocks, things, and abdomen, but it can be found also within the bone marrow. Brown adipose tissue is more abundant in the neonatal period specifically in the interscapular and perirenal regions in rodents, in human can be found also in the supraclavicular, chest and abdomen regions. BAT in adulthood is less represented [17]. Structurally, white and brown adipose tissue are different. White adipose tissue is characterized by unilocular/large lipid droplets and are supported by connective tissue with a thick network of capillaries. BAT adipocytes contain at the contrary many small lipid droplets and higher number of mitochondria because they are required for the regulation of non-shivering thermogenesis. The non-adipocytic component of WAT is called stromo-vascular fraction and includes extracellular matrix, that with its

components (e.g. collagen, proteoglycans, fibronectin, osteonectin, metalloproteinases) anchor adipocytes to ensure functional and structural integrity of the tissue [18].

In brown adipose depots thermogenesis is controlled by UCP1, a molecule expressed in response to adrenergic signal and located in the inner membrane of mitochondria. This signalling through UCP1 causes a proton leak across the inner membrane of mitochondria, converting chemical energy into the heat [19]. On the contrary, WAT primary function is to store excess energy as TGs to regulate energy homeostasis. When liver and muscles need energy, in absence of glucose, lipids are moved from adipocytes through lipolysis and released as TGs from the adipose tissue [20].

Both brown and white adipocytes originate from the mesoderm but white adipocytes derive from adipogenic lineage precursor cells that are Myf5-negative, while brown adipocytes derive from myogenic lineage precursor cells Myf5-positive, as Myf5 is a key myogenic regulatory factor [21]. BAT as a primary role in protection of the new-born from cold in the first moments of life, for this reason BAT develops and differentiates before birth. Instead, WAT formation starts early after birth under certain types of stimulation. The transition from pre-adipocytes to adipocytes is controlled by a series of transcription factors that include the nuclear receptor PPARγ, specific marker of adipose tissue and factor necessary for the maintenance of a terminal state of differentiation of the adipocytes, and members of the CCAAT-enhancer-binding protein (C/EBP) family, in particular C/EBP which is fundamental for adipogenesis in white adipose tissue [22].

There are two main type of white adipose tissue: the visceral (VAT) and the subcutaneous (SCAT) adipose tissue. Visceral adipose tissue is localized in the abdominal cavity, surrounding intraperitoneal organs and it can be further

divided in mesenteric, epididymal and perirenal visceral adipose tissue. Subcutaneous adipose tissue is below the skin in the hypoderm.

1.2.1 Adipose tissue inflammation

Obesity is characterized by the progressively expansion of VAT, enlargements of adipocytes, increase of the stromovascular components, and by a chronic state of low grade inflammation with progressive immune cell infiltration in the adipose tissue. Increased adipocytes size during obesity is associated with augmented pro-inflammatory cytokines secretion. AT is the primary source of many inflammatory cytokines, which in the adipose tissue are known as adipokines. Adipokines comprehend adiponectin, leptin, MCP-1, plasminogen activator inhibitor 1 (PAI-1), IL-6, visfatin, omentin, TNFα, retinol binding protein 4, serum amyloid A (SAA), C reactive protein, VEGF, resistin and many others [23]. Leptin levels increase in adipose tissue in expansion during obesity [24]. Leptin regulate satiety, food intake, reproductive function, energy expenditure. In the hypothalamus, leptin increases anorexigenic and decreases orexigenic peptide synthesis causing a reduction of the appetite [25]. Adiponectin is almost exclusively produced by adipocytes and modulates a number of metabolic processes such as fatty acids oxidation and glucose regulation [26]; in addition, it has also insulin sensitizing and anti-inflammatory properties. TNFα is a pro-inflammatory cytokine that correlates positively with body mass index, body fat, hyperinsulinemia and insulin resistance in humans [27], while the use of neutralizing antibodies against TNFα reduces inflammation, improves fatty liver diseases [28] and protects against diet-induced obesity in mice [29].

Inflammation of VAT is central in the development of systemic insulin resistance during obesity and is mediated primarily by adipose tissue

macrophages (ATM, their role will be discussed in detailed in the next paragraph) [30], but other immune cells play a critical role in AT-mediated inflammation. T lymphocytes (CD4+ and CD8+) produce high amounts of IFNγ that contribute to the pro-inflammatory microenvironment [31] and it has been shown to inhibit insulin signalling in human adipocytes [32]. It has been reported that depletion of VAT T cells lead to an improved insulin-sensitivity in obese mice [31], furthermore T cells present in adipose tissue seems to have an effector-memory phenotype with a restricted TCR repertoire, to suggest that fat accumulation leads to the generation of antigens recognized as not-self that drive T cell expansion [33]. Several studies were performed in B cells too. In a study, B cell deficient mouse on HFD results protect from insulin resistance despite weight gain [34], while conversely, the transfer of IgG from obese mice to a lean one cause glucose intolerance and insulin intolerance. Neutrophils are among the first immune cells to [35] and promote the inflammatory milieu by secreting neutrophil elastase [36], an enzyme which can promote inflammatory responses in several pathologies. While the number of monocytes, macrophages and T lymphocytes CD4+ or CD8+ increases during obesity, the number of a subclass of lymphocytes called T regulatory cells (Tregs), decreases. Tregs decrease in obesity is associated with a worsening of AT inflammation and insulin resistance. The reasons why Tregs are protective in obesity can be due, as shown in vitro, by the ability to improve glucose uptake by adipocytes [37] or because they interact with ATMs and are in an inverse correlation with M1 pro-inflammatory macrophages polarization [38].

1.2.2 Role of macrophages in adipose tissue immune-inflammatory response

Studies in animal models and in vitro highlight the critical role of adipose tissue macrophages (ATMs) in the establishment of the chronic inflammation

associated to obesity and metabolic dysfunctions as type 2 diabetes and insulin resistance [39, 40]. Crosstalk exists between adipocytes and macrophages, that promote the maintenance of the chronic inflammation in adipose tissue [41] through the continuous recruitment of circulating macrophages and monocytes. Macrophages can be divided in two class: the classically activated macrophages (M1) and alternatively activated macrophages (M2) [42]. M1 and M2 differ for the activator stimuli and for their functions (***Figure 2***). M1 are induced by pro-inflammatory mediators such as LPS and IFNγ and they are characterized by the production of pro-inflammatory cytokines as TNFα, Il-6, IL-12. During infections, M1 macrophages participate in the clearance of pathogens and generate reactive oxygen species (ROS). M1 through the generation of ROS induce tissue damage and impairment. To protect tissues from M1-mediated damage, M2 macrophages with their anti-inflammatory functions inhibit chronic inflammatory responses. M2 polarization can be induced in vitro with IL-2 and IL-13 [43]. M2 macrophages are believed to participate to the resolution of inflammation and tissue repair, in fact they produce mainly anti-inflammatory molecules as Arginase 1 (Arg1), YM1, Interleukine 1 (IL-1) receptor antagonist, IL-10. In an animal model the specific deletion in macrophages of the peroxisome proliferator activated receptor-c (PPARc), impair alternative macrophages activation predisposing to diet-induced obesity, insulin resistance and glucose tolerance, thus suggesting a beneficial role for M2 polarization in the regulation of nutrient homeostasis and obesity susceptibility [44]. M1 and M2 differ also for the type of chemokines produced. M1 produce CXCL9 and CXCL10 regulating Th1 polarized T cell responses, while M2 produce CCL22 that integrates the circuit of amplification and regulation of polarized Th2 or T regulatory lymphocytes responses.

In healthy tissues, macrophages derived from non-classical monocytes, express low levels of CCR2 (C-C motif chemokine receptor 2) [45], the receptor for the

chemokine MCP-1, while during inflammation the number of classical inflammatory monocytes LyC6^{hi} that express high levels of CCR2 increases. It has been shown that animals CCR2 deficient have decrease M1 macrophages in adipose tissue during obesity, possibly due to the reduced recruitment of classical monocytes [46], which have a high ability to migrate into inflamed tissue [47]. Hence, classical monocytes are important for the development of obesity as they have high ability to infiltrate tissues during inflammation and polarize to pro-inflammatory M1 macrophages.

Obesity is characterized by a shift from M2, anti-inflammatory macrophages, to M1 type responses [48]. Lean individuals in a non-inflammatory state maintain a 10-15% of resident ATMs [49]. In obese subjects this percentage increases (more than 50%). This increase of ATM in adipose tissue is due to the initial enlargement of adipocytes that release MCP-1, TNFα and saturated fatty acids which induce resident macrophages activation to the M1 phenotype [50]. Therefore, activated macrophages release MCP-1 thus promoting the recruitment of monocytes from the circulation into the site of inflammation [51]. This crosstalk between macrophages and adipocytes set up and support the chronic inflammation of obesity through the continuous engagement of new monocytes and macrophages from the circulation.

The 90% of macrophages infiltrating the adipose tissue can be found around dead adipocytes in structure called "crown-like structures", both in animals and in humans [52, 53]. These structures are more common in visceral compare to the subcutaneous fat depots [54], suggesting that the higher incidence of metabolic disorders associated with visceral fat accumulation could be due to a greater susceptibility to adipocytes necrosis of this tissue compared to the subcutaneous.

1.2.3 Importance of adipose tissue vascularization

Fat expansion requires concomitant neovascularization to enable correct delivery of oxygen and nutrients [55]. It has been proposed that the expansion of adipose tissue mass during the progression of obesity may lead to a relative oxygen deficit because angiogenesis is insufficient to maintain normoxia in the adipose tissue depots [56]. It was demonstrated in humans that adipose tissue blood flow decreases in obese compared to lean subjects, in agreement with a reduced vascularization of the tissue during obesity [57]. Homeostasis among adipocytes, immune cells and adipose stromal cells is controlled by several pro-angiogenic factors as FGF, VEGF or HGF. FGF2 (fibroblast growth factor 2) is the prototype member of a 13 members family that are heparin-binding growth factors [58]. In vitro FGF2 is a potent mitogen able to induce cell differentiation, and induces an angiogenic phenotype characterized by increased proliferation, migration, proteinase production and expression of specific integrins [59]. VEGFα (vascular endothelial growth factor α) is the prototype of the VEGF family and, through the binding of its receptors (VEGFR-1 and KDR), induces proliferation, migration and survival of endothelial cells, capillary morphogenesis and vascular permeability [60]. Mice on HFD with VEGF deletion have reduced adipose vascular density and show adipose tissue hypoxia, apoptosis, inflammation and metabolic defects (insulin resistance, increase total cholesterol and liver triglycerides). In contrast, the overexpression of VEGFα, utilizing an inducible adipose tissue-specific VEGFα overexpression model, leads to increase adipose vasculature and reduced hypoxia [61]. The latter changes are sufficient to counteract the established compromising effect of HFD on the metabolism, indicating that metabolic misbalance is reversible by adipose function. In some human studies, it was shown that reducing blood supply in obese adipose tissue was associated with beneficial effects and low incidence of complications [62], while the treatment of obese subjects with a

proapoptotic peptide, which targeted specifically white adipose tissue, resulted in a regression of metabolic anomalies [63]. Similar results were obtained in a mouse model genetically obese where the inhibition of angiogenesis cause weight loss and amelioration of the metabolic profile [64]. All together these observations suggest that at early stages, increase angiogenesis is beneficial for the adipose tissue because protects the tissue from hypoxia and adipocytes apoptosis, while at late stages both induction of vascularization and its inhibition can have beneficial effects; indeed, decreasing angiogenesis may promote apoptosis-mediated elimination of stressed adipocytes and consequently the regression of adiposity, on the other hand, increasing angiogenesis at later stages would alleviate adipose tissue inflammation [65] (***Figure 3***).

Angiogenetic factors are highly interconnected, and in particular FGF2 and VEGF mutually potentiate their angiogenetic effect. The addition of recombinant FGF-2 to endothelial cells in vitro or is induction results in increased VEGF expression. Furthermore, the use of neutralizing monoclonal antibodies to VEGF cause an inhibition of FGF-2-induced endothelial cell proliferation [66], the same effect was observed using blocking antibodies against VEGFR-1 [67]. Taken together these results indicate that VEGFR1 activation and VEGF action are required for FGF2-induced angiogenesis. VEGF as shown to have a possible role even in the recruitment of M2 alternatively activated macrophages. In fact, in THP1 cells, human monocytes cell line, the addiction of VEGF induces enhanced macrophages migration and induced M1 macrophages to shift to an M2 phenotype [68].

1.3 ANIMAL MODELS OF OBESITY

The use of animal models helps elucidating the molecular mechanism intrinsic of obesity and the development of new drugs. The most used animal for the study of obesity is the mouse, because has similar genetics and development. Mice have advantages compared to other animals used for research purposes. In fact, mice are small, easy to handle, and are cheap to maintain. There exist two ways to study obesity in animal models: the use of genetically modified animals or the use of high fat diet induced obesity.

1.3.1 Genetically obese mouse models

There are two animal models of obesity very well characterized due to spontaneous mutations that cause defect in the leptin-signalling pathway in the hypothalamus, the ob/ob mouse and db/db mouse. Leptin is mainly synthetized in the white adipocytes, is directly connected to body fat and to the amount of stored triglycerides; leptin helps to regulate energy balance by inhibiting hunger at the central level. Ob/ob mice are characterized by a single-base mutation in the leptin gene (ob gene) that lead to the synthesis of a premature form of leptin which is not bioactive [69]. In ob/ob mice the lack of leptin cause early-onset obesity associated with hyperphagia, reduced energy expenditure and hypothermia. This is one of the few forms of obesity that can be cured, giving exogenous leptin. Instead, db/db mice present a mutation in the leptin receptor, they are characterized by a marked hyperglycemia and they are resistant to leptin [70, 71]. Another animal model of obesity is the s/s mouse, a genetically engineered animal model, carriers of a mutation that specifically disrupts the transcription factor STAT3, which mediates leptin's effect on energy metabolism through melanocortin signaling [72, 73].

Linked to the downstream signalling of leptin there are different animal models of obesity. Leptin has different targets as proopiomelanocortin (POMC). POMC is the precursor of several bioactive peptides as α-melanocyte-stimulating hormone (α-MSH) which is a potent anorexigenic neuropeptide that reduces eating and increases energy expenditure acting on melanocortin receptor, Mc3r and Mc4r. POMC KO mice are characterized by severe obesity and heterozygous developed an intermediate phenotype. Another gene related to the leptin pathway is the agouti gene. Agouti gene is the first obesity gene to have been characterized at molecular level in mice [74]. This mutation caused an ectopic agouti gene expression instead of a transiently expression in hair follicles. The expression of agouti in the hypothalamus inhibits Mc4r functions, leading to obesity. Mc4r is normally expressed in hypothalamus where it plays a key role in the regulation of feeding and metabolism and is normally antagonized by agouti-related protein (AgRP); in agouti mice, agouti protein in the hypothalamus mimic AgRP binding and inhibiting Mc4r. Homozygous expression of this spontaneous mutation is lethal, while the heterozygous usually develop obesity within the first few months of life and also type II diabetes, hyperleptinemia, increased linear growth and infertility. Transgenic mice that overexpress agouti gene in adipose tissue have a higher body weight than non-transgenic mice with a similar food intake. Therefore, the increase fat mass may be the result of altered energy expenditure [75]. Agouti mice have increased levels of fatty acid synthetase (FAS) and stearoyl-CoA desaturase (SCD) [76]. The double knock-out mouse for POMC and AgRP has a similar phenotype and degree of obesity compared to POMC KO [77]. Targeted deletion of Mc3r gene also results in a late-onset obesity phenotype, but regulation of appetite and metabolism appear to be intact [78].

1.3.2 Diet-induced obesity model

Increase obesity in humans, apart from rare genetic mutations, is related to an excess of dietary fat intake. In human a high-fat diet with ≥30% of energy from fat induce obesity [79, 80]. Similarly, in mouse a positive relationship between the level of fat in the diet and body weight or fat gain has been reported; for this reason, the mouse model of high-fat diet induced obesity is largely used to study obesity. It is usually used a high fat diet containing 30-78% of kcal deriving from fat [81]. The use of a high-carbohydrate and low-fat diet is not efficient to induce obesity as the high-fat low-carbohydrate diet. The use of high-fed diet induce obesity can be advantageous for the study of different factors related to obesity as food intake, glucose homeostasis, insulin resistance and energy expenditure or they can be used to test the efficacy of new compounds for the treatment of obesity. Some mouse strains are more suitable and responsive to a diet-induced obesity. Strains as the C57BL/6J and C57BL/6NTac have a robust response to diet-induced obesity, while for example BALB/c is more resistant. Other factors can affect the response to diet-induced obesity. The number of animal per cage is important, as too many animals per cage tent to show more variable weight gain for the presence of a dominant mouse eating more food compared to the others, while housing only one animal per cage has been shown to gain weight less rapidly. The age at which the animals start the diet regimen is important. Usually for these types of experiments are used 6 to 10 weeks old mice, because young mice and old mice respond to HFD in a different way. The environment is as well important, as some reports have showed that in germ-free condition mice are more resistant to diet-induced obesity.

2. IMMUNITY

During obesity immunity is implicated in the maintenance of the chronic low-grade inflammation. Physiologically the immune system protects the body from neutralizing pathogens like bacteria, virus, parasites and fungi, it can recognize harmful substances and eliminate cell that escape their fate during illness, as for some cancerous cells, but when the immune response is uncontrolled it cause chronic inflammation that is harmful to health.

Immunity can be divided in two main branches: innate immunity and adaptive immunity. The innate immune system is the first line of defence and plays a crucial part in the initiation and subsequent direction of the adaptive immune responses. Adaptive immune cells help the innate counterparts in the elimination of foreign organisms by the recognition of specific "non-self" antigens processed by antigen presenting cells of the innate immunity, generating a response that it is tailored to an efficient elimination of pathogens with the production of specific cytokines and antibodies, and developing an immunological memory through memory B cells and memory T cells which are, able to rouse a rapid response during a second inflammatory response of the same pathogen.

2.1 INNATE IMMUNITY

Innate immunity depends upon both hematopoietic (mast cell, monocytes, macrophages, neutrophils, eosinophils, basophils, dendritic cells, natural killer cells) and non-hematopoietic cells (epithelial cells of the respiratory and gastrointestinal tract). In addition to a cellular component, in the innate immune responses have a fundamental role a humoral component and molecules known as cellular pattern recognition receptors (PRRs). PRRs are

able to recognize microbial components essential for the survival of the microorganism, known as pathogen associated molecular patterns (PAMPs), they are constitutively expressed by the host and independently from the immunological memory. Specific PAMPs are identified by specific PRRs and lead to the activation of distinct signalling pathways, these molecular mechanisms are highly preserved among species [82]. Examples of PRRs are C-type lectin receptors (CLRs), expressed by macrophages and dendritic cell where they mediate the phagocytoses and antigen presentation; it was shown that CLRs are able to modify Toll-like receptors (TLRs) activation of dendritic cells and drive immune responses by altering cytokine production. Other members of the PRRs family are scavenger receptors (e.g. CD36), surface glycoproteins that bind a broad range of ligand as LDL particles or lipopolysaccharides (LPS); complement receptors, in particular complement receptor 3 (CR3); toll-like receptors (TLRs), a family of ten elements and type-1 transmembrane proteins with leucine-reach repeat motifs implicated in the recognition of different types of PAMPs [83].

The humoral arm is composed by members of the complement cascade and soluble pattern recognition molecules (PMRs). Extracellular soluble PMRs represent the functional ancestor of antibodies and play a crucial role in the discrimination among self, non-self and modified-self. Furthermore, evidences were proven of a participation of soluble PMR in the regulation of inflammatory response and of their interaction with the cellular arm of the innate immune system [84]. Extracellular soluble PMRs is a big class of molecules, which comprises collectins, ficolins and pentraxins. Collectins are a family of defense lectins collagenous calcium-dependent, that bind preferentially monosaccharide units of the mannose type, they can interact with host cell receptors and facilitating microbial clearance through aggregation and complement activation [85]. Ficolins contain both a collagen-like and

fibrinogen-like domain and recognize carbohydrate molecules on pathogens, apoptotic and necrotic cells leading to the activation of the lectin pathway of complement or inducing a primitive phagocytosis driven by opsonization thus limiting the infection spread [86]. Pentraxins are a superfamily of highly conserved molecules, sharing a so-called *pentraxin signature* at the C-terminal domain characterized by an 8 conserved amino acids sequence (His-x-Cys-x-Ser/Thr-Trp-x-Ser, where "x" represents any amino acid) [87]. Pentraxins are divide in two groups based on their structure: long pentraxins and short pentraxins. Pentraxin 3 (PTX3) is the prototypic long pentraxin, while C-reactive protein (CRP) and the serum amyloid P-component (SAP) are the most well characterized short pentraxins.

2.2 PENTRAXIN 3

Pentraxin 3 (PTX3) is a homo-octameric secreted glycoprotein which shares the C-terminal domain with CRP and serum amyloid protein (SAP) (both short pentraxins), and possesses a unique and unrelated N-terminal domain, which accounts for PTX3-specific functions [88]. PTX3 was firstly identified in the 1990s as cytokine-inducible gene, it was identified as an IL-1 inducible gene in endothelial cells [88], and as a TNFα inducible gene in fibroblast [89].

2.2.1 PTX3 gene and protein structure

Human and murine PTX3 gene present the same organisation [90] and they display 92% amino acids conservation [91]. PTX3 gene is located on chromosome 3 (q22-25) and it is composed by three exons: the first encode for the signal peptide (17 amino acids), the second for the N-terminal domain

(from amino acid 18 to 179), while the third exon (amino acids 179-381), which correspond to the second exon of short pentraxins, encode for the C-terminal domain containing the pentraxin signature (***Figure 4***). In the human and murine promoters were found several enhancer-binding sites, for instance, binding elements for activator protein-1 (AP-1), which is responsible for the basal transcription of PX3, and nuclear factor kappa B (NF-κB) [92], that is involved in the transcriptional activation under inflammatory conditions. Unlike the human gene, murine PTX3 gene possesses multiple NF-IL-6 binding sites, while the human gene only one, and a greater number of transcriptional elements.

PTX3 is a multimeric glycoprotein of 340 kDa octameric protein, made from two tetramers and each identical protomer is held together by intra- and inter-chain disulphide bonds [93] [94] [95]. The N-terminal region assume a secondary structure forming four α-helices, while the C-terminal domain adopts a β-jelly roll topology and contains a single N-glycosylation site (Asn220), which is occupied by different complex type of oligosaccharides depending on the inflammatory cells and stimuli that induce PTX3 production. For instance, the status of glycosylation of PTX3 influences the ability of PTX3 to bind complement component 1q (C1q), in fact, the desialylation or complete deglycosylation of the protein increase its binding to C1q[96]. PTX3 complex as octamer shows grater activity, in particular PTX3 multimeric organization was shown to be essential for cumulus oophorous matrix assembly and stabilization [95].

2.2.2 ***PTX3 production***

PTX3 can be produced in different cell types (dendritic cells, neutrophils, adipocytes, endothelial cells, epithelial cells, smooth muscle cells, fibroblasts

and macrophages) and induced by various stimuli (***Figure 5***), as LPS, TNF and IL1β. Other factors can modulate the LPS-induced production of PTX3: dexamethasone, IL-4 and prostaglandin E inhibit PTX3 production, while IL-10 amplifies its expression [97]. Among cells of the myeloid lineage PTX3 is mainly produced by dendritic cells [91] after the stimulation with IL-10, CD40 and IL-1β, while it's inhibited by INFγ. Neutrophils are the only type of cells able to produce PTX3 in high amount and store it in specific granules released in response to TLR engagement by pathogens [98]. In adipocytes PTX3 is induced by TNF, his expression decreases after differentiation of the adipocytes, but it was observed an increase PTX3 mRNA expression in adipose tissue of obese and diabetic-obese mice as compared to WT [99]. TNF is an activator of PTX3 expression also in epithelial cells chondrocytes and brain cells. Endothelial cells from vasculature involved in atherosclerotic processes produced PTX3 after the interaction with oxidised LDL particles (ox-LDL) through the activation of NF-κB exerting an atherogenic function [100]. On the other hand, it was also observed a production of PTX3 in endothelial cells induced by HDL particles with the activation of one other intracellular pathway driven by PI3K/Akt exerting an anti-inflammatory and protective role.

2.2.3 PTX3 ligands

PTX3 plays a critical non-redundant role in the regulation of the humoral arm of innate immunity. The best described ligand of PTX3 is the complement component C1q [93]. Soluble or immobilized PTX3 binds C1q: when the interaction occurs with PTX3 immobilized on the surface of microbes it lead to the activation of the classical pathway of complement activation, while the interaction with soluble PTX3 mediates a dose-dependent inhibition of C1q haemolytic activity [101]. The interaction between PTX3 and C1q is Ca-

independent, differently from short pentraxins, but it is highly influenced by PTX3 glycosylation, indeed the removal of the glycosidic portion potentiates the binding and the activation of the pathway [96]. Complement activation is a cascade of subsequent activation of molecules after their cleavage by proteases which results in C3 and C4 deposition. The dual ability of PTX3 to bind C1q in the fluid phase or when it is immobilized suggests that PTX3 supports the clearance of microbes when immobilized, while protect against unwanted complement overactivation in the fluid phase [102]. PTX3 interacts directly further with the lectin pathways of complement, binding ficolin-1 [103] and ficolin-2 [104] attached to *Aspergillus fumigatus*, this interaction is Ca-dependent and occurs through their fibrinogen-like domain. PTX3 and ficolin1 or 2 interactions at the cell membrane of pathogens amplify synergistically complement- activated innate immune-responses. PTX3 can regulate furthermore the alternative pathway of complement activation thanks to its ability to bind to factor H [105], enhancing its deposition on apoptotic cells, and to C4b-binding protein (C4BP), binding C4BP, PTX3 inhibit its inhibitory activity on complement activation [106]. The activation of the complement alternative pathway, after PTX3 binding to factor H, can protect them against complement-mediated lysis [107], promoting instead their clearance in an anti-inflammatory context. PTX3 binds also the Fibroblast Growth Factor 2 (FGF2) [108]. FGF2 is a strong angiogenic factor that stimulates smooth muscle cells growth, repair [109], neovascularization during atherosclerosis, wound healing, and tumor growth [110]. PTX3 contains an FGF-2 binding domain in its N-terminal portion [111]; the binding of PTX3 to FGF2 lead to EC proliferation FGF2-dependent and angiogenesis inhibition [108]. Other identified ligands of PTX3 includes P-selectin, an adhesion molecule, and extracellular matrix proteins as TNF-stimulated gene 6.

2.2.4 *Relevance in humans: PTX3 and genetic variants*

PTX3 genetic variants have been studied in the context of different pathologies, to understand whether PTX3 SNPs present could associate with disease outcome. Three single nucleotide polymorphism (SNPs) (rs2305619, rs3816527 and rs1840680) have been studied in a multicentric association study focused on the relation between these SNP and plasma levels of the protein and the risk of AMI [112]. The analysis showed that, even if the SNPs and corresponding haplotypes were associated with different levels of PTX3 in the blood, they didn't influence directly the risk of AMI, but all-cause mortality after AMI. The same SNPs and haplotype were evaluated in association with pulmonary tuberculosis risk in West Africans [113]. Here, rs2305619 and rs1840680 and a PTX3 haplotype ("G-A-G" haplotype, resulting from the combination of rs2305619, rs3816527, rs1840680), were significantly less frequent in subject affected by tuberculosis. This haplotype association was also identified evaluating the impact of PTX3 genetic variants in the risk of Pseudomonas Aeruginosa (PA) airway colonization in cystic fibrosis patients; "G-A-G" haplotype was more common in non-PA colonized patients, while the "C-A-C" haplotype, for the same SNPs, was more common in PA patients [114].

In one other study, in the contest of hematopoietic stem cell transplantation, it was shown how the recipient of the hematopoietic stem cells from donor with the "C-A-C" haplotype, here indicated as h2/h2 haplotype, were more susceptible to develop invasive aspergillosis [115]. This haplotype was furthermore associated with a defect in PTX3 expression in broncho-alveolar-lavage fluid and neutropenia and lower, but not significant levels of plasmatic PTX3 levels. The increase susceptibility to aspergillosis in this case could be related to the reduced opsonization of the microorganism because of the

reduced amount of PTX3 in the site of infection, as exogenous addiction of PTX3 to PTX3-deficient neutrophils in vitro restored the functional deficit [115].

2.3 OTHER PENTRAXINS

2.3.1 Long Pentraxins

The long pentraxins family include not only PTX3 but include other proteins such as neural pentraxin 1 (NP1) and 2 (NP2), guinea pig apexin and PTX4. NP2 is a neural gene that plays a role in excitatory synaptogenesis. It was shown that NP2 together with NP1 forms highly organized complexes regulating the latent synaptogenic activity of NP1 [116]. NP2 plays furthermore a role in the clustering of AMPA-type glutamate receptors at established synapses, resulting in non-apoptotic cell death of dopaminergic nerve cells. Diseases associated with NP2 include narcolepsy and Kearns-Sayre Syndrome, characterized by progressive weakness or paralysis of the eye muscles. NP1 has been implicated in hypoxia-ischemia and amyloid β-induced neural death [117]. PTX4, as for the other long pentraxins, is characterized by an unrelated N-terminal domain and a C-terminal pentraxin domain, and it is well conserved from mammals to lower vertebrates, but it shows a unique pattern of mRNA expression that differs from other members of the family and it doesn't act as an acute phase gene even if produced also by the liver [118].

2.3.2 ***Short Pentraxins***

CRP and SAP are the two components of the short pentraxins class and are 25 kDa proteins characterized by a common quaternary structure organized in five or ten identical subunits arranged in a pentameric radial symmetry [119]. CRP was the first short pentraxin identified in 1930 [119], subsequently human SAP was identified, which has a 51% sequence identity to human CRP. The human CRP gene localized on chromosome 1 and comprehends two exons, encoding for the leader peptide (amino acids 1-18), the two initial amino acids of the mature peptide (amino acids 19-20) and C-terminal pentraxin-like domain (amino acids 21-224). CRP is the main acute-phase molecule in humans, its levels can increase 100 times in several pathological conditions. SAP, on the other hand, is the main acute-phase molecule in mouse and it remain invariant, around 30-50 mg/dL in humans. Differently from PTX3, that is produced by many cell types, CRP and SAP are produced by hepatocytes upon IL-6 and IL-1β stimulation [120]. Short pentraxins recognize several ligands present on microbes and apoptotic cells in a calcium-dependent manner, playing a fundamental role in humoral innate immunity. CRP bind apoptotic cells and pathogens through phosphatidylcholine moieties that are exposed on their cell membrane, activating the classical pathway of complement and promoting the opsonization and phagocytosis process [121]. CRP, as PTX3, is able to activate and regulate not only the classical [122] pathway of complement activation but also the non-classical pathway [123], and regulate factor H activation [124]; at the contrary SAP is able to activate only the classical pathway.

3. ROLE OF PTX3 IN PATHOLOGIES

3.1 PTX3 AND INFECTIONS

First studies on PTX3 activity and function recognized the ability of PTX3 to bind several pathogens, as *Aspergillus fumigatus*, *Pseudomonas Aeruginosa*, *Staphylococcus Aureus*, and its involvement in the resistance at some viral infections. Using transgenic mice lacking PTX3 it was shown that PTX3 plays a non-redundant role in innate resistance to infections caused by certain microorganisms thanks to complement engagement. In PTX3 KO mice was find a higher susceptibility to conidia, because of defects in the ability of neutrophils, macrophages and dendritic cell to recognize and kill it, and this was associated also to a low protective T helper 1 antifungal response; this susceptibility to conidia was restored adding recombinant PTX3 [94, 125]. The mechanism underline this recognition and phagocytosis of conidia by neutrophils, starts with the opsonization of conidia by PTX3, then neutrophils through Fcγ receptor II bind to PTX3 and complement dependent mechanism begins [126]. Treatment with recombinant PTX3 is also able to exert a therapeutic activity in chronic lung infections by *Pseudomonas aeruginosa*, a major cause of mortality and morbidity in cystic fibrosis patients, possibly due to, as established in animal models infected by *P. aeruginosa*, an enhanced clearance of bacteria from the lung and reduced production of pro-inflammatory cytokines and chemokines in the airways [127]. As anticipated, PTX3 as a role in viral infections too: PTX3 bind both human and murine cytomegalovirus reducing the viral entry and infectivity [128]; PTX3 reduces the susceptibility to murine hepatitis virus 1 pulmonary infection accelerating viral clearance, reducing neutrophil influx an ameliorating lung injury [129]. PTX3 is further an inhibitor of influenza A virus (IAV), as its sialylated glycan

is recognized by the hemagglutinin of susceptible strain of IAV leading to inhibition of virus-induced hemagglutination and neutralization of virus infectivity [130].

3.2 PTX3 IN CARDIOVASCULAR DISEASES

In man and mouse PTX3 behaves as an acute phase molecule, its plasma levels rapidly increase during sepsis, endotoxin shock and other inflammatory and infectious conditions. For instance, PTX3 plasma levels are higher in patients with chronic heart failure compare to healthy controls, and they increase with the severity of the pathology [131]. The possibility to use PTX3 as a prognostic biomarker for CVD death is due to its rapid increase after MI [132], as it peak after 7.5 hours from the events while CRP only after 50 hours, it is a more specific marker also for acute coronary syndrome compared to NAP-2 and cardiac troponin I in patients with unstable angina pectoris, NSTEMI and STEMI [133]. Patients with unstable angina, eligible for coronary intervention, exhibit PTX3 levels three times higher than the normal range [134]. Among cardiovascular diseases, PTX3 was largely studied in atherosclerosis. Atherosclerosis is characterized by an accumulation of cholesterol and oxidized LDL particles in the intima of arteries and the formation of plaques rich in cholesterol that cause at later stages the occlusion of the arteries with harmful effects. In atherosclerotic lesions major producers of PTX3 are endothelial cells and macrophages. Atherogenic lipoproteins in the plaque can induce the expression of inflammatory cytokines as IL-1 and IL-6 [135, 136], contributing to the recruitment of immune cells that perpetrate the state of chronic low-grade inflammation typical of the pathology. Mice lacking PTX3 on an ApoE background and on high fat diet, shown increased atherosclerosis. In particular, it was observed an increase in macrophage infiltration and lesions dimensions,

and an increase of cytokines, chemokines and adhesion molecules expression in the vascular wall [137], suggesting a protective role of PTX3 in atherosclerosis. Immunohistochemical staining reveal PTX3 deposition in advanced atherosclerotic lesions. During this scenario, PTX3 may limit atherosclerosis due to its ability to inhibit FGF2, which triggers smooth muscle cells migration and proliferation [138], or it may contribute to the clearance of lipid-loaded macrophages and foam cells by dendritic cells [139]. PTX3 non-redundant protective role has been demonstrated for myocardial infarction experimental models where mice lacking PTX3 shown a greater no-reflow area [140, 141] . In this contest PTX3 deficiency cause an increase of C3 deposition in the infarct area, and the interaction between PTX3 and factor H and is deposition on PTX3-coated surfaces, could represent a mechanism of protection from damage caused by an uncontrolled activation of the complement classical pathway [142]. In ischemic stroke PTX3 seams to exert a protective role, as PTX3 KO mice have a compromise blood-brain barrier and resolution of brain edema after ischemic event [143], but clinical results are in contrast, in fact PTX3 was observed to have a positive correlation with stroke severity and predict mortality after ischemic stroke [144, 145].

3.3 PTX3 DURING OBESITY

PTX3 is produced both in pre-adipocytes and mature adipocytes, both in visceral and subcutaneous adipose tissue [146], and its expression in adipose tissue is induced by TNF [99]. The current role of PTX3 in obesity is unclear. Most of the studies have been performed in animal models of obesity and studies in humans of correlation among PTX3 plasma levels and anthropometric parameters related to obesity have no clear conclusions, with some of them highlighted a positive correlation [99, 146-149], others a negative

correlation [150-154], or no correlations [155]. In a study including metabolic syndrome subjects with subclinical atherosclerosis there was evidence of a positive correlation between PTX3 and MetS, the correlation was positive also with triglycerides and negative with HDL [156]. A positive correlation was observed in other studies evaluating obese subjects. PTX3 plasma levels were found higher in obese subjects compared to the non-obese control group [148] and PTX3 expression from visceral adipose tissue was positively correlated with BMI, triglycerides, CRP, fibrinogen and adiponectin, LDL/HDL ratio and TNFα expression [146]. On the contrary, certain population studies identify a negative correlation: in a study conducted in a Japanese population of 2619 patient, plasma PTX3 levels were significantly lower in subjects with metabolic syndrome and correlate inversely with triglycerides and BMI; Ogawa T. et al observed an inverse correlation between PTX3 plasma levels and BMI, waist circumference, triglycerides, MetS and IL6 in 226 enrolled apparently healthy man [151]; similar results were observed in a study on a Sweden male population [153]. In animal models of obesity Abderrahim-Ferkoune et al [99], evaluating directly mRNA levels of PTX3 in adipose tissue, observed an increase of PTX3 transcript in ob/ob and db/db mice compared to control lean mice, while Miyaki et al [152] observed the opposite in TSOD mice, a model of diabetic-obese mice. To summarize current findings on the role of PTX3 in obesity and MetS, it is unclear whether PTX3 behaves as a bystander or actively participates to obesity-related inflammation, so additional studies need to be performed to clarify the role of PTX3 in obesity.

For what concern CRP, it correlates positively with obesity [157], while it doesn't differ between non-obese and metabolic syndrome affected but non-obese subjects [158], indicating a state of chronic low-grade inflammation in obese subjects.

3.4 PTX3 IN TUMORS

Inflammation plays a central role in tumor development and growth [159], therefore, given the role of PTX3 in immunity and its numerous functions, it is conceivable a possible role for this molecule in cancer. As for the role of PTX3 in obesity, the role of PTX3 in cancer has not been fully elucidated and it seems to have a dual role. In some cases PTX3 overexpression has been described as a bad prognostic marker (e.g. in pancreatic cancer [160] and in gastric cancer [161]), while other type of tumor it is considered an oncosuppressor. In melanoma it has an anti-tumor effects thanks to its ability to inhibit FGF2-induced proliferation, angiogenesis, epithelial-mesenchymal transition and metastatic potential of tumor cells [162]. PTX3 exert an anti-tumor effect also in multiple myeloma where it acts inhibiting FGF-mediated angiogenesis and inducing tumor cell death through the inhibition of plasma cell/bone marrow stroma cell cross-talk [163]. In mesenchymal and epithelial carcinoma, the oncosuppressive activity carried out by PTX3 is linked to the inhibition of complement-dependent tumor-promoting inflammation, in fact PTX3 deficient animal in an induced-model of mesenchymal and epithelial carcinoma are characterized by enhanced tumor burden, macrophage infiltration, angiogenesis and pro-inflammatory cytokine production [164]. Take advantage of PTX3 ability to inhibit FGF2 and the specificity of the binding, in the last few years, it was taken into account the possibility to create small molecules mimicking PTX3, in order to block angiogenesis and proliferation in tumor ligand-dependent FGFR activation. Ronca R. et al [163] identified the ARPCA sequence in PTX3, that correspond to the minimal FGF2-binding peptide able to bind FGF2 and prevent the binding whit its receptor. This finding gave the basis for the design of a pharmacophore model of the site of interaction between PTX3 an FGF2 leading to the identification of NSC12, a chemical ARPCA mimic. This molecule compared to common FGFR inhibitors, as

monoclonal antibodies and FGFR-derived decoy molecules acting as FGF traps, has less limitation because of its non-proteinaceous origin. NSC12 represents the leading compound for the development of orally active small molecules for therapeutic purposes in cancer. Data from phase I and II clinical trials indicate that the inhibition of the FGF/FGFR system may show anti-tumor activity as expected.

One interesting discovery related to PTX3 in cancer is that, in different type of cancers, from mesenchymal and epithelial human cancers [164] to esophageal squamous cell carcinoma [165], PTX3 gene present a different methylation-dependent silencing. In colorectal cancer it was detected a different pattern of methylation in different stages of the pathology. In early stages, enhancer-1 in PTX3 gene is silenced by methylation, while enhancer-2 methylation increases during carcinoma progression, suggesting that hypermethylation is involved in the onset and progression of colorectal cancer [166].

Aim of the project

Obesity is an epidemic that affects millions of people all over the world and is in continuous increase. This condition is characterized by fat accumulation at the level of the adipose tissue, mainly the visceral one, unleashing a state of chronic inflammation associated frequently with diabetes, hypertension and atherosclerosis.

Although PTX3 is produced by human adipocytes in visceral and subcutaneous adipose tissue [146] [167], the correlation between its levels and the onset and progression of obesity and MetS is less clear. Some authors highlighted a direct correlation between PTX3 plasma levels and obesity [148] or MetS [147], while others reported a neutral or an inverse correlation [150] [151]. Similarly, variable findings were reported in animal models of metabolic dysfunction: genetically obese (ob/ob) and obese-diabetic (db/db) mice showed higher levels of PTX3 mRNA in VAT compared to lean mice, an effect consistent with increased levels of TNFα [99]; whereas in Tsumura Suzuki obese-diabetic (TSOD) mice, a model of spontaneous type 2 diabetes [168], adipose tissue levels of PTX3 mRNA were found lower as compared to lean controls [152].

As PTX3 sits at the crossroad between innate immunity, inflammation and obesity [169] [87] [170], this project aims to characterize the role of PTX3 in obesity, thus identifying a therapeutic target for the cure of obesity and associated pathologies.

For this aim, we profiled the immuno-inflammatory and metabolic response to an obesogenic diet of PTX3 KO mice compared to WT littermates and investigated in humans the impact of a *PTX3* haplotype [115], on ectopic fat deposition and metabolic status to clarify whether PTX3 behaves as a bystander or actively participates to obesity-related inflammation.

Materials and Methods

1. Animal models

Male mice WT and PTX3 KO littermates on the C57BL/6 genetic background were bred in house and generated as in detail described previously [94]. Homozygous mutant mice display female subfertility due to abnormalities of the cumulus oophorus and are susceptible to invasive pulmonary aspergillosis associated with defective recognition of conidia by alveolar macrophages and dendritic cells and impaired induction of adaptive type 2 responses (*http://www.informatics.jax.org/marker/MGI:104641*). C57BL/6 WT mice were provided by Charles River Italy. Mice were kept in a temperature-controlled environment (20 ± 2°C, 50 ± 5% relative humidity) with a 12-hour light/dark cycle in an air-conditioned room and free access to food and water.

2. Genotyping

Animals were genotyped after the isolation of DNA from ear biopsy. Briefly, biopsy are incubated in 500 µl of lysis buffer (0.5% Sodium dodecyl sulphate, 0.2 M NaCl, 50 mM TrisHCl pH 8, 4 mM EDTA) with proteinase k (0.25 mg 37.7 mAnson U/mg, AppliChem) overnight at 56°C, than after centrifugation, 13000 rpm for 3 minutes, at the supernatant, is added 500 µl of phenol:chloroform:isoamyl alcohol 25:24:1. After another brief centrifugation, 13000 rpm for 5 minutes, the aqueous upper phase containing the DNA is collected and mix with 800 µl of 95% ethanol. Finally, after spinning samples 13000 rpm for 5 minutes, DNA precipitate at the bottom of the eppendorf, and after evaporation of the leftover ethanol DNA is resuspended in H_2O. Animals genotype was assessed by Polymerase Chain Reaction (PCR) as indicated in the protocol in ***Table 1***.

3. Diet-induced obesity model

Starting from eight weeks of age, male WT and PTX3 KO mice littermates were randomized in two groups, one fed a standard fat diet (SFD, 10% Kcal from fat, Research diet INC, Cat#D12450H) (***Table 2***), and one a high fat diet (HFD, 45% Kcal from fat, Research diet INC, Cat#D12451) (***Table 3***). Food intake and weight gain were measure weakly. At 10 and 20 weeks were performed glucose and insulin tolerance test, and fat deposition quantification through magnetic resonance for imaging. Mice were sacrificed at 20 weeks, liver, blood, visceral, subcutaneous and brown adipose tissue were collected and weighted, and an immunophenotypic analysis of the tissues was performed by flow cytometry, gene expression analysis and protein quantification (***Figure 6***). All animal procedures performed conform to the guidelines from directive 2010/63/EU of the European Parliament on the protection of animals used for scientific purposes and were approved by the Ethical Committee (Progetto di Ricerca 2012/02, Autorizzazione Ministeriale 811/2017).

4. Magnetic resonance for imaging (MRI)

MRI was used to evaluate VAT, SCAT and BAT depots in WT and PTX3 KO mice after 10 weeks and 20 weeks of HFD regimen. For this procedure, mice were anaesthetized with 2% isoflurane. Consecutive photos at the level of shoulder blades, chest and abdomen of each mouse were acquired and subsequently analysed with Photoshop® software for the quantification of adipose tissue deposition.

5. Glucose and Insulin tolerance test

Intraperitoneal glucose tolerance test (IP-GTT) and insulin tolerance test (ITT) were used to measure plasmatic clearance of glucose after intra-peritoneal injection of glucose or insulin respectively after 10 and 20 weeks of HFD or SFD. Briefly, for IP-GTT test, animals were fasted overnight (approximately 14 hours), then blood glucose levels at fasting and after 15, 30, 60, 90, 120 minutes from injection of glucose solution (20% w/v in PBS, 2 mg per grams of body weight) were measured with a glucometer (ONE-TOUCH Ultra glucometer). For ITT, the animals were fasted for 4 hours. Glucose plasma levels were measured at fasting and after 15, 30, 60, 90, 120 minutes from injection of human recombinant insulin (1 mU per gram of body weight, Humulin R100 Ul/mL).

6. Samples preparation for immunophenotyping by flow cytometry

Fresh collected blood was stained after the lysis of red blood cells with ACK solution ($KHCO_3$ 10mM, NH_4Cl 150 mM, EDTA 0.1 mM) for 10 minutes at room temperature. Bone marrow was taken from femoral bones, flushing bone marrow out of the bone with a syringe with PBS, then it was obtained a cell suspension and red blood cells were lysed using ACK solution. Fresh visceral and subcutaneous adipose tissues were placed on ice in a 6 well plate and cut in small pieces in 2 mL of PBS 5% BSA solution, then collagenase (200 mg/mL final concentration; NB4 standard grade, Serva) and $CaCl_2$ (5 mM final concentration) were added and samples were incubated at 37°C for 40 minutes under agitation. Samples were then top up with MACS (PBS, 2% FCS, 2 mM EDTA) and filtered on a sterile bandage and subsequently on a 100 μm and 70 μm cells strainer. After the lysis of red blood cells with ACK for 5 minutes on

ice, samples were washed, spin and resuspended in 50 μL of antibodies mix (Supplementary Table 1). All flow cytometry antibodies were used at 1:100 dilutions unless otherwise specified, optimal antibody concentrations for staining were calculated based on manufacturer instructions. For immunophenotyping a cell suspension containing $1x10^6$ cells or 50 μL of blood were acquired with FACS Calibur (BD Bioscience) or Novocyte 3000 (ACEA Biosciences). Cell sorting was performed with FACSAria II flow cytometer (BD Bioscience). Antibodies used are listed in the Supplementary Information (***Table 4***).

7. Blood biochemistry measurements

Blood samples were collected in EDTA tubes by tail vein at 10 weeks and intracardiac puncture at 20 weeks and plasma was separated by centrifugation (8000 rcf for 10 minutes) at 4°C. Total plasma cholesterol and triglycerides were measured from frozen plasma by standard enzymatic techniques using the Cholesterol CP KIT (ABX Pentra, HORIBA Medical) or the triglyceride CP KIT (ABX Pentra, HORIBA Medical). Briefly, for cholesterol quantification it is prepared in 96 wells plate a calibrator curve with serial dilution of cholesterol standard (200 mg/dL, ABX Pentra). 10 μl of samples plasma to be analysed are load in the same plate and then is added to the plate 200 μl of reagent (ABX Pentra Cholesterol CB) per well. The plate is incubated for 15 minutes at 37°C protected from light. The same procedure is used for tryglicerides quantification, using the appropriate standard (200 mg/dL TG standard ABX Pentra) and reagent (ABX Pentra triglycerides CB). After incubation with the reagent, cholesterol and triglyceride concentration were read by spectrophotometer at 490 nm (Bio-Rad iMark microplate reader). Plasma

insulin concentrations were quantified using mouse Ultrasensitive ELISA kit (Mercodia) as indicated by the manufacturer.

PTX3 plasma levels in human blood samples at enrolment were determined as previously described [171] with sandwich ELISA (detection limit 0.1 ng/mL, inter-assay variability from 8% to 10%) developed in-house, by personnel blind to patients' characteristics. Data are reported as ng/mL.

8. Histology

Part of the visceral and subcutaneous adipose tissue were fixed overnight in 4% buffer formalin (Sigma-Aldrich), embedded in paraffin and tissue section (5μm) stained with haematoxylin and eosin (Sigma-Aldrich). 10X images were obtained using a Zeiss Axiovert microscope. Quantification of adipocytes areas was performed using Adobe Photoshop software: manually is selected an area with intact adipocytes covering the 60-80% of the section and then the calculated area (1 pixel = 0.6289 μm) is divided for the number of adipocytes counted in that selected area (at least three independent measurement per mouse). Crown-like structures were counted from 8 visceral sections per mouse (n = 6) by an operator blinded of the genotypes.

9. Real time PCR

Total RNA from cells and visceral adipose tissue was isolated using Nucleo Spin RNA kit (Machery NAGEL) and RNAsi Lipid Tissue Mini kit (QIAGEN), respectively, as indicated in the manufacturer instruction. Adipose tissue homogenization was performed using Tissue Ruptor instrument(Qiagen) and Qiazol contained in the kit. RNA quality and quantity were assessed using

absorption measurements (NanoDrop™ 1000 Spectrophotometer, Thermo Fisher Scientific) and transcribed in cDNA (400 ng RNA) with iScriptTM cDNA synthesis kit (BioRad). Gene expression analysis was done using SYBR Green Supermix (ThermoFisher Scientific) in CFX connect light cycler (BioRad, Cat#1708841). Expression was calculated using the ΔΔCt method (Livak and Schmittgen, 2001) and normalized to a housekeeping gene (*Rpl*, L Ribosomal Protein). Primers for qPCR were designed with the help of online tools (https://www.eurofinsgenomics.eu/). The thermal cycling profile was a two-step amplification (95°C for 5 min, followed by 45 cycles of 95°C for 10 s and 55 °C for 30 s). The sequences of the qPCR Primers are reported in the ***Table 5***.

10. Immunoblotting

Adipose tissue was homogenized in RIPA buffer (0.1% sodium dodecyl sulphate, 0.5% sodium deoxycholate, 1% Nonidet P-40, 150 mM NaCl, and 50mM Tris HCl, pH 8.0, supplemented with protease inhibitors). Tissues were lysed at 4°C for 15 minutes and clarified by centrifugation at 12.000 rpm. Quantification of protein extracted from the tissue was performed using Lowry assay protocol. Briefly, it is prepared a standard curve with different dilution of albumin 1 μg/mL in 5 mL tubes. 5μl of samples are load in other tubes and brought to 200 μL with ddH_2O. Then is added to the tubes 1 mL of solution A:B 50:1 (Solution A: NaOH 0.1 N, $NaHCO_3$ 2%; solution B: $CuSO_4$ 0.5%, sodium potassium tartrate 1%, NaON 0.1 N) for 10 minutes at 37°C. After another incubation with 100 μL of 1:1 Folin:H_2O solution for 30 minutes at 37°C, samples are read by spectrophotometer at 490 nm (Bio-Rad iMark microplate reader). Lysates were separated by SDS-PAGE on a 12% polyacrylamide gel, transferred to nitrocellulose. Nonspecific binding to the membrane were blocked with 1h incubation in milk 5% PBS 0.1% Triton X100. Primary antibody

used are anti-VEGF "Vascular Endothelial Growth Factor" (Biorbyt orb256347), anti-CD31 "Cluster of Differentiation 31" (Cell Signaling 77699) and anti-α Tubulin. Incubation with primary antibodies was performed overnight at 4°C. Secondary antibodies were HRP-conjugated; incubation of the secondary antibodies was performed for 1h at room temperature. HRP activity was identify by enhanced chemiluminescence (Clarity Western ECL, BioRad) and Odyssey Imaging System.

11. Human study – the PLIC cohort

Human data were obtained from samples of the PLIC study (Progressione delle Lesioni Intimali Carotidee). PLIC is a prospective observational study, including a total of 2,606 subjects, representative of the general population residents in northern area of Milan (Italy). The population was followed for up to fifteen years at the Centre for the Study of Atherosclerosis, Bassini Hospital (Cinisello Balsamo, Milan) in order to study predictive value of cardio-metabolic parameters for the evolution and clinical manifestation of atherosclerosis. The study was approved by the Scientific Committee of the Università degli Studi di Milano (Cholesterol and Health: Education, Control and Knowledge – Studio CHECK ((SEFAP/Pr.0003) – reference number Fa-04-Feb-01). Each subject signed the informed consent for the collection of blood samples and clinical data for research purposes. The study was conducted in accordance with the principles of the Declaration of Helsinki. The PLIC population has been extensively described [172-178].

Clinical, familial and pharmacological histories of each individual have been collected. Information on obesity, BMI and waist-to-hip ratio were available as

well. Genetic information on PTX3 polymorphisms was conducted on 1,122 subjects, representative of the entire cohort.

DNA was extracted from blood peripheral blood mononuclear cells (PBMCs), as previously described [174] using QIAGEN DNA Blood Mini Kit (Qiagen), and it was genotyped for three polymorphisms, previously annotated [115] via Taqman allelic discrimination (ThermoFisher): a) rs2305619 (+281A/G) on intron 1 (HapMap MAF=0.500), b) rs1840680 (+1449A/G) on intron 2 (HapMap MAF=0.491) and c) rs3816527 (+734A/C, missense Ala48Asp) on exon 2 (1000Genomes MAF=0.285). Allelic frequencies of all three variants followed Hardy-Weinberg equilibrium. Genetic allele frequencies were identical from +281GG genotype and those from the +1449GG genotype, because of their complete linkage disequilibrium (which was not the case for other genetic forms and those from +734A/C). Thus, the combination of genotypes AA and AG was the reference category accounting for h1/h1 in +281A/G and the combination of genotypes CC and CA was the reference category accounting for h1/h1 in +734C/A. By contrast h2/h2 haplotype included genotypes GG in +281A/G and AA in +734C/A [115]. A table showing the main characteristics of the cohort studied is presented in ***Table 6***.

12. Human study – Anthropometric measurements

Measurements of body composition and regional adipose tissue distribution was performed via Dual Energy X-ray Absorptiometry (DEXA), as previously described [178] using a Lunar iDXA (Ge Healthcare, Madison, WI). Scans were then analysed through enCORE software (version 14.0), in order to set regions of interest for detection and quantification, discriminating among bone mass (calculating density as well), lean and adipose tissue. Android fat was

computed automatically over the android region, a region-of-interest automatically defined by the enCORE software, whose caudal limit is automatically placed at the top of the iliac crest and whose height is set to 20% of the distance from the top of the iliac crest to the base of the skull to define its cephalad limit.

13.Statistical analysis

Statistical analysis was performed using Prism (GraphPad) and SPSS v.23 (IBM Corp., Chicago, IL) for human data. Both mice and human data are expressed as mean ± SEM and a *P* value of less than 0.05 was considered significant (**P*<0.05, ***P*<0.01, ****P*<0.001). For comparison between two groups an unpaired two-sides test with a 95% confidence interval was used. In detail, for groups with more than 7 observations, after checking for the normal distribution of data, a parametric Student's t test was applied, whereas for groups with less than 6 observations or not normally distributed a Mann-Whitney non-parametric test was used, as also indicated in the figure legends. For human data, Mann-Whitney and Kolmogorov-Smirnov non-parametric test were used.

Results

1. Diet-induced obesity model

In order to study the role of PTX3 during obesity, we take advantage of a well-known model of diet-induced obesity. The effects of diet-induced obesity on WT mice compared to a standard-fat diet are shown in ***Figure 7*** to ***Figure 10***. Wild type mice were fed a high fat diet (HFD) or a standard fat diet (SFD) for 20 weeks. As expected, HFD-fed mice showed increased body weight and increased visceral and subcutaneous adipose tissue deposition (***Figure 7***). Moreover HFD-fed mice displayed an impaired glucose tolerance and insulin sensitivity as assessed by GTT and ITT (***Figure 8***). They also presented an increased infiltration of monocytes and macrophages into the visceral adipose tissue (***Figure 9A***) which associated to increased monocyte-chemoattractant protein 1 (*Mcp1*) and *Cd68* mRNA expression (***Figure 9B***). Adipose tissue expansion associates with a worsening of the inflammatory status both locally and systemically [179]. Therefore, we investigated whether plasma levels of PTX3 change during the onset of obesity. In agreement with the increased immune-inflammatory profile, PTX3 plasma levels were significantly increased after 10 and 20 weeks of HFD compared to SFD regimen (***Figure 10***).

2. Effect of diet-induce obesity in *PTX3 KO mice*

This observation prompted us to investigate whether PTX3 plays a causal role or simply reflects the underlying inflammatory response associated to obesity and for this reason we decided to use PTX3 KO mice. WT and PTX3 KO mice were fed up to 20 weeks with HFD or a control diet (SFD). While PTX3 deficiency doesn't affect weight gain in SFD fed mice (***Figure 11A, 11B***), in animals on HFD it was associated with significant reduced weight gain compared to WT (***Figure 11C, 11D***). The difference in the weight gain is not

explicable to a different daily food intake between the two groups on HFD as it was comparable (***Figure 11E***). Differences in weight gain were associated with analysis showing a reduced visceral and subcutaneous adipose tissue deposition at both 10 and 20 weeks of HFD in PTX3 KO mice compared to WT mice (***Figure 12A-C)*** assessed by magnetic resonance imaging (MRI); whereas the amount of brown adipose tissue in the intrascapular area was similar between the two experimental groups (***Figure 12D, 12E***). This phenotype was confirmed at sacrifice, where the amount of VAT and SCAT but not of BAT was significantly reduced in PTX3 KO mice compared to WT mice. Similar weights for liver, pancreas and spleen were also observed (***Figure 13***).

3. Glucose and lipid homeostasis evaluation

The reduced weight gain and fat deposition in PTX3 KO mice, suggest that PTX3 plays a non-redundant role during HFD-induced obesity and brought us to explore whether the phenotype observed might have been the consequence of impaired glucose metabolism. To this end, we measured basal glycemia following overnight fasting and performed an intraperitoneal glucose (IP-GTT) and insulin tolerance test (ITT) after 4 hours fasting in WT and PTX3 KO mice after 10 and 20 weeks of diet. Basal glycemia was similar between WT and PTX3 KO mice following 10-weeks or 20-weeks of HFD (WT 121±10 mg/dL, PTX3 KO 111±9 mg/dL at 10 weeks; WT 145±13 mg/dL, PTX3 KO 130±3 mg/dL at 20 weeks respectively), as were glucose curves over time after IP-GTT (***Figure 14A, 14B***) or ITT (***Figure 14C, 14D***). Likewise, there were no differences in the response to IP-GTT and ITT in the two groups on SFD (***Figure 15A-D***). Lipid profile (cholesterol and triglycerides) was not different between PTX3 KO and WT mice after 20 week-HFD, maintaining only a significant difference in the levels of cholesterol comparing animal on SFD with the group on HFD (***Figure***

16A, 16B). We analysed further insulin and resistin plasmatic concentration in the animals on HFD which result similar between the two groups (***Figure 16C, 16D***).

These results of a similar glucose and insulin response after HFD and similar lipid profile, ruled out that the differences between WT and KO observed in the weight gain and fat depots are due to a direct impact of PTX3 on glucose and lipid homeostasis.

4. Circulating and bone marrow immune cell profiling

Next, we investigated whether the decreased weight gain and fat accumulation might have been related to a different inflammatory profile in PTX3 KO mice. First, we profiled bone marrow immune cells. The absolute number of cells in bone marrow of WT and PTX3 KO mice on HFD was similar, as was the percentage of CD11b positive cells, and the distribution of monocytes and neutrophils (***Figure 17***). Then we profile circulating immune cell signature in PTX3 KO and WT mice on HFD and SFD (***Figure 18-19***). There was a general increase of CD11b+ cells, monocyte and neutrophils number comparing animals on SFD with animals on HFD (***Figure 18***). Looking at animals on HFD, a significant decrease in the number of circulating neutrophils was observed (***Figure 18C***), while the absolute count of blood monocytes was similar between WT and PTX3 KO (***Figure 18D***) as was the case for monocytes subsets distribution (***Figure 18D, 18E***). The number of circulating $CD3^+$ and $CD19^+$ lymphocytes (***Figure 19***) and the distribution of different $CD4^+$ and $CD8^+$ T cells subsets (T naive, T effector cells, T central and effector memory) (***Figure 20***) was similar between WT and PTX3 KO mice both when animals where on HFD or on SFD.

5. *PTX3 deficiency promotes pro-resolution macrophage skewing*

Despite of a similar circulating immune profile, the analysis of the inflammatory profile in the visceral and subcutaneous adipose tissue of HFD-fed PTX3 KO mice showed a significant decreased expression of markers associated with inflammation in VAT **(*Figure 21A***), such as *Mcp1* and *Il-6*, compared to WT mice, while in SCAT we observed only a slight decrease of these cytokines (***Figure 21B***). This profile was associated with a significant reduction in the number of monocytes, macrophages, and neutrophils infiltrating the visceral adipose tissue of PTX3 KO mice compared to WT (***Figure 22A, 22B***). Differently, only macrophages number was reduced in subcutaneous adipose tissue of PTX3 KO mice compared to WT (***Figure 22C***). In addition, the phenotypic characterization of monocytes and macrophages isolated from the visceral adipose tissue revealed that monocytes from PTX3 KO VAT presented a reduced expression of *Ccr2* (*M*CP1 receptor) but not of *Cx3cr1* (CX3CL1 or Fractalkine receptor, marker highly expressed on alternative activated monocytes) compared to WT (***Figure 23A***), pointing toward a pro-resolving profile of monocytes. In SCAT we didn't observed the same monocytes profile, the expression of Ccr2 and Cx3cr1 was similar between WT and PTX3 KO monocytes (***Figure 23B***). In parallel PTX3 KO VAT macrophages presented a significant increased expression of *Arg1* (Arginase1) and *Ym1*, M2-like molecules, compared to WT macrophages (***Figure 23C***). This difference was specific for VAT macrophages but not for macrophages infiltrating the SCAT (***Figure 23D***). In agreement with the reduced inflammatory profile, the distribution of crown like structures surrounding dying or dead adipocytes, where macrophages resorb the remnants of these dying cells [54], was significantly decreased in PTX3 KO VAT (***Figure 23E***).

These results suggest that PTX3 deficiency associates with lower monocytes recruitment and macrophages M1-polarization in visceral adipose tissue.

6. *Enhanced vascularization limits visceral adipocytes hypertrophy in* **PTX3 KO** *mice*

Obesity associates with hypertrophic visceral adipocytes that, undergoing cell death, promote an inflammatory response [179]. Physiological adipose tissue expansion is controlled by the rate of vascularization and angiogenesis that plays a crucial role favouring a correct oxygen supply to adipocytes. Accordingly, adipocytes became hypertrophic after HFD regimen both in VAT and SCAT (***Figure 24A, 24C***), and we found that adipocytes from PTX3 KO VAT (***Figure 24A, 24B*)** and SCAT (***Figure 24C, 24D***) displayed less pronounced hypertrophy compared to WT mice when on HFD. Given the anti-angiogenetic role of PTX3, accomplished by binding and thus inhibiting Fibroblast Growth Factor 2 (FGF2) [111, 180], we investigated adipose tissue vascularization in the absence of PTX3, evaluating the expression of key markers of angiogenesis, as *Cd31* (Cluster of Differentiation 31) and *Vegfa* (Vascular Endothelial Growth Factor a). As shown in ***Figure 25A,*** *Cd31* and *Vegfa mRNA* expression was significantly increased in VAT from PTX3 KO compared to that from WT mice, while there were no differences in their expression in SCAT (***Figure 25B***). We confirmed the higher angiogenesis in VAT analysing the protein expression of VEGF that resulted enhanced in PTX3 KO mice (***Figure 25C, 25E***). These results suggest that PTX3 deficiency results in less pronounced inflammatory profile and enhanced angiogenesis in the visceral adipose tissue.

7. *Genetic determined lower PTX3 levels in humans relates with a reduced visceral adipose tissue accumulation*

To translate our findings in humans, we investigated whether the presence of two different haplotypes (h1/h1 vs h2/h2) on the PTX3 locus [115], which result in lower PTX3 levels, associated with differences in the metabolic profile. The carriers of the h2/h2 haplotype showed a significant reduction in PTX3 plasma levels compared to subjects with the h1/h1 haplotype [h1/h1 median 3.65 ng/mL (3.13, 4.15); h2/h2 median 3.47 (3.07, 3.96) (***Figure 26A***) which was associated with a significant reduction in BMI [h1/h1 median 27.45 kg/m² (25, 30.09); h2/h2 median 26.6 kg/m² (24.25, 29.41)] (***Figure 26B***). We next measured adipose tissue accumulation by Dual-energy X-ray absorptiometry (DEXA) (***Figure 26C***) and observed that subjects with the h2/h2 haplotype also presented a significant reduction in adipose tissue accumulation in the android area (an index of visceral adiposity) [h1/h1 median 48.35% (42.25, 52.88); h2/h2 median 46.70% (39.65, 52.95)](***Figure 26D***) but a similar distribution in the gynoid area (an index of subcutaneous adiposity) [h1/h1 median 42.30% (32.65, 52.03); h2/h2 median 44.20% (33.60, 51.90)] (***Figure 26E***), resulting in a significant difference in android-gynoid ratio [h1/h1 median 1.12 (0.98, 1.35); h2/h2 median 1.06 (0.93, 1.27)] (***Figure 26F***). These data extended the observations in animal models supporting the relevance of PTX3 on indexes of obesity also in humans.

Discussion

Obesity is a complex pathology characterized by an excess of fat accumulation and chronic inflammation that increases the risk of cardiovascular diseases and is correlated with a series of comorbidities as diabetes, hypertriglyceridemia, high blood pressure, insulin resistance. The chronic low-grade inflammation that characterizes these pathologies is the result of high amount of pro-inflammatory molecules, as adipokines (e.g. TNFα, IL6) released by adipocytes and immune cells, in particular monocytes and macrophages infiltrating the tissue. PTX3, the prototype of long pentraxins, is involved in many inflammatory processes. It is produced by different cells types as neutrophils, endothelial cells, macrophages and also adipocytes. The role of PTX3 in obesity is still unclear, there are a series of work with contradictory results and observations linking PTX3 and obesity. The aim of this project was to clarify the role of PTX3 in obesity and understand if ptx3 behaves as a bystander or actively participates to obesity-related inflammation using well established model of diet-induced obesity on PTX3 KO mice.

The work demonstrates that PTX3 deficiency reduces the development of obesity: PTX3 KO mice gain less weight compare to WT. This reduced weight gain is due to a reduced accumulation of fat both at the visceral and subcutaneous level. Diet-induced obesity in PTX3 KO mice is associated with a reduced immuno-inflammatory response, in terms of cytokines production, numbers of monocytes and macrophages infiltrating the visceral adipose tissue and the pro-resolutive profile of these cells. Furthermore, we find an enhanced grade of vascularization in visceral adipose tissue of PTX3 KO mice compared to WT (***Figure 27***). Moreover, carriers of a PTX3 h2/h2 haplotype which results in reduced PTX3 plasma levels present decreased adipose tissue accumulation.

Healthy AT behaves as a pool of "anti-inflammatory", "pro-resolving" and long-lived memory immune cells [181]. Excessive accumulation of fat, as a result of over nutrition and increased circulating levels of free fatty acids,

however, prompts an inflammatory response which is paralleled by the infiltration of activated effector immune cells in AT [182], and by a systemic increased of circulating activated immune cells [183], which further support adipose-tissue inflammation and insulin resistance. Whether this inflammatory response follows or contributes to adipocyte hypertrophy is still a matter of discussion, but it is recognized that the improvement of the immuno-inflammatory responses counteracts the metabolic complications associated to obesity. Indeed, MCP-1 deficiency, a key chemoattractant protein, reduces macrophage accumulation in adipose tissue, insulin resistance, and hepatic steatosis associated with obesity [184], while the blockade of the costimulatory molecule CD40 and its signalling intermediates, TNF receptor-associated factors 6 (TRAF6), ameliorates insulin resistance and hepatosteatosis by reducing CD8+ T cell infiltration into adipose tissue [185]. Similarly, our data show that PTX3 deficiency preserves the M2-like phenotype of adipose tissue macrophages thus preventing fat accumulation and inflammation during HFD-induced obesity. PTX3 is a member of the pentraxin family, soluble mediators of innate immune arm, whose levels rapidly increase following an inflammatory insult [169]. Whereas CRP accurately reflects the inflammatory state associated to obesity [158], PTX3 appears to play a role in modulating the immune response in different contexts [169]: by limiting PMN recruitment [142], protecting from atherosclerosis [137] and thrombosis [186], decreasing cardiac necrosis [141] and platelet-leukocyte aggregation after myocardial infarction [187], reducing restenosis [111] and fibrotic scar formation [156] and behaving as onco-suppressor [164]. On the other hand, PTX3 has been also involved in promoting inflammation after intestinal ischemia and reperfusion [188]. All these evidences delineate the complex role of PTX3 that might depend on cell/tissue origin and can be affected by the glycosylation variability of the N-terminal domain [189]. We show that deficiency of PTX3 protects from adipose tissue expansion during diet induced-obesity through the maintenance

of an anti-inflammatory milieu, mainly as the consequence of the prevalence of M2-macrophages. Similar to this, PTX3 deficiency was shown to result in increased M2 macrophage polarization in the context of experimental models of mesenchymal and epithelial carcinogenesis thus limiting the protective pro-inflammatory response, but rather maintaining a tolerogenic environment to tumour growth [164]. The maintenance of M2-like macrophage polarization is indeed observed in lean adipose tissue where they support adipose homeostasis [44], whereas during obesity, the balance is tilted toward the recruitment of M1-like macrophages, primarily found in crown-like structures (CLSs) around large dying adipocytes [54]. These macrophages, by secreting inflammatory cytokines as TNFα, IL-1β, IL-6, nitric oxide (NO) [190], induce the recruitment of monocytes and/or their differentiation into M1-like phenotype and promote adipocyte resistance to insulin that sustains metabolic syndrome progression. In our model, this maintenance of the M2 phenotype could be the consequence of the pro-angiogenic environment resulting from PTX3 deficiency [164]. Indeed PTX3, by binding to FGF2 and reducing angiogenesis [111], controls vascularization. Angiogenesis is a complex process which exerts different functions based on the physio-pathological mechanism in which it is involved. Angiogenesis is detrimental in atherosclerosis where contributes to plaque growth and instability [191], while its promotion in adipose tissue by angiogenetic factors, such as VEGF and FGF2 (secreted by both adipocytes and activated macrophages) favours the delivery of oxygen and nutrients to adipocytes [61], thus preventing hypoxia caused by adipocyte hypertrophy, as a consequence of excessive fat accumulation [55]. In line with these observations, we demonstrated that PTX3 deficiency is accompanied by increased CD31 and VEGF expression in adipose tissue thus perhaps contributing to the improved vascularization, to reduced fat accumulation and macrophage skewing to the M2 phenotype in PTX3 KO mice. Of note, VEGF was already shown to be a targetable strategy for the prevention of obesity

promoting vessel blood formation [192]. It was shown that FGF2 induced angiogenesis is mediated by VEGF, while the inhibition of VEGF blocked FGF2 induced angiogenesis. Furthermore, recently it has been demonstrated the ability of VEGF to induce the phenotype switch from M1 to M2 in THP-1 cells [68]. These observations sustain our hypothesis that PTX3 might contribute to obesity through a mechanism involving angiogenesis acting on FGF2, and then, as a consequence of a more inflamed and less vascularized tissue, it's promoted macrophages infiltration and their polarization towards a pro-inflammatory phenotype.

Considering that PTX3 shares a 82% sequence similarity between mouse and man [88], we next investigated whether the findings in animal models might be translated to humans. We confirmed previous findings showing that PTX3 plasma levels mark the immunoinflammatory response associated to obesity [147], by demonstrating that specific genetic settings which were found to alter PTX3 plasma levels in Ghanaian women [193] and in lung-transplant recipients with primary graft dysfunction [194] results in a significant decrease in BMI and visceral fat accumulation, further suggesting in humans a direct connection between lower genetically determined PTX3 plasma levels and improved metabolic profile.

As a consequence, although the inhibition of PTX3 might be beneficial for the treatment of obesity, the other protective effects associated to PTX3 [164, 169] suggest the need for the development of tissue selective PTX3 targeting strategies to fully exploit its pharmacological potential.

Figures and Tables

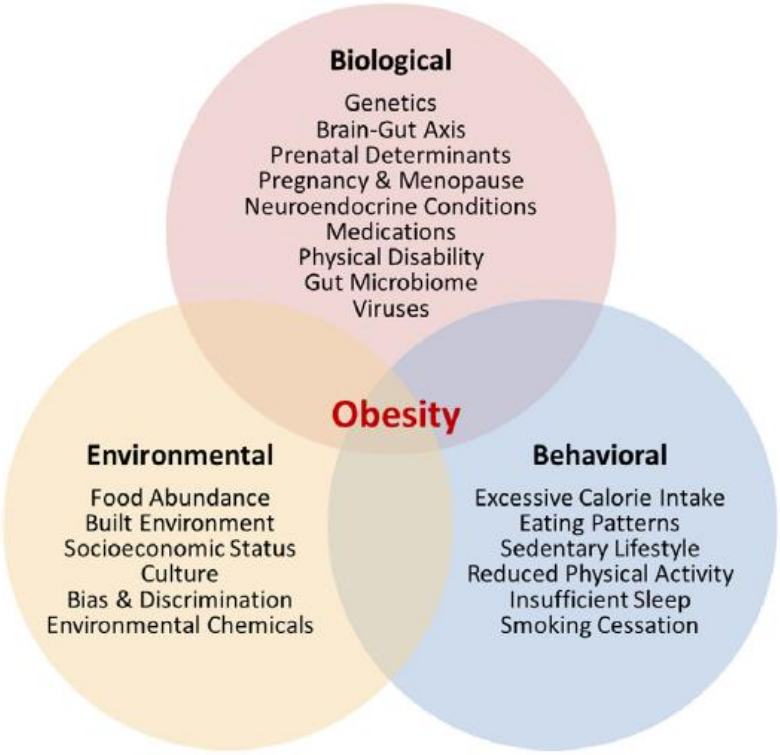

Figure 1. Obesity, a multifactorial disease.

Obesity is a complex disease that results from the interaction of multiple factors. This figure depicts the biological, environmental, and behavioral factors that contribute to positive energy balance, excess weight gain, and therefore obesity. (Kadouh C. H. et al, Techniques in Gastrointestinal Endoscopy 19, 2017)

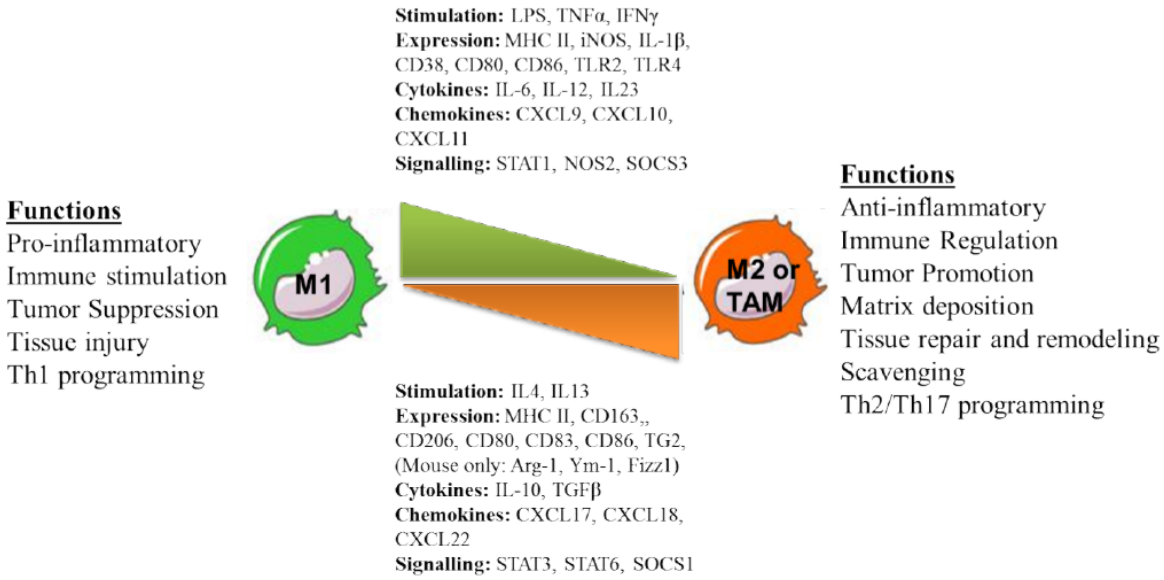

Figure 2. M1 and M2 macrophages phenotype and functions.

Schematic representation of phenotypic as well functional plasticity of macrophages. M1 macrophages, classically activated, are usually induced by INFγ or LPS and produce proinflammatory cytokines stimulating the immune response and tissue injury. M2 alternatively activated macrophages, are activated usually after IL4 and IL13 stimulation, and are implicated in tissue repair and modelling but also in tumor promotion. (Nadella V. et al, Integr Cancer Sci Therap, 2016)

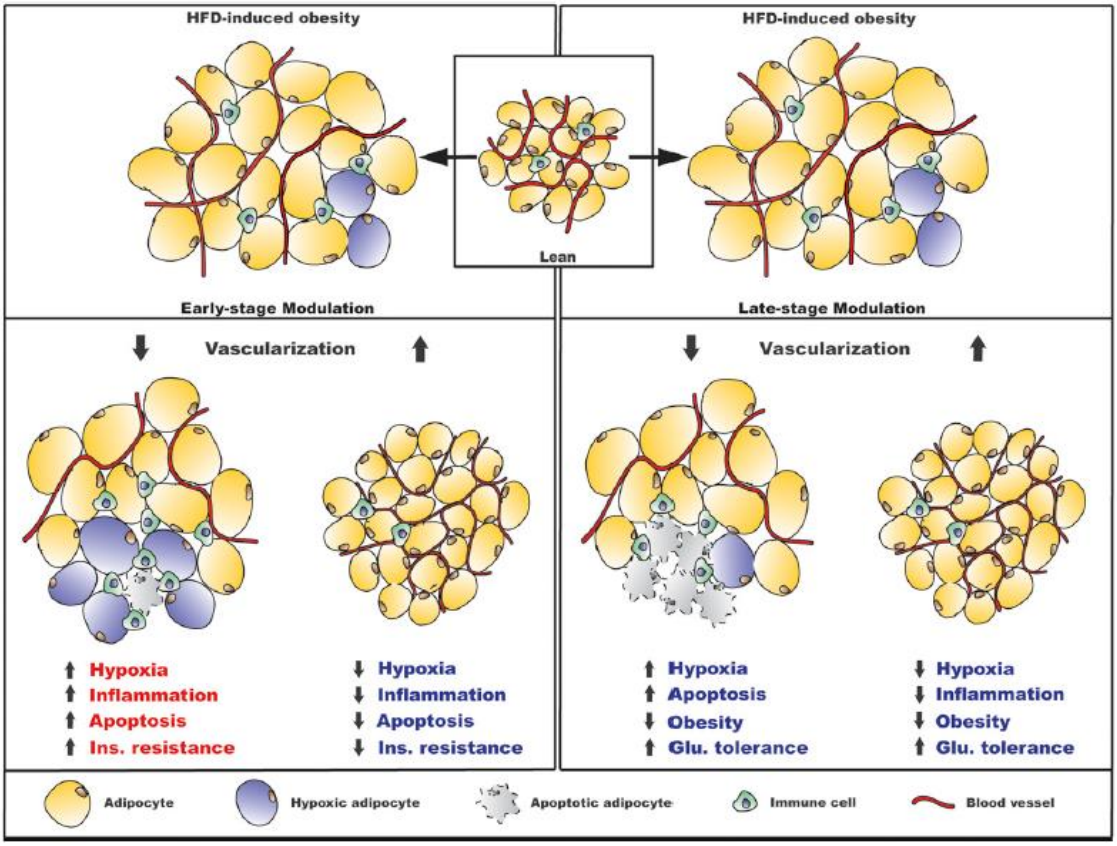

Figure 3. Stage-Dependent Effects of Adipose Tissue Vascularization.

Adipose tissue undergoes hypertrophic and hyperplastic alterations during the course of obesity. Induction of vascularization has beneficial effects at early and late stages of the disease, as it results in decreased hypoxia and inflammation. In late stages reduced vasculature can reduce obesity but with an increase in hypoxia and apoptosis of the adipocytes. (Yilmaz M. et al, Cell Metab, 2013)

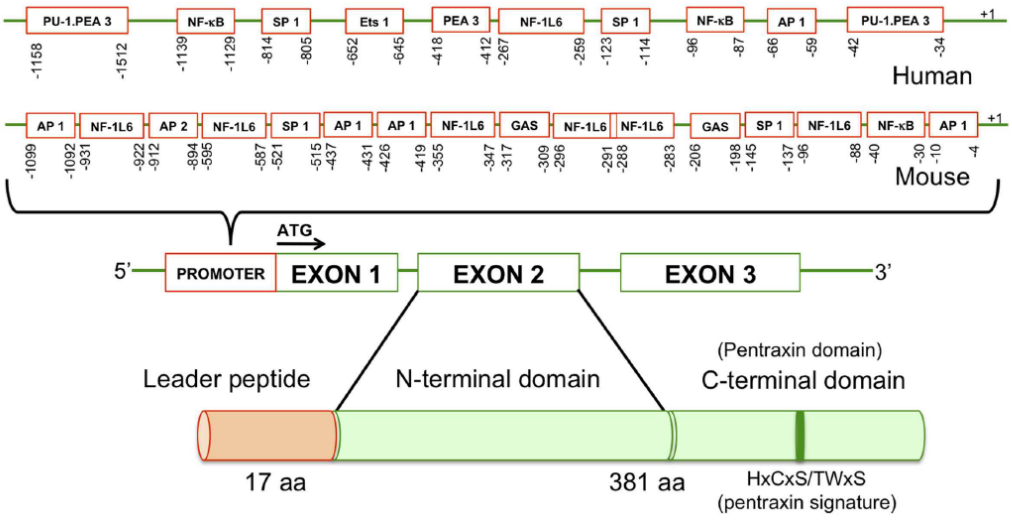

Figure 4. Molecular structure of PTX3 in human and mouse.

PTX3 gene is organized into promoter region and three exons: the first exon encodes for leader peptide (17 amino acids) while the second and the third exons encode for N- and C-terminal domains of the protein (381 amino acids). Promoter region contains multiple transcription binding sites. (Balhara J. et al, Front. Immunol, 2013)

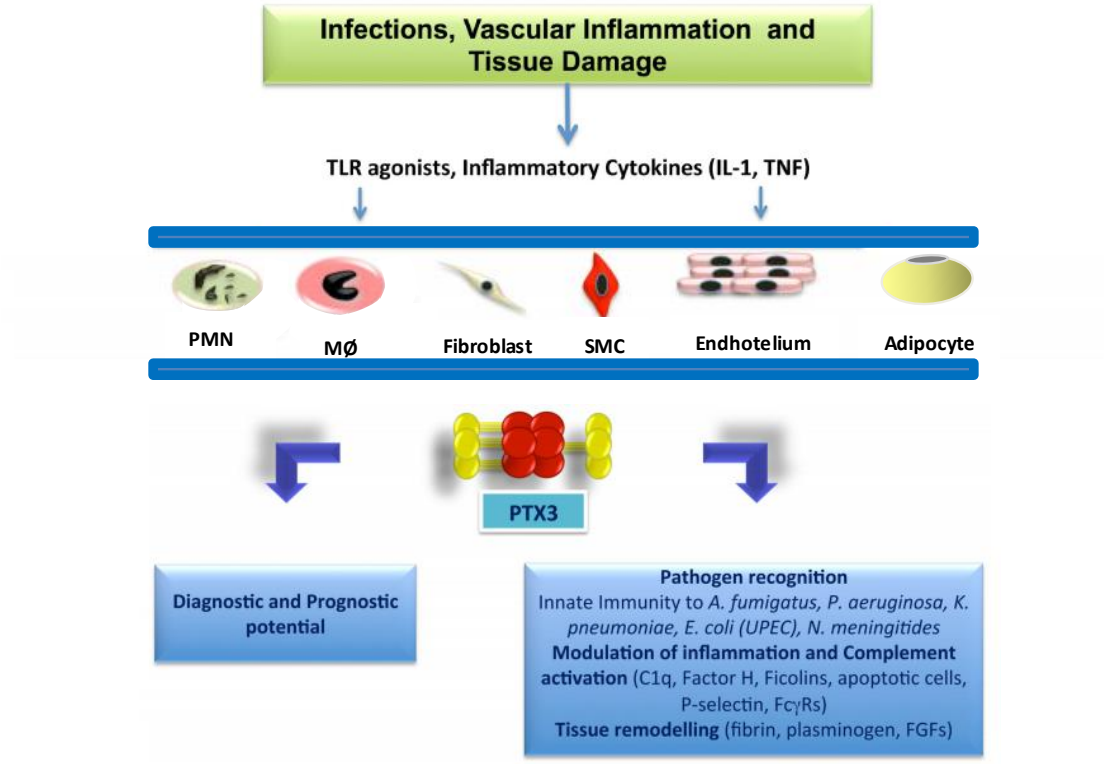

Figure 5. Schematic view of the functional role of PTX3.

After infections, tissue damage or vascular inflammation, PTX3 production and release by neutrophils and other cells types increase rapidly so that it can be a potential diagnostic and prognostic marker of inflammation and tissue damage. Among its functions there are regulation of inflammation, tissue repair and modulation of complement activation. (Adapted from Magrini E. et al, Trends Mol Med, 2016)

PCR master mix:	
GoTaq 5X Flexi buffer (Promega)	10 µl
$MgCL_2$ 25 mM (Promega)	6 µl
dNTP (Promega)	1 µl
Primer FW mut 10 µM 5'-CTGCTCTTTACTGAAGGCTC-3'	1 µl
Primer Rev 10 µM 5'-TCCTCGGTGGGATGAAGTCCA-3'	1 µl
Primer FW 10 µM 5'-AGCAATGCACCTCCTTGCGAT-3'	1 µl
GoTaq G2 DNA polimerase (Promega)	0.5 µl
H_2O RNA-free	28.5 µl
DNA	2 µl

PCR thermal protocol:	
95°C, 5min	
10 cicles	95°C, 30 sec
	65°C, 30 sec
	12°C, 1 min
25 cicles	95°C, 30 sec
	54.5°C, 30 sec
	72°C, 30 sec
72°C, 15 min	
4°C	

Table 1. PCR protocol for the genotyping.

Class Description	Ingredient	Grams
Protein	Casein, Lactic, 30 Mesh	200.0 g
Protein	Cystine, L	3.0 g
Carbohydrate	Starch, Corn	452.2 g
Carbohydrate	Sucrose, Fne granulated	176.8 g
Carbohydrate	Lodex 10	75 g
Fiber	Solka Floc, FCC200	50.0 g
Fat	Soybean Oil, USP	25.0 g
Fat	Lard	20.0 g
Mineral	S10026B	50.0 g
Vitamin	Choline Bitartrate	2.0 g
Vitamin	V10001C	1.0 g
Dye	Dye, Yellow FD&C #5, Alum. Lake 35-42%	0.0 g
Dye	Dye, Red FD&C #40, Alum. Lake 35-42%	0.0 g

Protein:	20% kcal
Fat:	10% kcal
Carbohydrate:	70% kcal
Energy Density:	3.82 kcal/g

Table 2. Standard Fat Diet (D12450H) composition.

Class Description	Ingredient	Grams
Protein	Casein, Lactic, 30 Mesh	200.0 g
Protein	Cystine, L	3.0 g
Carbohydrate	Sucrose, Fne granulated	176.8 g
Carbohydrate	Lodex 10	100 g
Carbohydrate	Starch, Corn	72.8 g
Fiber	Solka Floc, FCC200	50.0 g
Fat	Soybean Oil, USP	25 g
Fat	Lard	177.5 g
Mineral	S10026B	50.0 g
Vitamin	Choline Bitartrate	2.0 g
Vitamin	V10001C	1.0 g
Dye	Dye, Red FD&C #40, Alum. Lake 35-42%	0.0 g

Protein:	20% kcal
Fat:	45% kcal
Carbohydrate:	35% kcal
Energy Density:	4.7 kcal/g

Table 3. High fat diet (D12451) composition.

Blood and bone marrow staining		
Rat anti-mouse ANTIBODIES	SOURCE	IDENTIFIER
anti-CD3e PerCP-Cy5.5	BD Bioscience	Cat#560527
anti-CD19 PECy7	eBioscience	Cat#25-0193-81
anti-CD4 BV786	BD Bioscince	Cat#563727
anti-CD8 BV650	BD Bioscience	Cat#563234
anti-CD44 eFluor450	eBioscience	Cat#48-0441-82
anti-CD62L BV605	BD Bioscience	Cat#563252
anti-CD11b PE	Immunotools	Cat#22159114
anti-Ly6C eFluor450	eBioscience	Cat#48-5932-82
anti-Ly6G FITC	eBioscience	Cat#11-9668-82

Vat and Scat staining		
Rat anti-mouse ANTIBODIES	SOURCE	IDENTIFIER
anti-CD45 PerCP	BD Bioscience	Cat#553093
anti-CD11b BV421	BD Bioscience	Cat#562605
anti-Ly6G PE	BD Bioscience	Cat#551461
anti-Ly6C FITC	BD Bioscience	Cat#553104
anti-F4/80 PECy7	eBioscience	Cat#25-4801-82

Table 4. List of fluorescent-conjugated antibodies.

List of antibodies used for flow cytofluorimetric analysis of blood, bone marrow and adipose tissues from WT and PTX3 KO mice.

Rpl	FW: 5′-GCGCCTCAAGTGGTGTTGGAT-3′	REV: 5′-GAGCAGCAGGGACCACCAT-3′
Mcp-1	FW: 5-TCTCACTGAAGCCAGCTCTCTCT-3	REV: 5′-CAGGCCCAGAAGCATGACA-3′
Il-6	FW: 5′-CTGCAAGAGACTTCCATCCAGTT-3′	REV: 5′-AGGGAAGGCCGTGGTTGT-3′
Il-10	FW: 5′-CAGCCGGGAAGACAATAACTG-3′	REV:5′-CCGCAGCTCTAGGAGCATGT-3′
Tnfa	FW: 5′-CTGAGGTCAATCTGCCCAAGTAC-3′	REV: 5′-CTTCACAGAGCAATGACTCCAAAG-3′
Cd31	FW: 5′-GAG CGG ATA ATT GCC ATT CC-3′	REV:5′-CTA TCA CCC TGA CCC TCA GGA T-3′
Vegfa	FW: 5′-GAC TGG ATT CGC CAT TTT CTT ATA TC-3′	REV: 5′-GGA ATC CCA GAA ACA ACC CTA AT-3′
Cx3cr1	FW:5′-TCAGCATCGACCGGTACCTT-3′	REV: 5′-CTGCACTGTCCGGTTGTTCAT-3′
Ccr2	FW: 5′-TCATCCACGGCATACTATCAA-3′	REV: 5′-GTGGCCCCTTCATCAAGCT-3′
Ym1	FW: 5′-GGCCAATAGAAGGGAGTTTCAA-3′	REV: 5′-CAAAGGCATAGATCAGGTGAGTACA-3′
Arg1	FW: 5′- TGGGTGGATGCTCACACTGA-3′	REV: 5′- CAGGTTGCCCATGCAGATT-3′
Tie1	FW: 5′-CAAGGTCACACACACGGTGAA-3′	REV-5′-GCCAGTCTAGGGTATTGAAGTAGGA-3′

Table 5. List of primers for mRNA quantification.

List of primers used for gene expression analysis of VAT, SCAT and cells isolated from adipose tissues of WT and PTX3 KO mice.

	h1/h1 (n= 201)	h2/h2 (n= 921)	P
Age (years)	63 (56-69)	63 (56-68)	0.620
Gender (n, men)	94	357	**0.045**
Waist/hip ratio	0.90 (0.84-0.95)	0.87 (0.82-0.93)	**0.003**
Fasting glucose levels (mg/dL)	98.0 (90.0-107.0)	97.0 (90.0-105.0)	0.124
Type 2 Diabetes (n, yes)	17	59	0.295
Systolic blood pressure (mmHg)	130 (120-140)	130 (120-140)	0.795
Diastolic blood pressure (mmHg)	80 (75-85)	80 (70-80)	0.079
Hypertension (n, yes)	93	384	0.236
Total cholesterol (mg/dL)	232.0 (205.0-260.5)	230.0 (203.0-258.0)	0.237
HDL-C (mg/dL)	55.0 (46.0-68.0)	56.0 (49.0-68.0)	0.105
Triglycerides (mg/dL)	103.0 (76.0-137.5)	92.0 (68.0-127.7)	**0.003**
LDL-C (mg/dL)	150.6 (128.8-180.3)	149.6 (125.0-175.0)	0.297
ApoB (mg/dL)	117.5 (104.0-137.0)	116.0 (101.0-131.0)	**0.027**
ApoA-I (mg/dL)	154.0 (127.0-170.0)	157.0 (136.0-170.0)	0.081
Hypolipemic treatments (n, yes)	52	263	0.440
Alanine Transaminase, ALT (U/L)	22.0 (18.0-28.0)	21.0 (16.0-28.0)	0.155
Aspartate Transaminase, AST (U/L)	22.0 (19.0-25.0)	22.0 (18.0-26.0)	0.851
Gamma-Glutamyl Transpeptidase (U/L)	26.0 (22.0-37.0)	25.0 (20.0-37.0)	0.143
Creatinine (mg/dL)	0.92 (0.79-1.04)	0.88 (0.78-1.01)	0.055
Glomerular Filtration Rate (mL/min/1.73 m^2)	78.97 (63.69-96.00)	76.97 (64.22-94.10)	0.510
Anti-aggregants (n, yes)	26	125	0.809
C-reactive Protein (mg/L)	2.46 (0.93-4.82)	1.76 (0.69-3.76)	**0.014**

Table 6. Descriptive table of h1/h1 and h2/h2 subjects.

Clinical characteristics, biological parameters and therapies of carriers of PTX3 haplotypes from the PLIC Study cohort.

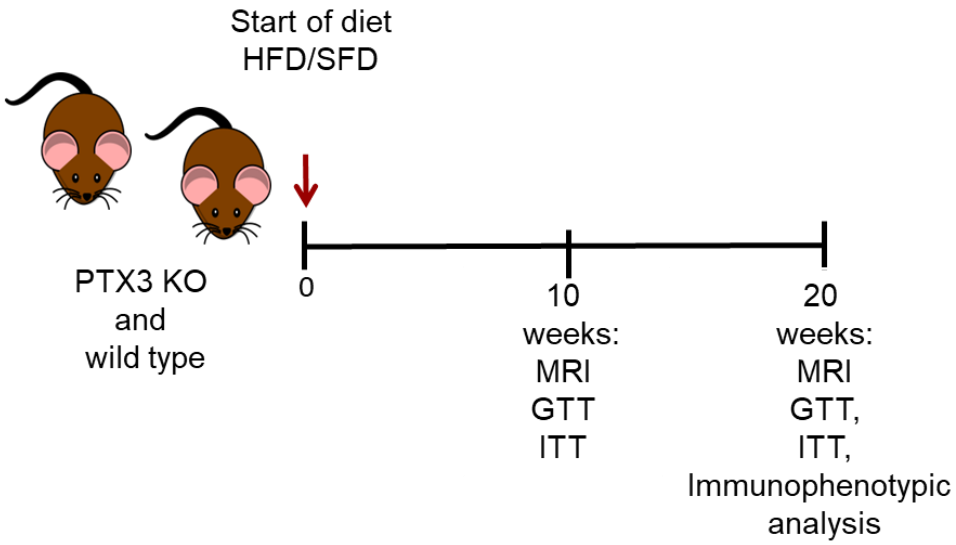

Figure 6. Experimental plan.

PTX3 KO and WT mice were fad a high fat diet (HFD) or a standard fat diet (SFD), as control, for 20 weeks. At 10 weeks of diet magnetic resonance imaging (MRI) acquisition, glucose tolerance test (GTT) and insulin tolerance test (ITT) test were performed. The same procedures were repeated at 20 weeks of diet, followed after the sacrifice by an immunophenotypic analysis of the animal models.

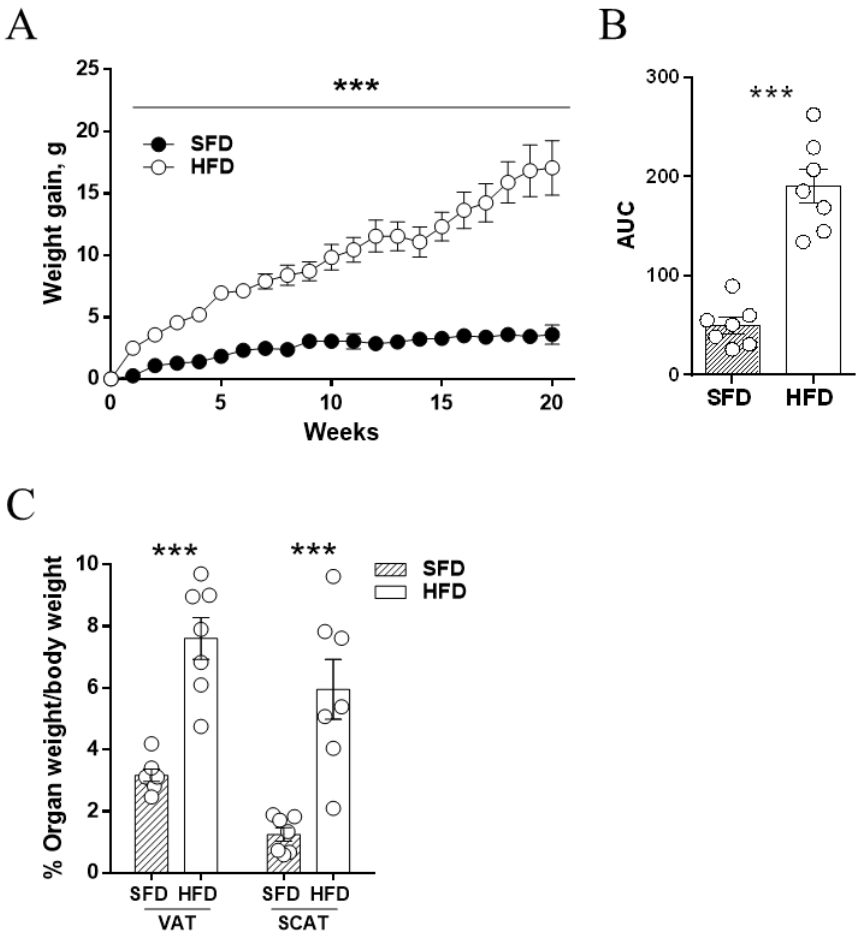

Figure 7. Effect of diet induce obesity on body weight and organs weight.

(A-B) Weight gain of C57BL/6 WT mice on SFD and HFD for 20 weeks and relative area under the curve (AUC), n=7 per group. (C) Visceral (VAT) and subcutaneous (SCAT) adipose tissue percentage of organ weight compared to final body weight of WT and PTX3 KO mice on SFD and HFD for 20 weeks, n=7 per group. Data are presented as mean±SEM. Statistical analysis was performed with Student's t test, *p<0.05, **p<0.01, ***p<0.001.

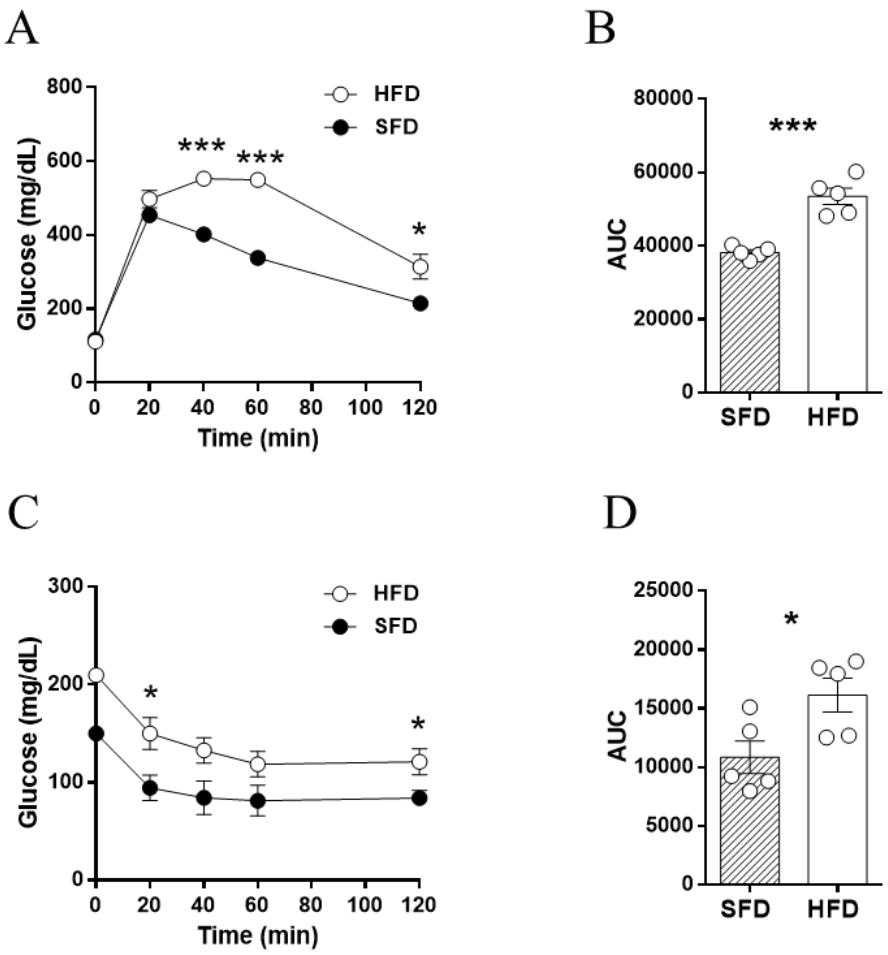

Figure 8. Effect of diet induce obesity on glucose homeostasis.

(A-B) GTT on WT animals at 20 weeks of SFD and HFD regimen and related AUC, n=5 per group. (C-D) ITT on WT animals at 20 weeks of SFD and HFD regimen and related AUC, n=5 per group. Data are presented as mean±SEM. Statistical analysis was performed with Mann-Whitney test, *p<0.05, ***p<0.001.

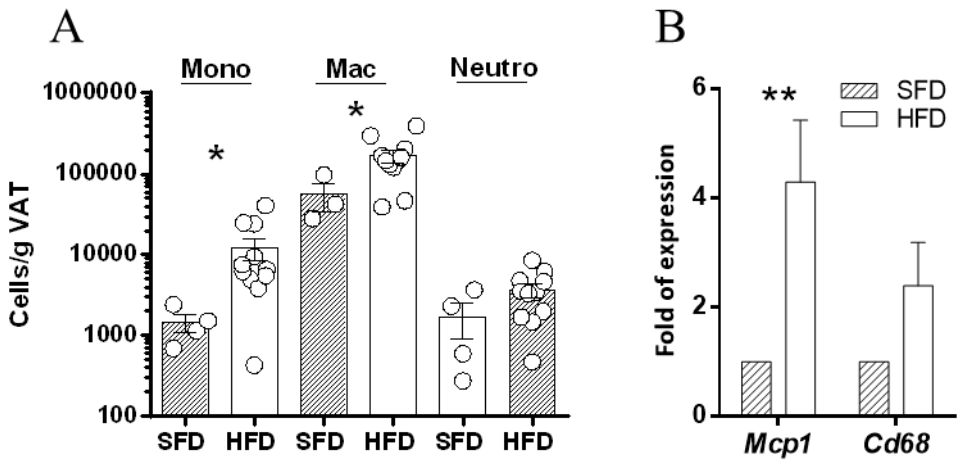

Figure 9. Effect of diet induce obesity on visceral adipose tissue inflammation.

Number of monocytes (mono), macrophages (Mac) and neutrophils (Neutro) per gram of VAT of WT on SFD or HFD for 20 weeks, n=3-11 per group. (B) mRNA expression relative to *Rpl* (L Ribosomal Protein) in VAT of mice on SFD or HFD for 20 weeks, n=4-9 per group. Data are presented as mean±SEM. Statistical analysis was performed with Mann-Whitney test; *p<0.05, **p<0.01.

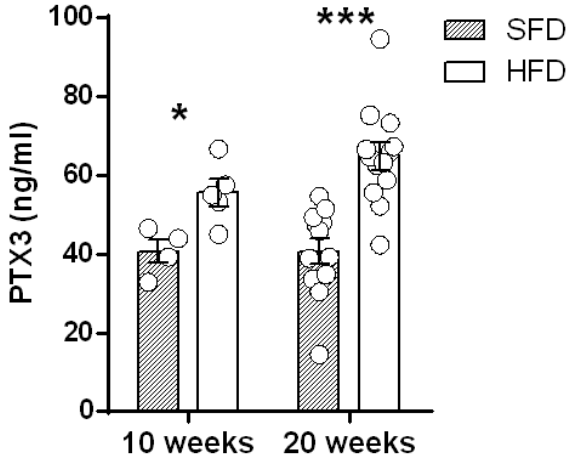

Figure 10. Effect of diet induce obesity on PTX3 plasma levels.

Plasma PTX3 levels measured at 10 weeks and 20 weeks after the starting of the HFD in C57BL/6 mice. Data are presented as mean±SEM. Statistical analysis was performed with Student's t test (B), *p<0.05, ***p<0.001.

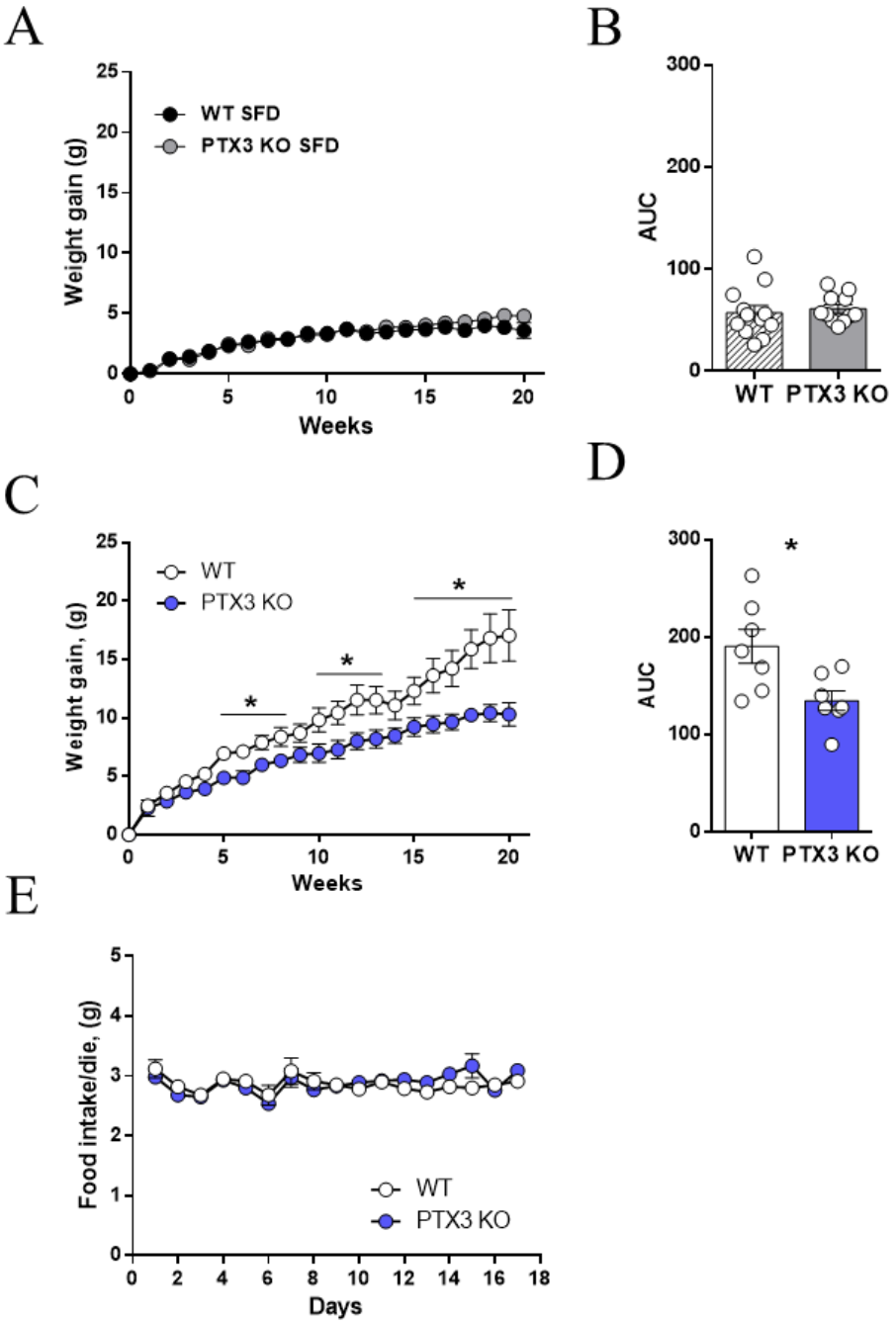

Figure 11. PTX3 is implicated in diet-induced obesity.

(A-B) Weight gain and AUC of weight gain of groups on standard fat diet, n=11-12 per group. (C-D) Weight gain of WT and PTX3 KO mice on HFD measured weekly and AUC of weight gain, n=7 per group. (E) Daily intake measured in WT and PTX3 KO mice on HFD expressed as grams eaten per day, n=3 per group. Data are presented as mean±SEM. Statistical analysis was performed with Student's t test (B), *p<0.05.

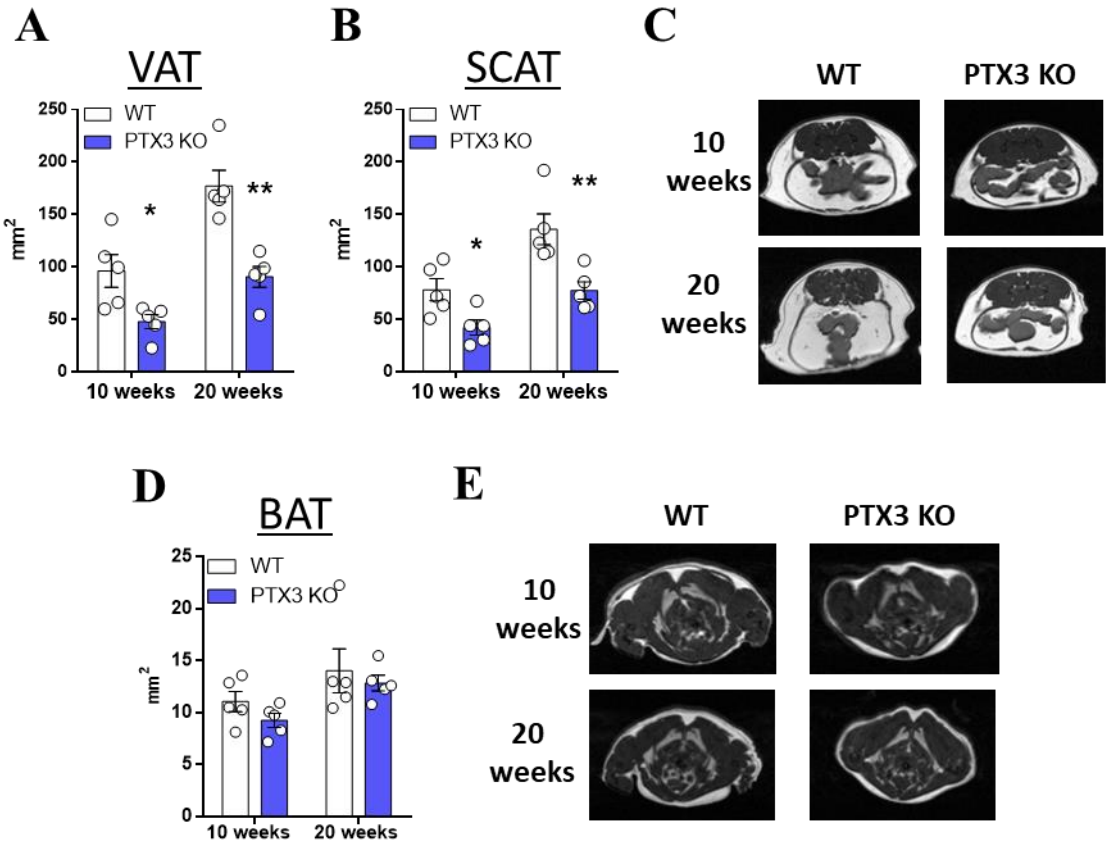

Figure 12. Reduced accumulation of fat in PTX3 KO mice on HFD.

(A-B) MRI of visceral (A) and subcutaneous (B) adipose tissue in WT and PTX3 KO mice on HFD performed at 10 weeks and 20 weeks, n=5 per group. (C) Representative magnetic resonance images of WT and PTX3 KO mice on HFD performed at 10 and 20 weeks. (D) Area of brown adipose tissue at 10 and 20 weeks of HFD measured from magnetic resonance images, n=5 per group. (E) Representative MRI picture used for the quantification of brown adipose tissue in (D) graph. Data are presented as mean±SEM. Statistical analysis was performed with Mann Whitney test, *$p<0.05$, **$p<0.01$.

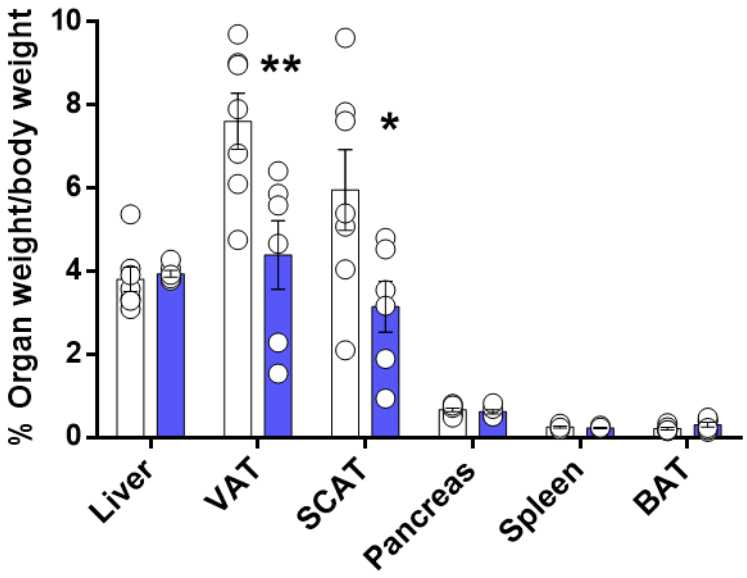

Figure 13. Reduced VAT and SCAT in PTX3 KO mice on HFD

Percentage of organ weight (liver, pancreas, spleen, visceral, subcutaneous and brown adipose tissue) compared to final body weight at 20 week-HFD, n=6-7 per group. Data are presented as mean±SEM. Statistical analysis was performed with Student's t test, *p<0.05, **p<0.01.

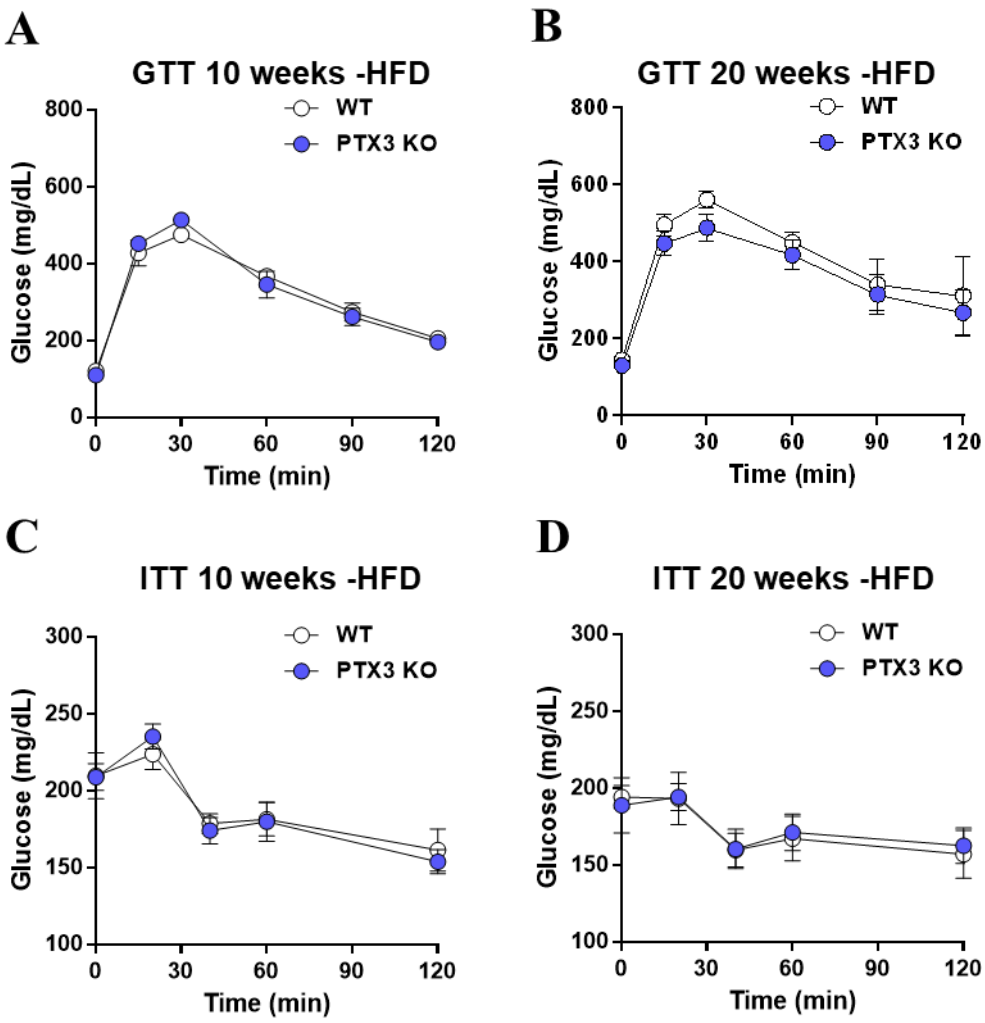

Figure 14. PTX3 deficiency doesn't affect glucose homeostasis during diet-induced obesity.

(A-B) Glucose tolerance test (GTT) performed at 10 (A) and 20 (B) weeks from the beginning of the HFD in WT and PTX3 KO mice, n=5 per group. Glycemia was measured before i.p. glucose injection and after 15, 30, 60, 90 and 120 minutes. (C-D) Insulin tolerance test (ITT) performed at 10 (C) and 20 (D) weeks from the beginning of the HFD in WT and PTX3 KO mice, n=5 per group. Glycemia was measured before i.p. insulin injection and after 20, 40, 60 and 120 minutes. Data are presented as mean±SEM. Statistical analysis was performed with Mann Whitney test.

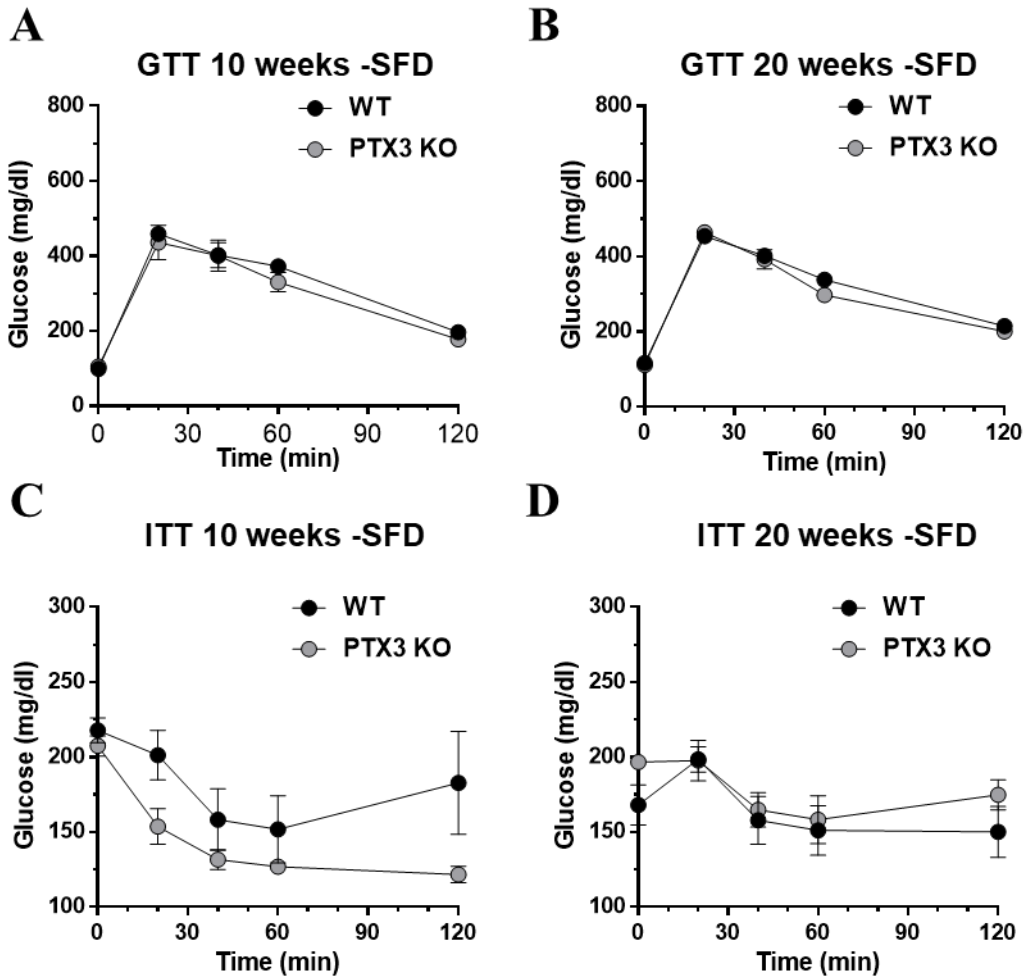

Figure 15. Similar glucose homeostasis in PTX3 KO and WT mice on SFD.

(A-B) GTT performed on WT and PTX3 KO mice on SFD at 10 weeks (A) and 20 weeks (B) from the beginning of the diet, n=5 per group. (C-D) ITT test performed on SFD fed WT and PTX3 KO mice at 10 (C)and 20 (D) weeks from the beginning of the diet regimen, n=5 per group. Data are presented as mean±SEM. Statistical analysis was performed with Mann Withney test.

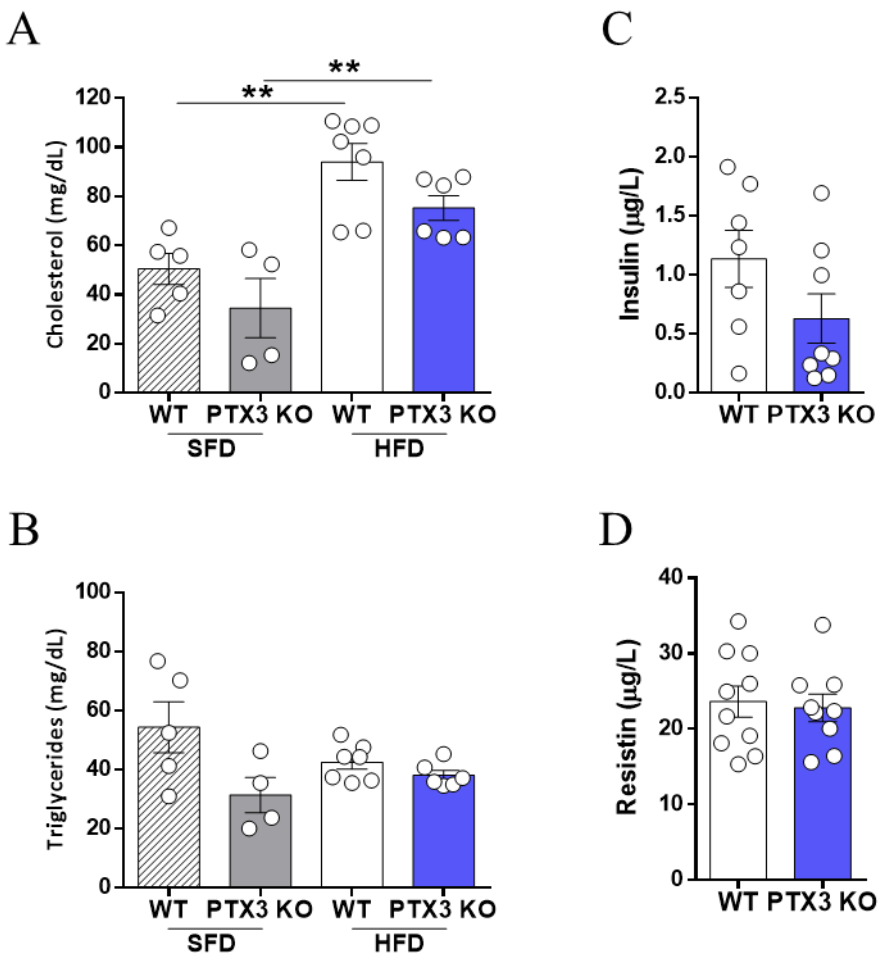

Figure 16. PTX3 does not affect lipid metabolism.

(A) Cholesterol, (B) triglycerides, (C) insulin and resistin concentrations in WT and PTX3 plasma after 20 weeks of SFD or HFD, as indicated; n=6-10 per group. Data are presented as mean±SEM. Statistical analysis was performed with Mann Withney test (A, B) or Student's t test (C, D), *p<0.05, **p<0.01.

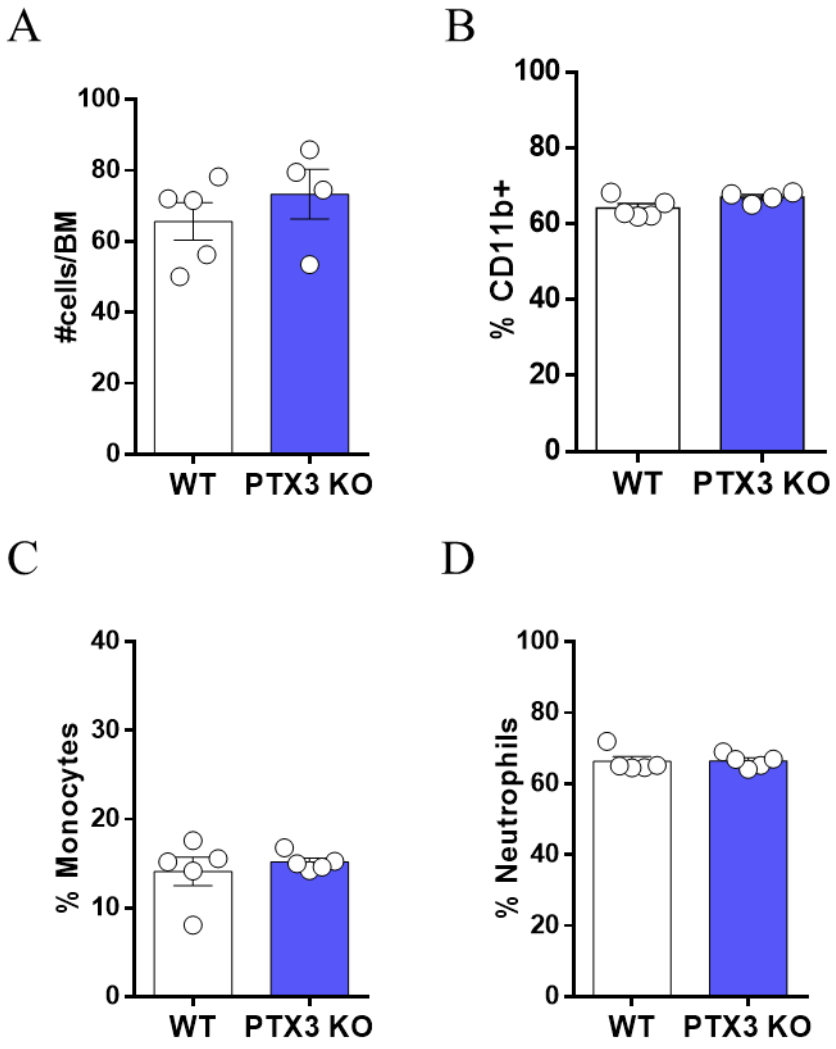

Figure 17. Bone marrow monocytes and neutrophils distribution.

(A) Absolut number of cells in bone marrow of WT and PTX3 KO mice after 20 weeks of HFD. (B) Percentage of CD11b+ in WT and PTX3 KO mice after 20 weeks of HFD. (C-D) Percentage of monocytes (C) and neutrophils (D) in bone marrow of WT and PTX3 KO mice on HFD (n=4-5 per group). Data are presented as mean±SEM. Statistical analysis was performed with Mann-Whitney test.

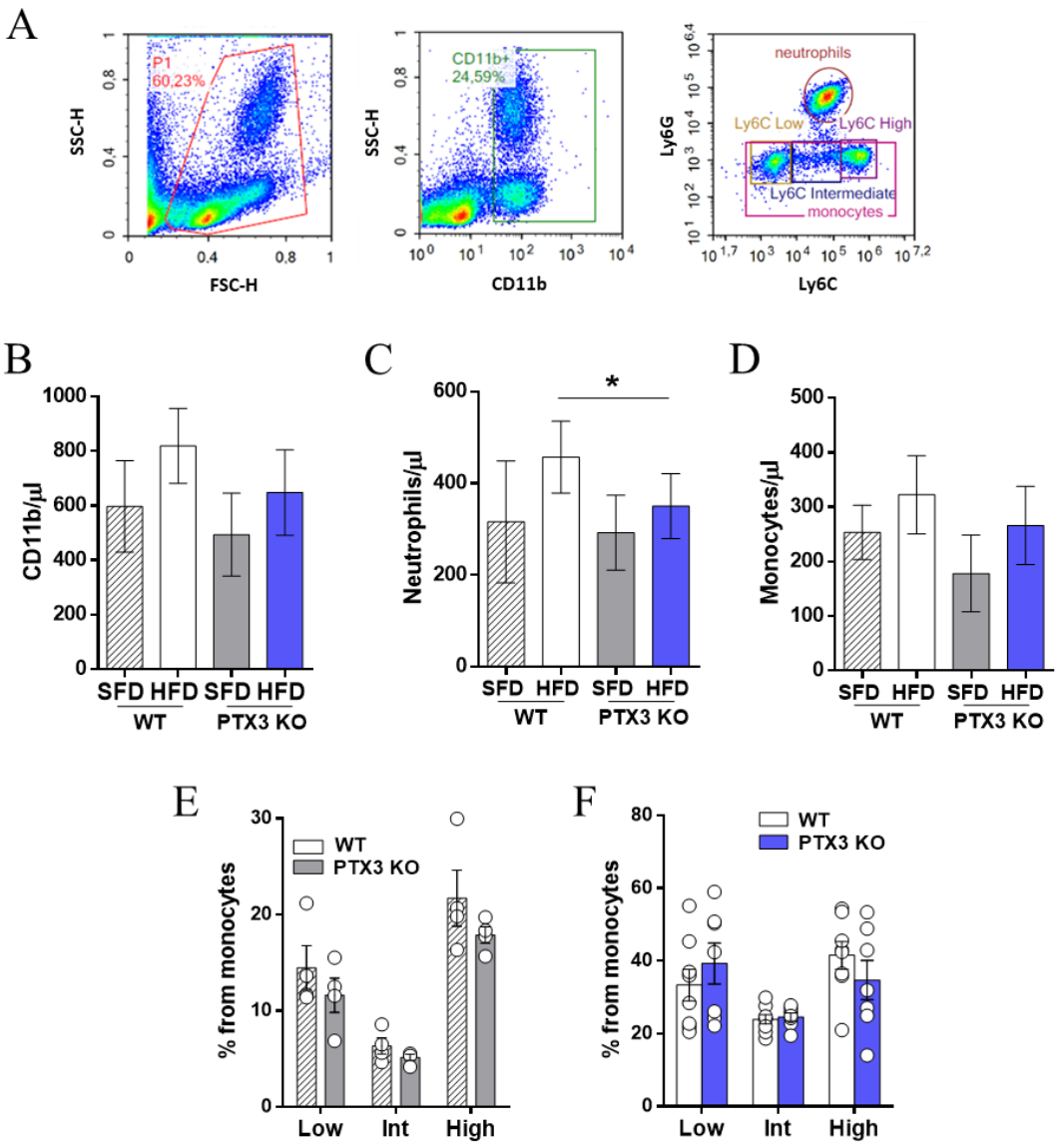

Figure 18. Blood monocytes and neutrophils characterization by flow cytometry.

(A) Gating strategy: selected CD11b+ cells and among them through the use of specific antibody anti-Ly6C and Ly6G are identified monocytes (Ly6C+Ly6G-) and neutrophils (Ly6C+Ly6G+). (B-D) Cells per µl of blood in WT and PTX3 KO mice after 20 weeks of SFD or HFD, in particular CD11b+ cells (B), neutrophils (C) and monocytes (D), n=4 per group. (E, F) Monocytes subsets distribution in blood of WT and PTX3 KO mice on SFD (E) and HFD (F), n=4-12 per group. Data are presented as mean±SEM. Statistical analysis was performed with Mann-Whytney test.

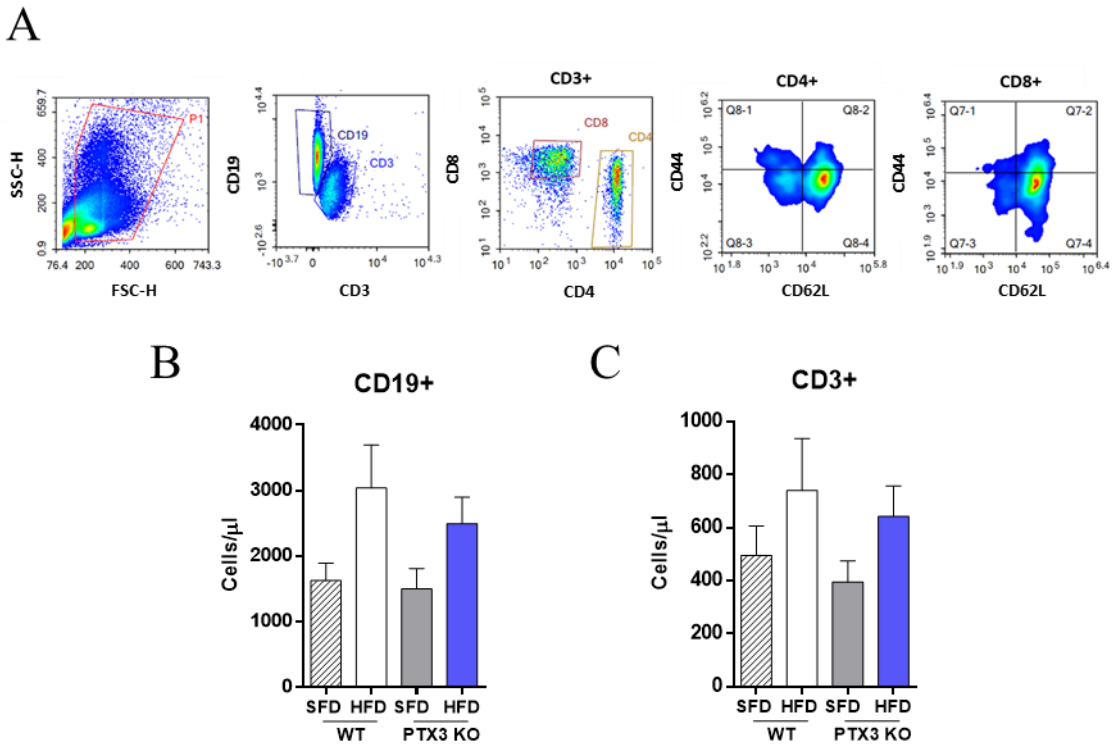

Figure 19. Strategy for the characterization of blood T lymphocytes by flow cytometry.

(A) Gating strategy for the identification of B cells (CD3-CD19+), T lympphocytes (CD3+CD19-), T helper lymphocytes (CD3+CD4+) and T cytotoxic lymphocytes (CD3+CD8+) T lymphocytes and their subsets (T effector memory CD44+CD62L+, T effector CD44-CD62L-, T naive CD44-CD62L+, T. central memory CD44+CD62L+). (B) CD19+ T cells per µl of blood in WT and PTX3 KO mice after 20 weeks of SFD or HFD, n=4 per group. (C) CD3+ T cells per µl of blood in WT and PTX3 KO mice after 20 weeks of SFD or HFD, n=4 per group. Data are presented as mean±SEM. Statistical analysis was performed with Mann-Whitney.

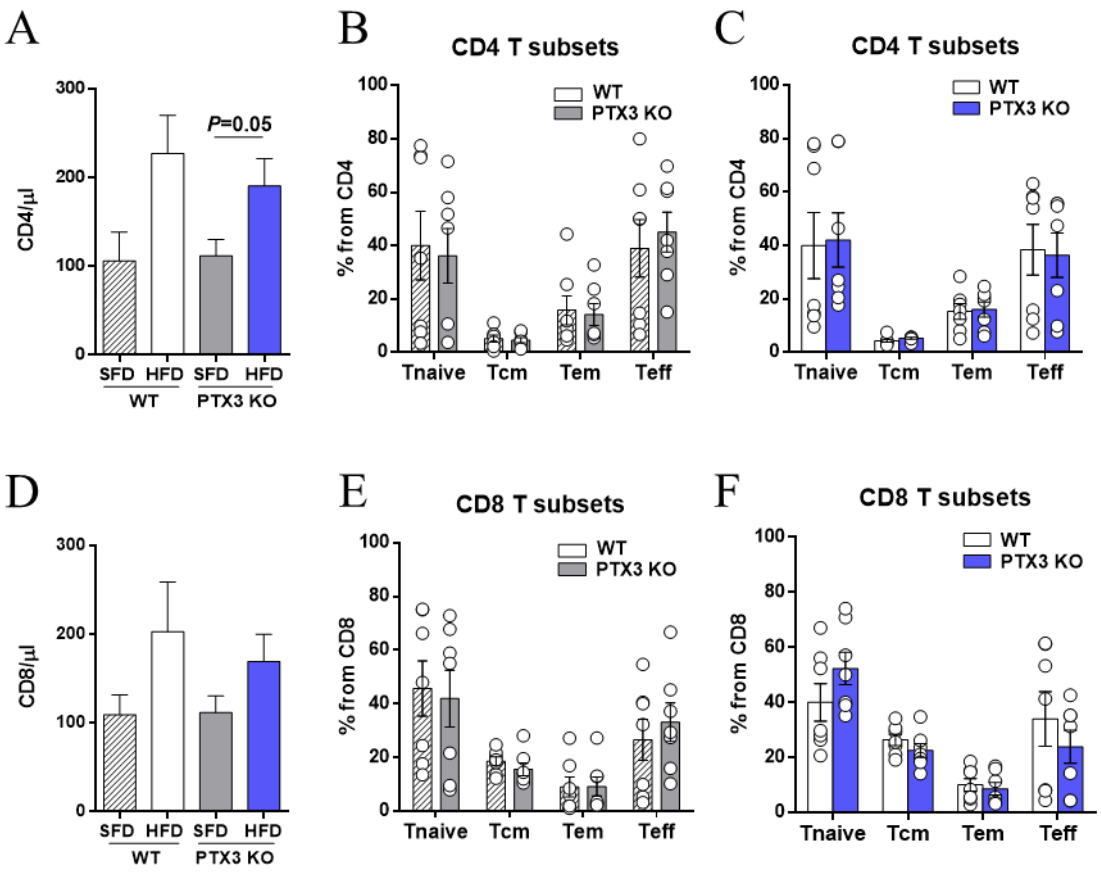

Figure 20. Blood CD4+ and CD8+ T lymphocytes characterization by flow cytometry.

(A) CD4+ T cells per µl of blood in WT and PTX3 KO mice after 20 weeks of SFD or HFD, n=4 per group. (B, C) CD4+ T cells subsets distribution in blood of WT and PTX3 KO mice on SFD (B) and HFD (C), n=7-11 per group. (D) CD8+ T cells per µl of blood in WT and PTX3 KO mice after 20 weeks of SFD or HFD, n=4 per group. (E, F) CD8+ T cells subsets distribution in blood of WT and PTX3 KO mice on SFD (E) and HFD (F), n=7-11. Data are presented as mean±SEM. Statistical analysis was performed with Mann-Whitney test.

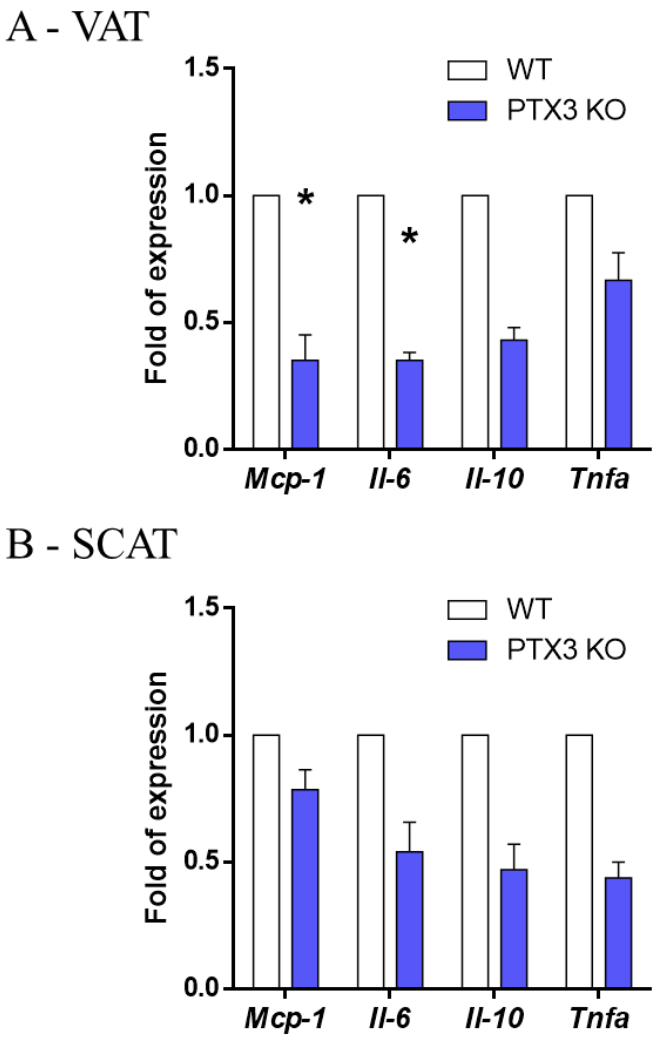

Figure 21. PTX3 deficiency associates with reduced VAT inflammation.

mRNA expression relative to RPL (L Ribosomal Protein) of inflammatory genes in VAT (A) and SCAT (B) of WT and PTX3 KO mice on 20-week HFD, n=5-10 per group. Data are presented as mean±SEM. Statistical analysis was performed with Student's t test or Mann-Whitney, *p<0.05

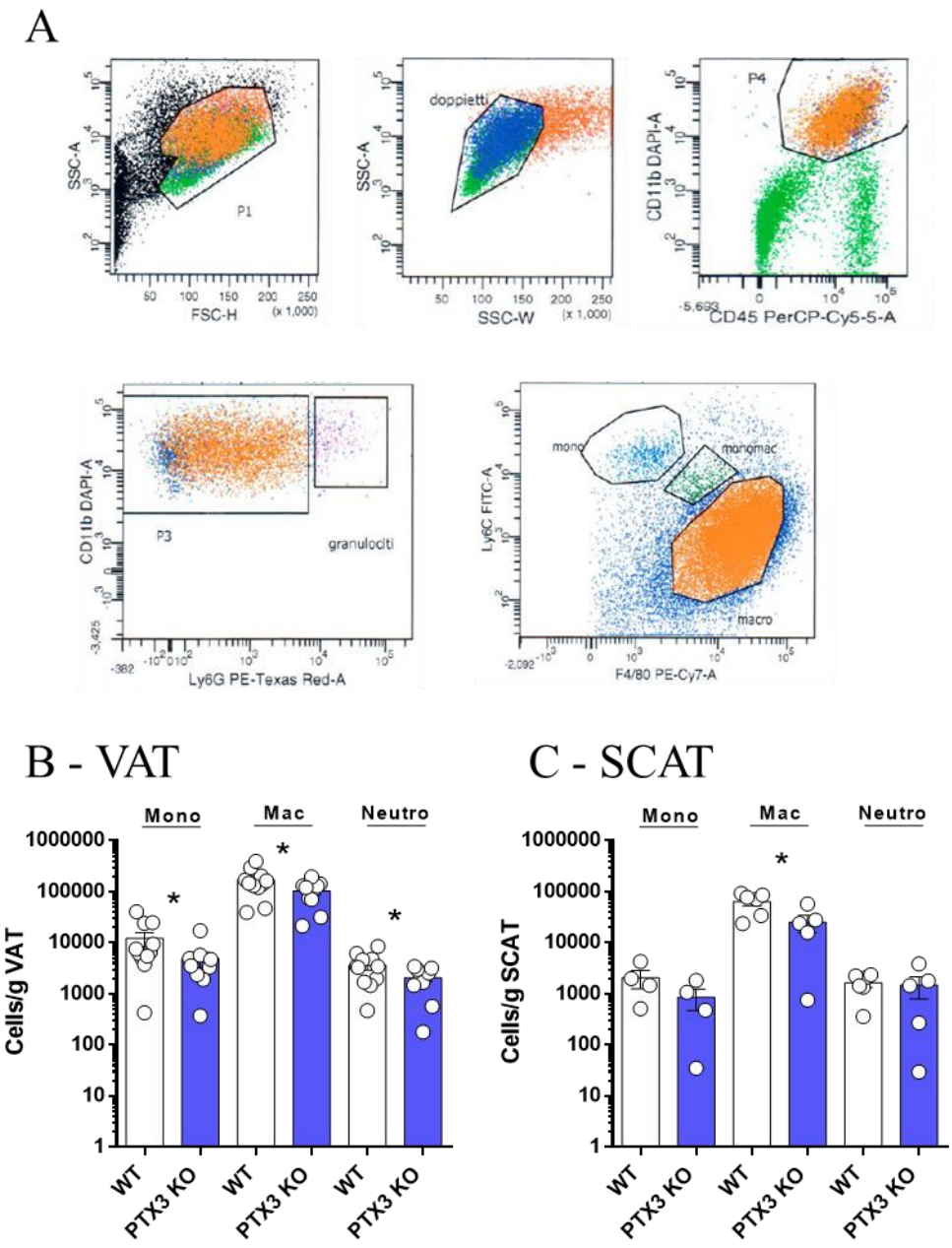

Figure 22. PTX3 deficiency associates with reduced VAT recruitment of innate immune cells.

(A) Sorting strategy for monocytes, neutrophils and macrophages from visceral and subcutaneous adipose tissue. (B-C) Numbers corrected for tissue weight of sorted monocytes (mono), macrophages (mac) and neutrophils (neutro) in VAT (B), n=9-10 per group, and SCAT (C), n=4-6 per group, of WT and PTX3 KO on 20-week HFD. Data are presented as mean±SEM. Statistical analysis was performed with Mann-Whitney test, *$p<0.05$.

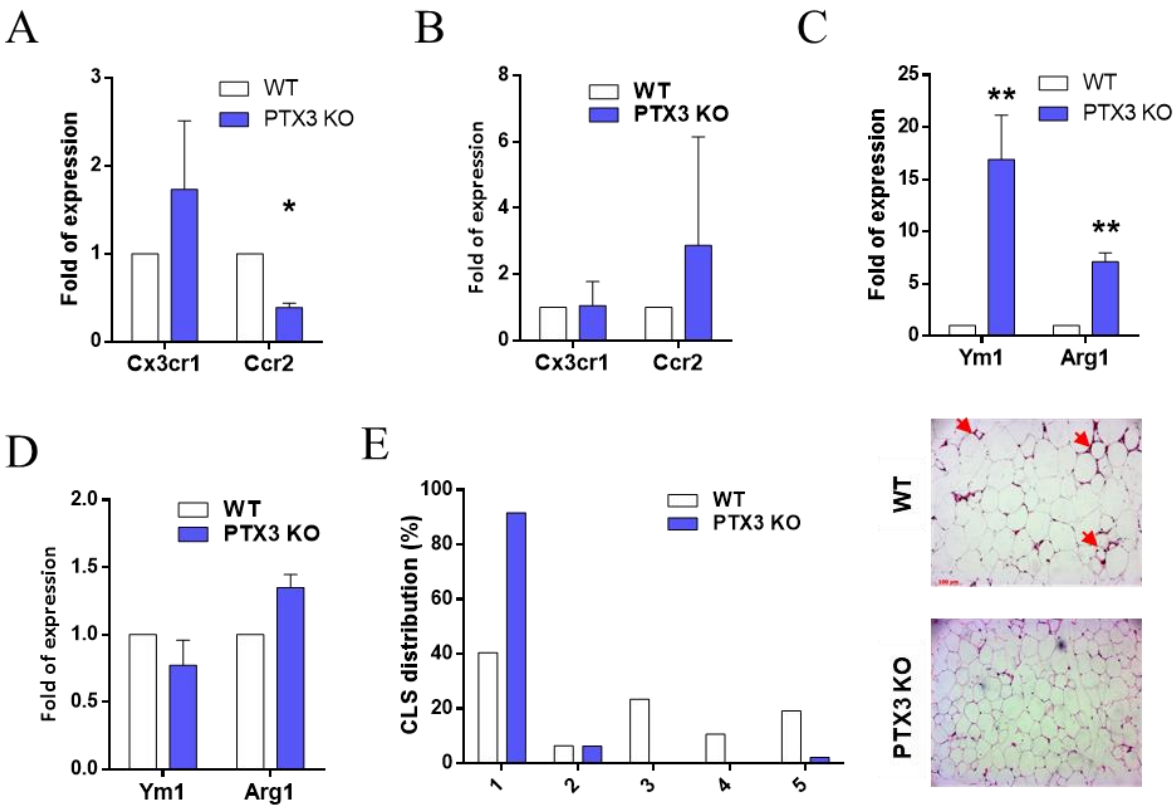

Figure 23. PTX3 deficiency associates with a more pro-resolving monocytes and macrophages profile.

(A-B) mRNA expression relative to RPL in monocytes sorted from VAT (A) and SCAT (B) of WT and PTX3 KO mice on 20-week HFD, n=3-5 per group. (C-D) mRNA expression relative to RPL in macrophages sorted from VAT (C) and SCAT (D) of WT and PTX3 KO mice on 20-week HFD, n=3-5 per group. (E) Quantification of the numbers of crown like structure, and representative images, in VAT sections from WT and *Ptx3*$^{-/-}$ mice on 20-week HFD (legends: from score 1 -no crown detected- to score 5 -equal or more than 4 crowns-), n=6 per group. Data are presented as mean±SEM. Statistical analysis was performed with Mann-Whitney test, *p<0.05, **p<0.01.

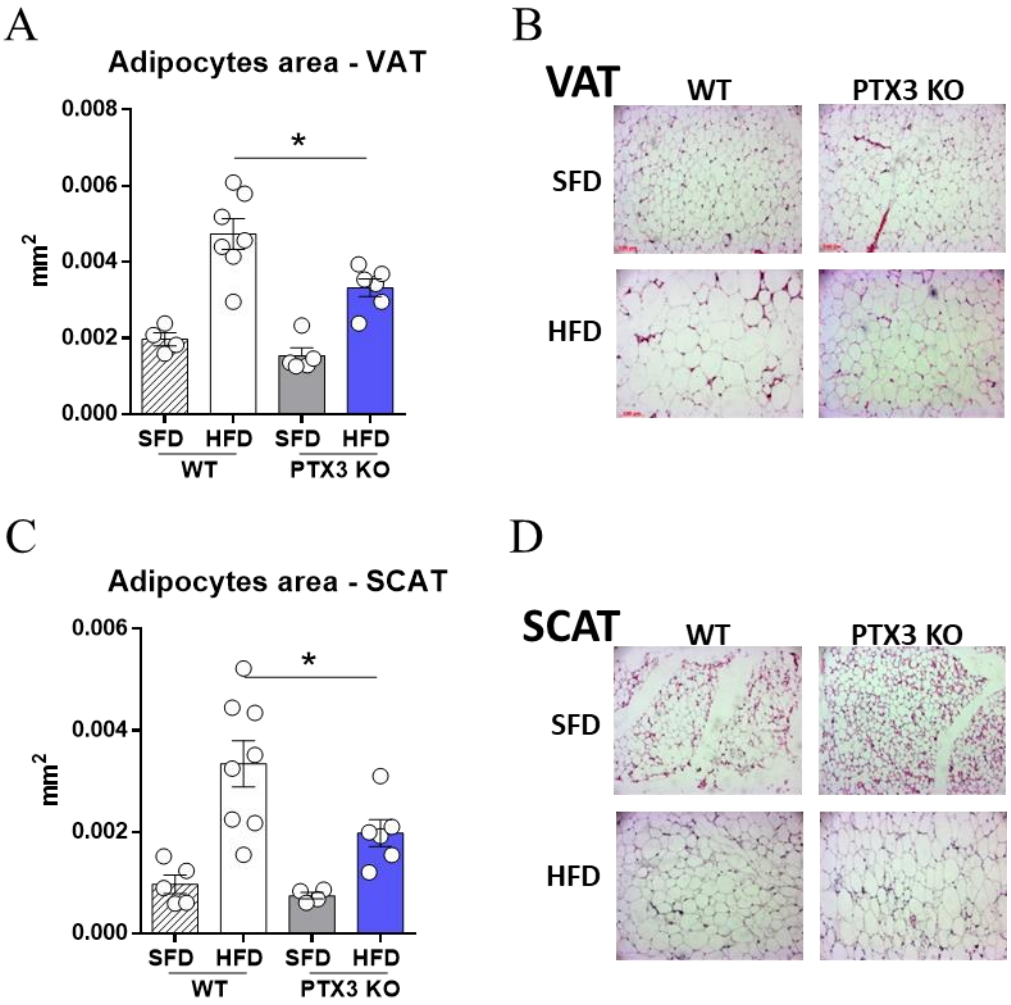

Figure 24. PTX3 KO mice on HFD present smaller adipocytes compared to WT on HFD.

(A) Quantification of adipocyte area in VAT of WT and PTX3 KO on 20-week of SFD or HFD, n=5-8 per group. (B) Representative pictures of VAT sections stained with haematoxylin and eosin are shown. (C) Quantification of adipocyte area in SCAT of WT and PTX3 KO on 20-week of SFD or HFD, n=5-8 per group. (D) Representative pictures of SCAT sections stained with haematoxylin and eosin are shown. Data are presented as mean±SEM. Statistical analysis was performed with Mann-Whitney test, *$p<0.05$.

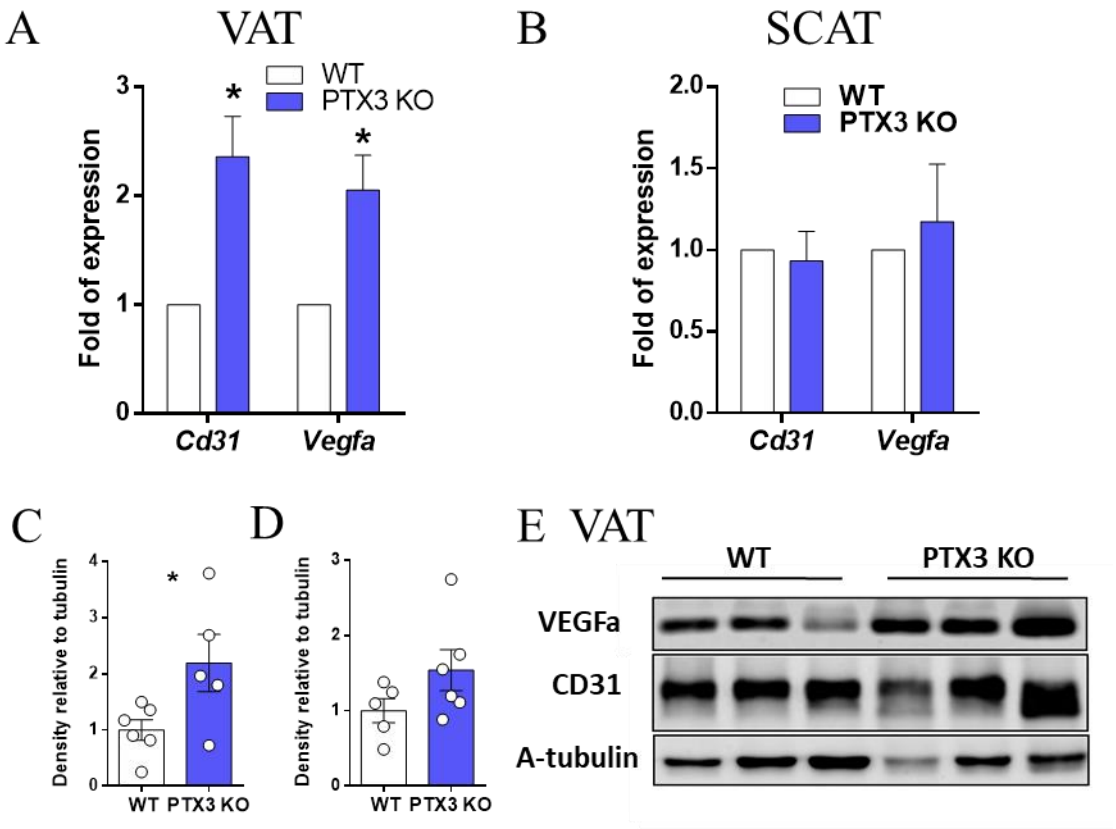

Figure 25. PTX3 KO mice present enhanced vascularization of VAT.

(A-B) mRNA expression relative to RPL of genes related to vascularization in VAT(A) and SCAT (B) of WT and PTX3 KO mice on 20-week HFD, n=5-8 per group. (C-D) Quantification of Vegfa (C) and Cd31 (D) in VAT of WT and PTX3 KO mice on 20-week HFD, n=5-6 per group. (E) Representative panel for VEGF and CD31 Western blot are shown. Data are presented as mean±SEM. Statistical analysis was performed with Mann-Whitney test, *p<0.05.

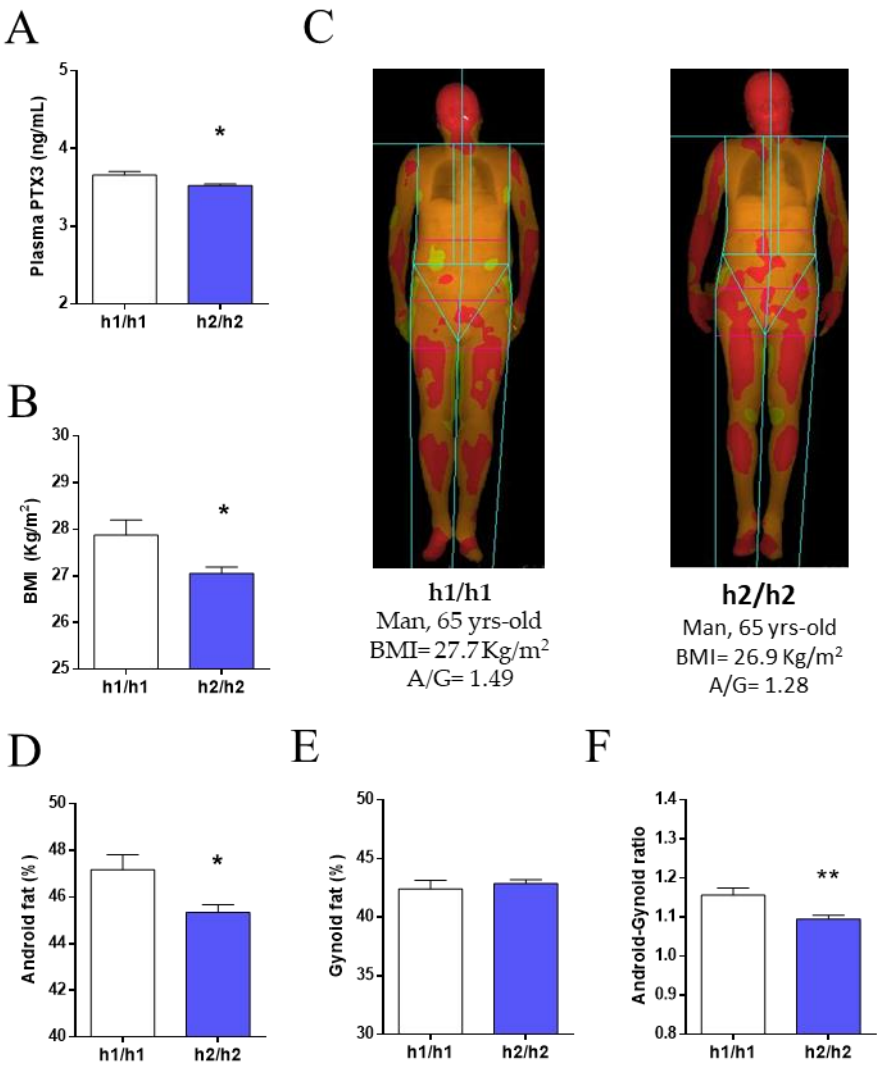

Figure 26. Characterization of h1/h1 and h2/h2 PTX3 haplotype carriers from PLIC study.

(A) PTX3 plasma levels in h1/h1 and h2/h2 subjects from the PLIC study; h1/h1 n=163, h2/h2 n=817. (B) Body Mass Index (BMI), h1/h1 n=201, h2/h2 n=921. (C) Representative images obtained by DEXA scan of two individuals of the h1/h1 and h2/h2 haplotypes for PTX3. (D) Android fat mass and (E) gynoid fat mass were evaluated by DEXA scan in the two groups, h1/h1 n=210, h2/h2 n=941. (F) Android-gynoid ration. Data are presented as mean±SEM. Statistical analysis was performed with Kolmogorov-Smirnov non-parametric test (A), Mann-Whitney non-parametric test (B, D, E, F), *$p<0.05$.

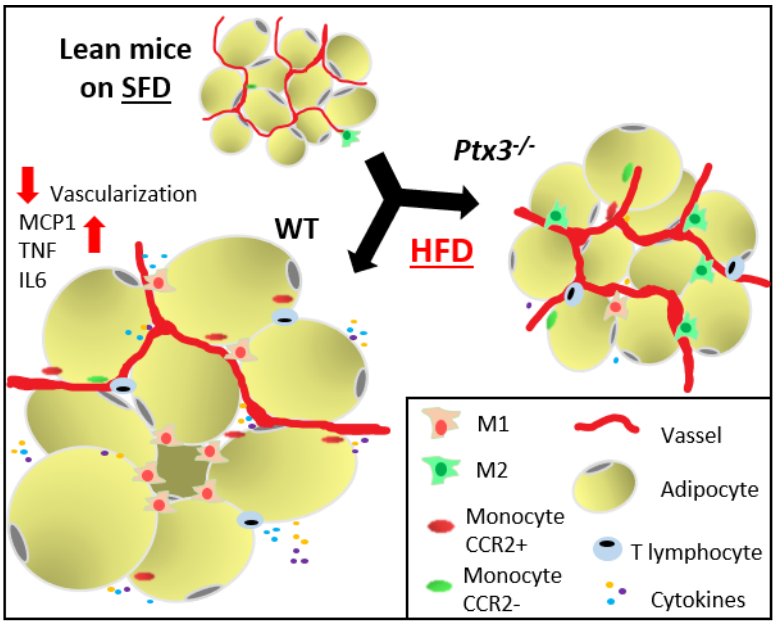

Figure 27. PTX3 deficiency protects from HFD-induced obesity.

PTX3 KO mice show less pronounced visceral adipose tissue hypertrophy compared to WT mice. This effect is associated with increased vascularization, decreased infiltration of pro-inflammatory monocytes and macrophages.

References

1. Spiegel, K., et al., *Brief communication: Sleep curtailment in healthy young men is associated with decreased leptin levels, elevated ghrelin levels, and increased hunger and appetite.* Ann Intern Med, 2004. **141**(11): p. 846-50.
2. Drewnowski, A., *The economics of food choice behavior: why poverty and obesity are linked.* Nestle Nutr Inst Workshop Ser, 2012. **73**: p. 95-112.
3. Phelan, S., *Obesity in the American population: calories, cost, and culture.* Am J Obstet Gynecol, 2010. **203**(6): p. 522-4.
4. Rao, K.R., N. Lal, and N.V. Giridharan, *Genetic & epigenetic approach to human obesity.* Indian J Med Res, 2014. **140**(5): p. 589-603.
5. Park, H.S., J.Y. Park, and R. Yu, *Relationship of obesity and visceral adiposity with serum concentrations of CRP, TNF-alpha and IL-6.* Diabetes Res Clin Pract, 2005. **69**(1): p. 29-35.
6. Reinehr, T., et al., *High-sensitive C-reactive protein, tumor necrosis factor alpha, and cardiovascular risk factors before and after weight loss in obese children.* Metabolism, 2005. **54**(9): p. 1155-61.
7. Eder, K., et al., *The major inflammatory mediator interleukin-6 and obesity.* Inflamm Res, 2009. **58**(11): p. 727-36.
8. Bastard, J.P., et al., *Recent advances in the relationship between obesity, inflammation, and insulin resistance.* Eur Cytokine Netw, 2006. **17**(1): p. 4-12.
9. Marti, A., A. Marcos, and J.A. Martinez, *Obesity and immune function relationships.* Obes Rev, 2001. **2**(2): p. 131-40.
10. Wellen, K.E. and G.S. Hotamisligil, *Inflammation, stress, and diabetes.* J Clin Invest, 2005. **115**(5): p. 1111-9.
11. Grundy, S.M., *Hypertriglyceridemia, atherogenic dyslipidemia, and the metabolic syndrome.* Am J Cardiol, 1998. **81**(4A): p. 18B-25B.
12. Austin, M.A., et al., *Atherogenic lipoprotein phenotype. A proposed genetic marker for coronary heart disease risk.* Circulation, 1990. **82**(2): p. 495-506.
13. Gao, Z., et al., *Serine phosphorylation of insulin receptor substrate 1 by inhibitor kappa B kinase complex.* J Biol Chem, 2002. **277**(50): p. 48115-21.
14. Aguirre, V., et al., *The c-Jun NH(2)-terminal kinase promotes insulin resistance during association with insulin receptor substrate-1 and phosphorylation of Ser(307).* J Biol Chem, 2000. **275**(12): p. 9047-54.
15. Ye, J., *Regulation of PPARgamma function by TNF-alpha.* Biochem Biophys Res Commun, 2008. **374**(3): p. 405-8.
16. Sarzani, R., et al., *Renin-angiotensin system, natriuretic peptides, obesity, metabolic syndrome, and hypertension: an integrated view in humans.* J Hypertens, 2008. **26**(5): p. 831-43.
17. Lean, M.E., *Brown adipose tissue in humans.* Proc Nutr Soc, 1989. **48**(2): p. 243-56.
18. Divoux, A. and K. Clement, *Architecture and the extracellular matrix: the still unappreciated components of the adipose tissue.* Obes Rev, 2011. **12**(5): p. e494-503.
19. Nedergaard, J., et al., *UCP1: the only protein able to mediate adaptive non-shivering thermogenesis and metabolic inefficiency.* Biochim Biophys Acta, 2001. **1504**(1): p. 82-106.
20. Gibbons, G.F., K. Islam, and R.J. Pease, *Mobilisation of triacylglycerol stores.* Biochim Biophys Acta, 2000. **1483**(1): p. 37-57.
21. Timmons, J.A., et al., *Myogenic gene expression signature establishes that brown and white adipocytes originate from distinct cell lineages.* Proc Natl Acad Sci U S A, 2007. **104**(11): p. 4401-6.
22. Farmer, S.R., *Transcriptional control of adipocyte formation.* Cell Metab, 2006. **4**(4): p. 263-73.

23. Fasshauer, M. and M. Bluher, *Adipokines in health and disease.* Trends Pharmacol Sci, 2015. **36**(7): p. 461-70.
24. Tilg, H. and A.R. Moschen, *Adipocytokines: mediators linking adipose tissue, inflammation and immunity.* Nat Rev Immunol, 2006. **6**(10): p. 772-83.
25. Mantzoros, C.S., et al., *Leptin in human physiology and pathophysiology.* Am J Physiol Endocrinol Metab, 2011. **301**(4): p. E567-84.
26. Diez, J.J. and P. Iglesias, *The role of the novel adipocyte-derived hormone adiponectin in human disease.* Eur J Endocrinol, 2003. **148**(3): p. 293-300.
27. Jellema, A., J. Plat, and R.P. Mensink, *Weight reduction, but not a moderate intake of fish oil, lowers concentrations of inflammatory markers and PAI-1 antigen in obese men during the fasting and postprandial state.* Eur J Clin Invest, 2004. **34**(11): p. 766-73.
28. Cawthorn, W.P. and J.K. Sethi, *TNF-alpha and adipocyte biology.* FEBS Lett, 2008. **582**(1): p. 117-31.
29. Liang, H., et al., *Blockade of tumor necrosis factor (TNF) receptor type 1-mediated TNF-alpha signaling protected Wistar rats from diet-induced obesity and insulin resistance.* Endocrinology, 2008. **149**(6): p. 2943-51.
30. Osborn, O. and J.M. Olefsky, *The cellular and signaling networks linking the immune system and metabolism in disease.* Nat Med, 2012. **18**(3): p. 363-74.
31. Winer, S., et al., *Normalization of obesity-associated insulin resistance through immunotherapy.* Nat Med, 2009. **15**(8): p. 921-9.
32. McGillicuddy, F.C., et al., *Interferon gamma attenuates insulin signaling, lipid storage, and differentiation in human adipocytes via activation of the JAK/STAT pathway.* J Biol Chem, 2009. **284**(46): p. 31936-44.
33. Yang, H., et al., *Obesity increases the production of proinflammatory mediators from adipose tissue T cells and compromises TCR repertoire diversity: implications for systemic inflammation and insulin resistance.* J Immunol, 2010. **185**(3): p. 1836-45.
34. Winer, D.A., et al., *B cells promote insulin resistance through modulation of T cells and production of pathogenic IgG antibodies.* Nat Med, 2011. **17**(5): p. 610-7.
35. Elgazar-Carmon, V., et al., *Neutrophils transiently infiltrate intra-abdominal fat early in the course of high-fat feeding.* J Lipid Res, 2008. **49**(9): p. 1894-903.
36. Talukdar, S., et al., *Neutrophils mediate insulin resistance in mice fed a high-fat diet through secreted elastase.* Nat Med, 2012. **18**(9): p. 1407-12.
37. Feuerer, M., et al., *Lean, but not obese, fat is enriched for a unique population of regulatory T cells that affect metabolic parameters.* Nat Med, 2009. **15**(8): p. 930-9.
38. Deiuliis, J., et al., *Visceral adipose inflammation in obesity is associated with critical alterations in tregulatory cell numbers.* PLoS One, 2011. **6**(1): p. e16376.
39. Koppaka, S., et al., *Reduced adipose tissue macrophage content is associated with improved insulin sensitivity in thiazolidinedione-treated diabetic humans.* Diabetes, 2013. **62**(6): p. 1843-54.
40. Menghini, R., et al., *TIMP3 overexpression in macrophages protects from insulin resistance, adipose inflammation, and nonalcoholic fatty liver disease in mice.* Diabetes, 2012. **61**(2): p. 454-62.
41. Wellen, K.E. and G.S. Hotamisligil, *Obesity-induced inflammatory changes in adipose tissue.* J Clin Invest, 2003. **112**(12): p. 1785-8.
42. Gordon, S. and P.R. Taylor, *Monocyte and macrophage heterogeneity.* Nat Rev Immunol, 2005. **5**(12): p. 953-64.
43. Gordon, S., *Alternative activation of macrophages.* Nat Rev Immunol, 2003. **3**(1): p. 23-35.
44. Odegaard, J.I., et al., *Macrophage-specific PPARgamma controls alternative activation and improves insulin resistance.* Nature, 2007. **447**(7148): p. 1116-20.
45. Geissmann, F., S. Jung, and D.R. Littman, *Blood monocytes consist of two principal subsets with distinct migratory properties.* Immunity, 2003. **19**(1): p. 71-82.

46. Weisberg, S.P., et al., *CCR2 modulates inflammatory and metabolic effects of high-fat feeding.* J Clin Invest, 2006. **116**(1): p. 115-24.
47. Sunderkotter, C., et al., *Subpopulations of mouse blood monocytes differ in maturation stage and inflammatory response.* J Immunol, 2004. **172**(7): p. 4410-7.
48. de Heredia, F.P., S. Gomez-Martinez, and A. Marcos, *Obesity, inflammation and the immune system.* Proc Nutr Soc, 2012. **71**(2): p. 332-8.
49. Schipper, H.S., et al., *Adipose tissue-resident immune cells: key players in immunometabolism.* Trends Endocrinol Metab, 2012. **23**(8): p. 407-15.
50. Suganami, T., J. Nishida, and Y. Ogawa, *A paracrine loop between adipocytes and macrophages aggravates inflammatory changes: role of free fatty acids and tumor necrosis factor alpha.* Arterioscler Thromb Vasc Biol, 2005. **25**(10): p. 2062-8.
51. Kamei, N., et al., *Overexpression of monocyte chemoattractant protein-1 in adipose tissues causes macrophage recruitment and insulin resistance.* J Biol Chem, 2006. **281**(36): p. 26602-14.
52. Cinti, S., et al., *Adipocyte death defines macrophage localization and function in adipose tissue of obese mice and humans.* J Lipid Res, 2005. **46**(11): p. 2347-55.
53. Strissel, K.J., et al., *Adipocyte death, adipose tissue remodeling, and obesity complications.* Diabetes, 2007. **56**(12): p. 2910-8.
54. Murano, I., et al., *Dead adipocytes, detected as crown-like structures, are prevalent in visceral fat depots of genetically obese mice.* J Lipid Res, 2008. **49**(7): p. 1562-8.
55. Cao, Y., *Angiogenesis modulates adipogenesis and obesity.* J Clin Invest, 2007. **117**(9): p. 2362-8.
56. Goossens, G.H. and E.E. Blaak, *Adipose tissue dysfunction and impaired metabolic health in human obesity: a matter of oxygen?* Front Endocrinol (Lausanne), 2015. **6**: p. 55.
57. Jansson, P.A., A. Larsson, and P.N. Lonnroth, *Relationship between blood pressure, metabolic variables and blood flow in obese subjects with or without non-insulin-dependent diabetes mellitus.* Eur J Clin Invest, 1998. **28**(10): p. 813-8.
58. Bikfalvi, A., et al., *Biological roles of fibroblast growth factor-2.* Endocr Rev, 1997. **18**(1): p. 26-45.
59. Moscatelli, D., M. Presta, and D.B. Rifkin, *Purification of a factor from human placenta that stimulates capillary endothelial cell protease production, DNA synthesis, and migration.* Proc Natl Acad Sci U S A, 1986. **83**(7): p. 2091-5.
60. Yancopoulos, G.D., et al., *Vascular-specific growth factors and blood vessel formation.* Nature, 2000. **407**(6801): p. 242-8.
61. Sung, H.K., et al., *Adipose vascular endothelial growth factor regulates metabolic homeostasis through angiogenesis.* Cell Metab, 2013. **17**(1): p. 61-72.
62. Brakenhielm, E., et al., *Angiogenesis inhibitor, TNP-470, prevents diet-induced and genetic obesity in mice.* Circ Res, 2004. **94**(12): p. 1579-88.
63. Kolonin, M.G., et al., *Reversal of obesity by targeted ablation of adipose tissue.* Nat Med, 2004. **10**(6): p. 625-32.
64. Rupnick, M.A., et al., *Adipose tissue mass can be regulated through the vasculature.* Proc Natl Acad Sci U S A, 2002. **99**(16): p. 10730-5.
65. Yilmaz, M. and G.S. Hotamisligil, *Damned if you do, damned if you don't: the conundrum of adipose tissue vascularization.* Cell Metab, 2013. **17**(1): p. 7-9.
66. Seghezzi, G., et al., *Fibroblast growth factor-2 (FGF-2) induces vascular endothelial growth factor (VEGF) expression in the endothelial cells of forming capillaries: an autocrine mechanism contributing to angiogenesis.* J Cell Biol, 1998. **141**(7): p. 1659-73.
67. Kanda, S., Y. Miyata, and H. Kanetake, *Fibroblast growth factor-2-mediated capillary morphogenesis of endothelial cells requires signals via Flt-1/vascular endothelial growth factor receptor-1: possible involvement of c-Akt.* J Biol Chem, 2004. **279**(6): p. 4007-16.

68. Wheeler, K.C., et al., *VEGF may contribute to macrophage recruitment and M2 polarization in the decidua.* PLoS One, 2018. **13**(1): p. e0191040.
69. Zhang, Y., et al., *Positional cloning of the mouse obese gene and its human homologue.* Nature, 1994. **372**(6505): p. 425-32.
70. Chua, S.C., Jr., et al., *Phenotypes of mouse diabetes and rat fatty due to mutations in the OB (leptin) receptor.* Science, 1996. **271**(5251): p. 994-6.
71. Coleman, D.L., *Obese and diabetes: two mutant genes causing diabetes-obesity syndromes in mice.* Diabetologia, 1978. **14**(3): p. 141-8.
72. Bates, S.H., et al., *Roles for leptin receptor/STAT3-dependent and -independent signals in the regulation of glucose homeostasis.* Cell Metab, 2005. **1**(3): p. 169-78.
73. Bates, S.H., et al., *STAT3 signalling is required for leptin regulation of energy balance but not reproduction.* Nature, 2003. **421**(6925): p. 856-9.
74. Bultman, S.J., E.J. Michaud, and R.P. Woychik, *Molecular characterization of the mouse agouti locus.* Cell, 1992. **71**(7): p. 1195-204.
75. Mynatt, R.L., et al., *Combined effects of insulin treatment and adipose tissue-specific agouti expression on the development of obesity.* Proc Natl Acad Sci U S A, 1997. **94**(3): p. 919-22.
76. Jones, B.H., et al., *Adipose tissue stearoyl-CoA desaturase mRNA is increased by obesity and decreased by polyunsaturated fatty acids.* Am J Physiol, 1996. **271**(1 Pt 1): p. E44-9.
77. Corander, M.P., et al., *Loss of agouti-related peptide does not significantly impact the phenotype of murine POMC deficiency.* Endocrinology, 2011. **152**(5): p. 1819-28.
78. Butler, A.A. and R.D. Cone, *The melanocortin receptors: lessons from knockout models.* Neuropeptides, 2002. **36**(2-3): p. 77-84.
79. Bray, G.A. and B.M. Popkin, *Dietary fat intake does affect obesity!* Am J Clin Nutr, 1998. **68**(6): p. 1157-73.
80. Jequier, E., *Pathways to obesity.* Int J Obes Relat Metab Disord, 2002. **26 Suppl 2**: p. S12-7.
81. Buettner, R., J. Scholmerich, and L.C. Bollheimer, *High-fat diets: modeling the metabolic disorders of human obesity in rodents.* Obesity (Silver Spring), 2007. **15**(4): p. 798-808.
82. Akira, S., S. Uematsu, and O. Takeuchi, *Pathogen recognition and innate immunity.* Cell, 2006. **124**(4): p. 783-801.
83. McGuinness, D.H., P.K. Dehal, and R.J. Pleass, *Pattern recognition molecules and innate immunity to parasites.* Trends Parasitol, 2003. **19**(7): p. 312-9.
84. Deban, L., et al., *Pentraxins in innate immunity: lessons from PTX3.* Cell Tissue Res, 2011. **343**(1): p. 237-49.
85. van de Wetering, J.K., L.M. van Golde, and J.J. Batenburg, *Collectins: players of the innate immune system.* Eur J Biochem, 2004. **271**(7): p. 1229-49.
86. Zhang, X.L. and M.A. Ali, *Ficolins: structure, function and associated diseases.* Adv Exp Med Biol, 2008. **632**: p. 105-15.
87. Garlanda, C., et al., *Pentraxins at the crossroads between innate immunity, inflammation, matrix deposition, and female fertility.* Annu Rev Immunol, 2005. **23**: p. 337-66.
88. Breviario, F., et al., *Interleukin-1-inducible genes in endothelial cells. Cloning of a new gene related to C-reactive protein and serum amyloid P component.* J Biol Chem, 1992. **267**(31): p. 22190-7.
89. Lee, G.W., T.H. Lee, and J. Vilcek, *TSG-14, a tumor necrosis factor- and IL-1-inducible protein, is a novel member of the pentaxin family of acute phase proteins.* J Immunol, 1993. **150**(5): p. 1804-12.
90. Bottazzi, B., et al., *An integrated view of humoral innate immunity: pentraxins as a paradigm.* Annu Rev Immunol, 2010. **28**: p. 157-83.
91. Introna, M., et al., *Cloning of mouse ptx3, a new member of the pentraxin gene family expressed at extrahepatic sites.* Blood, 1996. **87**(5): p. 1862-72.

92. Basile, A., et al., *Characterization of the promoter for the human long pentraxin PTX3. Role of NF-kappaB in tumor necrosis factor-alpha and interleukin-1beta regulation.* J Biol Chem, 1997. **272**(13): p. 8172-8.
93. Bottazzi, B., et al., *Multimer formation and ligand recognition by the long pentraxin PTX3. Similarities and differences with the short pentraxins C-reactive protein and serum amyloid P component.* J Biol Chem, 1997. **272**(52): p. 32817-23.
94. Garlanda, C., et al., *Non-redundant role of the long pentraxin PTX3 in anti-fungal innate immune response.* Nature, 2002. **420**(6912): p. 182-6.
95. Inforzato, A., et al., *Structural characterization of PTX3 disulfide bond network and its multimeric status in cumulus matrix organization.* J Biol Chem, 2008. **283**(15): p. 10147-61.
96. Inforzato, A., et al., *Structure and function of the long pentraxin PTX3 glycosidic moiety: fine-tuning of the interaction with C1q and complement activation.* Biochemistry, 2006. **45**(38): p. 11540-51.
97. Doni, A., et al., *Regulation of PTX3, a key component of humoral innate immunity in human dendritic cells: stimulation by IL-10 and inhibition by IFN-gamma.* J Leukoc Biol, 2006. **79**(4): p. 797-802.
98. Jaillon, S., et al., *The humoral pattern recognition receptor PTX3 is stored in neutrophil granules and localizes in extracellular traps.* J Exp Med, 2007. **204**(4): p. 793-804.
99. Abderrahim-Ferkoune, A., et al., *Characterization of the long pentraxin PTX3 as a TNFalpha-induced secreted protein of adipose cells.* J Lipid Res, 2003. **44**(5): p. 994-1000.
100. Gustin, C., et al., *Upregulation of pentraxin-3 in human endothelial cells after lysophosphatidic acid exposure.* Arterioscler Thromb Vasc Biol, 2008. **28**(3): p. 491-7.
101. Nauta, A.J., et al., *Biochemical and functional characterization of the interaction between pentraxin 3 and C1q.* Eur J Immunol, 2003. **33**(2): p. 465-73.
102. Inforzato, A., et al., *Pentraxins in humoral innate immunity.* Adv Exp Med Biol, 2012. **946**: p. 1-20.
103. Gout, E., et al., *M-ficolin interacts with the long pentraxin PTX3: a novel case of cross-talk between soluble pattern-recognition molecules.* J Immunol, 2011. **186**(10): p. 5815-22.
104. Ma, Y.J., et al., *Synergy between ficolin-2 and pentraxin 3 boosts innate immune recognition and complement deposition.* J Biol Chem, 2009. **284**(41): p. 28263-75.
105. Deban, L., et al., *Binding of the long pentraxin PTX3 to factor H: interacting domains and function in the regulation of complement activation.* J Immunol, 2008. **181**(12): p. 8433-40.
106. Braunschweig, A. and M. Jozsi, *Human pentraxin 3 binds to the complement regulator c4b-binding protein.* PLoS One, 2011. **6**(8): p. e23991.
107. Trouw, L.A., et al., *C4b-binding protein and factor H compensate for the loss of membrane-bound complement inhibitors to protect apoptotic cells against excessive complement attack.* J Biol Chem, 2007. **282**(39): p. 28540-8.
108. Rusnati, M., et al., *Selective recognition of fibroblast growth factor-2 by the long pentraxin PTX3 inhibits angiogenesis.* Blood, 2004. **104**(1): p. 92-9.
109. Basilico, C. and D. Moscatelli, *The FGF family of growth factors and oncogenes.* Adv Cancer Res, 1992. **59**: p. 115-65.
110. Presta, M., et al., *Fibroblast growth factor/fibroblast growth factor receptor system in angiogenesis.* Cytokine Growth Factor Rev, 2005. **16**(2): p. 159-78.
111. Camozzi, M., et al., *Identification of an antiangiogenic FGF2-binding site in the N terminus of the soluble pattern recognition receptor PTX3.* J Biol Chem, 2006. **281**(32): p. 22605-13.
112. Barbati, E., et al., *Influence of pentraxin 3 (PTX3) genetic variants on myocardial infarction risk and PTX3 plasma levels.* PLoS One, 2012. **7**(12): p. e53030.

113. Olesen, R., et al., *DC-SIGN (CD209), pentraxin 3 and vitamin D receptor gene variants associate with pulmonary tuberculosis risk in West Africans.* Genes Immun, 2007. **8**(6): p. 456-67.
114. Chiarini, M., et al., *PTX3 genetic variations affect the risk of Pseudomonas aeruginosa airway colonization in cystic fibrosis patients.* Genes Immun, 2010. **11**(8): p. 665-70.
115. Cunha, C., et al., *Genetic PTX3 deficiency and aspergillosis in stem-cell transplantation.* N Engl J Med, 2014. **370**(5): p. 421-32.
116. Xu, D., et al., *Narp and NP1 form heterocomplexes that function in developmental and activity-dependent synaptic plasticity.* Neuron, 2003. **39**(3): p. 513-28.
117. Hossain, M.A., *Hypoxic-ischemic injury in neonatal brain: involvement of a novel neuronal molecule in neuronal cell death and potential target for neuroprotection.* Int J Dev Neurosci, 2008. **26**(1): p. 93-101.
118. Martinez de la Torre, Y., et al., *Evolution of the pentraxin family: the new entry PTX4.* J Immunol, 2010. **184**(9): p. 5055-64.
119. Emsley, J., et al., *Structure of pentameric human serum amyloid P component.* Nature, 1994. **367**(6461): p. 338-45.
120. Pepys, M.B. and G.M. Hirschfield, *C-reactive protein: a critical update.* J Clin Invest, 2003. **111**(12): p. 1805-12.
121. Abernethy, T.J. and O.T. Avery, *The Occurrence during Acute Infections of a Protein Not Normally Present in the Blood : I. Distribution of the Reactive Protein in Patients' Sera and the Effect of Calcium on the Flocculation Reaction with C Polysaccharide of Pneumococcus.* J Exp Med, 1941. **73**(2): p. 173-82.
122. Roumenina, L.T., et al., *Interaction of C1q with IgG1, C-reactive protein and pentraxin 3: mutational studies using recombinant globular head modules of human C1q A, B, and C chains.* Biochemistry, 2006. **45**(13): p. 4093-104.
123. Ng, P.M., et al., *C-reactive protein collaborates with plasma lectins to boost immune response against bacteria.* EMBO J, 2007. **26**(14): p. 3431-40.
124. Okemefuna, A.I., et al., *Complement factor H binds at two independent sites to C-reactive protein in acute phase concentrations.* J Biol Chem, 2010. **285**(2): p. 1053-65.
125. D'Angelo, C., et al., *Exogenous pentraxin 3 restores antifungal resistance and restrains inflammation in murine chronic granulomatous disease.* J Immunol, 2009. **183**(7): p. 4609-18.
126. Moalli, F., et al., *Role of complement and Fc{gamma} receptors in the protective activity of the long pentraxin PTX3 against Aspergillus fumigatus.* Blood, 2010. **116**(24): p. 5170-80.
127. Moalli, F., et al., *The therapeutic potential of the humoral pattern recognition molecule PTX3 in chronic lung infection caused by Pseudomonas aeruginosa.* J Immunol, 2011. **186**(9): p. 5425-34.
128. Bozza, S., et al., *Pentraxin 3 protects from MCMV infection and reactivation through TLR sensing pathways leading to IRF3 activation.* Blood, 2006. **108**(10): p. 3387-96.
129. Han, B., et al., *Protective effects of long pentraxin PTX3 on lung injury in a severe acute respiratory syndrome model in mice.* Lab Invest, 2012. **92**(9): p. 1285-96.
130. Reading, P.C., et al., *Antiviral activity of the long chain pentraxin PTX3 against influenza viruses.* J Immunol, 2008. **180**(5): p. 3391-8.
131. Suzuki, S., et al., *Pentraxin 3, a new marker for vascular inflammation, predicts adverse clinical outcomes in patients with heart failure.* Am Heart J, 2008. **155**(1): p. 75-81.
132. Peri, G., et al., *PTX3, A prototypical long pentraxin, is an early indicator of acute myocardial infarction in humans.* Circulation, 2000. **102**(6): p. 636-41.
133. Ustundag, M., et al., *Comparative diagnostic accuracy of serum levels of neutrophil activating peptide-2 and pentraxin-3 versus troponin-I in acute coronary syndrome.* Anadolu Kardiyol Derg, 2011. **11**(7): p. 588-94.

134. Inoue, K., et al., *Establishment of a high sensitivity plasma assay for human pentraxin3 as a marker for unstable angina pectoris.* Arterioscler Thromb Vasc Biol, 2007. **27**(1): p. 161-7.
135. Klouche, M., et al., *Atherogenic properties of enzymatically degraded LDL: selective induction of MCP-1 and cytotoxic effects on human macrophages.* Arterioscler Thromb Vasc Biol, 1998. **18**(9): p. 1376-85.
136. Klouche, M., et al., *Enzymatically degraded, nonoxidized LDL induces human vascular smooth muscle cell activation, foam cell transformation, and proliferation.* Circulation, 2000. **101**(15): p. 1799-805.
137. Norata, G.D., et al., *Deficiency of the long pentraxin PTX3 promotes vascular inflammation and atherosclerosis.* Circulation, 2009. **120**(8): p. 699-708.
138. Lindner, V., et al., *Inhibition of smooth muscle cell proliferation in injured rat arteries. Interaction of heparin with basic fibroblast growth factor.* J Clin Invest, 1992. **90**(5): p. 2044-9.
139. Peoples, G.E., et al., *T lymphocytes that infiltrate tumors and atherosclerotic plaques produce heparin-binding epidermal growth factor-like growth factor and basic fibroblast growth factor: a potential pathologic role.* Proc Natl Acad Sci U S A, 1995. **92**(14): p. 6547-51.
140. Ishino, M., et al., *Deficiency of Long Pentraxin PTX3 Promoted Neointimal Hyperplasia after Vascular Injury.* J Atheroscler Thromb, 2015. **22**(4): p. 372-8.
141. Salio, M., et al., *Cardioprotective function of the long pentraxin PTX3 in acute myocardial infarction.* Circulation, 2008. **117**(8): p. 1055-64.
142. Deban, L., et al., *Regulation of leukocyte recruitment by the long pentraxin PTX3.* Nat Immunol, 2010. **11**(4): p. 328-34.
143. Rodriguez-Grande, B., et al., *The acute-phase protein PTX3 is an essential mediator of glial scar formation and resolution of brain edema after ischemic injury.* J Cereb Blood Flow Metab, 2014. **34**(3): p. 480-8.
144. Ryu, W.S., et al., *Pentraxin 3: a novel and independent prognostic marker in ischemic stroke.* Atherosclerosis, 2012. **220**(2): p. 581-6.
145. Qin, L.Z., et al., *PTX3 expression in the plasma of elderly ACI patients and its relationship with severity and prognosis of the disease.* Eur Rev Med Pharmacol Sci, 2016. **20**(19): p. 4112-4118.
146. Alberti, L., et al., *Expression of long pentraxin PTX3 in human adipose tissue and its relation with cardiovascular risk factors.* Atherosclerosis, 2009. **202**(2): p. 455-60.
147. Zanetti, M., et al., *Circulating pentraxin 3 levels are higher in metabolic syndrome with subclinical atherosclerosis: evidence for association with atherogenic lipid profile.* Clin Exp Med, 2009. **9**(3): p. 243-8.
148. Miyaki, A., et al., *Is pentraxin 3 involved in obesity-induced decrease in arterial distensibility?* J Atheroscler Thromb, 2010. **17**(3): p. 278-84.
149. Qin, S., et al., *Prenatal Exposure to Lipopolysaccharide Induces PTX3 Expression and Results in Obesity in Mouse Offspring.* Inflammation, 2017. **40**(6): p. 1847-1861.
150. Miyazaki, T., et al., *Plasma pentraxin 3 levels do not predict coronary events but reflect metabolic disorders in patients with coronary artery disease in the CARE trial.* PLoS One, 2014. **9**(4): p. e94073.
151. Ogawa, T., et al., *Reciprocal contribution of pentraxin 3 and C-reactive protein to obesity and metabolic syndrome.* Obesity (Silver Spring), 2010. **18**(9): p. 1871-4.
152. Miyaki, A., Y. Choi, and S. Maeda, *Pentraxin 3 production in the adipose tissue and the skeletal muscle in diabetic-obese mice.* Am J Med Sci, 2014. **347**(3): p. 228-33.
153. Witasp, A., et al., *Inflammatory biomarker pentraxin 3 (PTX3) in relation to obesity, body fat depots and weight loss.* Obesity (Silver Spring), 2014. **22**(5): p. 1373-9.

154. Yamasaki, K., et al., *Determination of physiological plasma pentraxin 3 (PTX3) levels in healthy populations.* Clin Chem Lab Med, 2009. **47**(4): p. 471-7.
155. Jenny, N.S., et al., *Associations of pentraxin 3 with cardiovascular disease: the Multi-Ethnic Study of Atherosclerosis.* J Thromb Haemost, 2014. **12**(6): p. 999-1005.
156. Doni, A., et al., *An acidic microenvironment sets the humoral pattern recognition molecule PTX3 in a tissue repair mode.* J Exp Med, 2015. **212**(6): p. 905-25.
157. Visser, M., et al., *Elevated C-reactive protein levels in overweight and obese adults.* JAMA, 1999. **282**(22): p. 2131-5.
158. Aronson, D., et al., *Obesity is the major determinant of elevated C-reactive protein in subjects with the metabolic syndrome.* Int J Obes Relat Metab Disord, 2004. **28**(5): p. 674-9.
159. Mantovani, A., et al., *Cancer-related inflammation.* Nature, 2008. **454**(7203): p. 436-44.
160. Kondo, S., et al., *Clinical impact of pentraxin family expression on prognosis of pancreatic carcinoma.* Br J Cancer, 2013. **109**(3): p. 739-46.
161. Choi, B., et al., *Upregulation of brain-derived neurotrophic factor in advanced gastric cancer contributes to bone metastatic osteolysis by inducing long pentraxin 3.* Oncotarget, 2016. **7**(34): p. 55506-55517.
162. Ronca, R., et al., *Long pentraxin-3 inhibits epithelial-mesenchymal transition in melanoma cells.* Mol Cancer Ther, 2013. **12**(12): p. 2760-71.
163. Ronca, R., et al., *Long-Pentraxin 3 Derivative as a Small-Molecule FGF Trap for Cancer Therapy.* Cancer Cell, 2015. **28**(2): p. 225-39.
164. Bonavita, E., et al., *PTX3 is an extrinsic oncosuppressor regulating complement-dependent inflammation in cancer.* Cell, 2015. **160**(4): p. 700-714.
165. Wang, J.X., et al., *Aberrant methylation of the 3q25 tumor suppressor gene PTX3 in human esophageal squamous cell carcinoma.* World J Gastroenterol, 2011. **17**(37): p. 4225-30.
166. Rubino, M., et al., *Epigenetic regulation of the extrinsic oncosuppressor PTX3 gene in inflammation and cancer.* Oncoimmunology, 2017. **6**(7): p. e1333215.
167. Osorio-Conles, O., et al., *Plasma PTX3 protein levels inversely correlate with insulin secretion and obesity, whereas visceral adipose tissue PTX3 gene expression is increased in obesity.* Am J Physiol Endocrinol Metab, 2011. **301**(6): p. E1254-61.
168. Suzuki, W., et al., *A new mouse model of spontaneous diabetes derived from ddY strain.* Exp Anim, 1999. **48**(3): p. 181-9.
169. Bonacina, F., et al., *Long pentraxin 3: experimental and clinical relevance in cardiovascular diseases.* Mediators Inflamm, 2013. **2013**: p. 725102.
170. Violi, F. and D. Pastori, *Pentraxin 3 - A Link Between Obesity, Inflammation and Vascular Disease?* Circ J, 2016. **80**(2): p. 327-8.
171. Knoflach, M., et al., *Pentraxin-3 as a marker of advanced atherosclerosis results from the Bruneck, ARMY and ARFY Studies.* PLoS One, 2012. **7**(2): p. e31474.
172. Norata, G.D., et al., *Leptin:adiponectin ratio is an independent predictor of intima media thickness of the common carotid artery.* Stroke, 2007. **38**(10): p. 2844-6.
173. Lorenz, M.W., et al., *Carotid intima-media thickness progression to predict cardiovascular events in the general population (the PROG-IMT collaborative project): a meta-analysis of individual participant data.* Lancet, 2012. **379**(9831): p. 2053-62.
174. Baragetti, I., et al., *-374 T/A RAGE polymorphism is associated with chronic kidney disease progression in subjects affected by nephrocardiovascular disease.* PLoS One, 2013. **8**(4): p. e60089.
175. Baragetti, A., et al., *Telomere shortening over 6 years is associated with increased subclinical carotid vascular damage and worse cardiovascular prognosis in the general population.* J Intern Med, 2015. **277**(4): p. 478-87.

176. Baragetti, A., et al., *Subclinical atherosclerosis is associated with Epicardial Fat Thickness and hepatic steatosis in the general population.* Nutr Metab Cardiovasc Dis, 2016. **26**(2): p. 141-53.
177. Boardman-Pretty, F., et al., *Functional Analysis of a Carotid Intima-Media Thickness Locus Implicates BCAR1 and Suggests a Causal Variant.* Circ Cardiovasc Genet, 2015. **8**(5): p. 696-706.
178. Baragetti, A., et al., *PCSK9 deficiency results in increased ectopic fat accumulation in experimental models and in humans.* Eur J Prev Cardiol, 2017. **24**(17): p. 1870-1877.
179. Kloting, N. and M. Bluher, *Adipocyte dysfunction, inflammation and metabolic syndrome.* Rev Endocr Metab Disord, 2014. **15**(4): p. 277-87.
180. Leali, D., et al., *Long pentraxin 3/tumor necrosis factor-stimulated gene-6 interaction: a biological rheostat for fibroblast growth factor 2-mediated angiogenesis.* Arterioscler Thromb Vasc Biol, 2012. **32**(3): p. 696-703.
181. Mathis, D., *Immunological goings-on in visceral adipose tissue.* Cell Metab, 2013. **17**(6): p. 851-9.
182. Woolford, S.J., et al., *Maternal perspectives on growth and nutrition counseling provided at preschool well-child visits.* J Natl Med Assoc, 2007. **99**(2): p. 153-8.
183. Mauro, C., et al., *Obesity-Induced Metabolic Stress Leads to Biased Effector Memory CD4(+) T Cell Differentiation via PI3K p110delta-Akt-Mediated Signals.* Cell Metab, 2017. **25**(3): p. 593-609.
184. Kanda, H., et al., *MCP-1 contributes to macrophage infiltration into adipose tissue, insulin resistance, and hepatic steatosis in obesity.* J Clin Invest, 2006. **116**(6): p. 1494-505.
185. Chatzigeorgiou, A., et al., *Blocking CD40-TRAF6 signaling is a therapeutic target in obesity-associated insulin resistance.* Proc Natl Acad Sci U S A, 2014. **111**(7): p. 2686-91.
186. Bonacina, F., et al., *Vascular pentraxin 3 controls arterial thrombosis by targeting collagen and fibrinogen induced platelets aggregation.* Biochim Biophys Acta, 2016. **1862**(6): p. 1182-90.
187. Maugeri, N., et al., *Early and transient release of leukocyte pentraxin 3 during acute myocardial infarction.* J Immunol, 2011. **187**(2): p. 970-9.
188. Souza, D.G., et al., *The long pentraxin PTX3 is crucial for tissue inflammation after intestinal ischemia and reperfusion in mice.* Am J Pathol, 2009. **174**(4): p. 1309-18.
189. Inforzato, A., et al., *The "sweet" side of a long pentraxin: how glycosylation affects PTX3 functions in innate immunity and inflammation.* Front Immunol, 2012. **3**: p. 407.
190. Lumeng, C.N., et al., *Increased inflammatory properties of adipose tissue macrophages recruited during diet-induced obesity.* Diabetes, 2007. **56**(1): p. 16-23.
191. Moreno, P.R., et al., *Neovascularization in human atherosclerosis.* Circulation, 2006. **113**(18): p. 2245-52.
192. Elias, I., et al., *Adipose tissue overexpression of vascular endothelial growth factor protects against diet-induced obesity and insulin resistance.* Diabetes, 2012. **61**(7): p. 1801-13.
193. May, L., et al., *Genetic variation in pentraxin (PTX) 3 gene associates with PTX3 production and fertility in women.* Biol Reprod, 2010. **82**(2): p. 299-304.
194. Diamond, J.M., et al., *Variation in PTX3 is associated with primary graft dysfunction after lung transplantation.* Am J Respir Crit Care Med, 2012. **186**(6): p. 546-52.